Role of the nuclear lamina for stem cell mediated homeostasis

Sep 30, 2015

Dissertation for the award of the degree
"Doctor rerum naturalium (Dr. rer. nat.)"

in the GGNB program "Genes and Development"

at the Georg - August - Universität Göttingen

Faculty of Biology

submitted by

Roman Petrovsky
born in Freital, Germany

MEMBERS OF THE THESIS COMMITTEE AND EXAMINATION BOARD

Prof. Dr. Jörg Großhans (Supervisor, reviewer)
Department of Developmental Biochemistry, University of Göttingen

Prof. Dr. Reinhard Schuh (Reviewer)
Department of Molecular Developmental Biology, Max Planck Institute for Biophysical Chemistry

Prof. Dr. Ahmed Mansouri
Department of Molecular Cell Biology, Max Planck Institute for Biophysical Chemistry

MEMBERS OF THE EXAMINATION BOARD

Dr. Halyna Shcherbata
Max Planck Research Group "Gene Expression and Signaling", Max Planck Institute for Biophysical Chemistry

Dr. Gerd Vorbrüggen
Max Planck Research Group "Molecular Cell Dynamics", Max Planck Institute for Biophysical Chemistry

Prof. Dr. Ralph Kehlenbach
Department of Molecular Biology, University Medical Center Göttingen

Date of oral examination: 02.12.2015

AFFIDAVIT

I hereby declare that I prepared the PhD thesis “Role of the nuclear lamina for stem cell mediated homeostasis” on my own with no other sources and aids than quoted.

_____ Roman Petrovsky

Contents

Acknowledgments

I take this opportunity to thank all the people who were directly or indirectly involved in the successful completion of my doctoral work. First of all, I would like to thank my supervisor Prof. Jörg Großhans for providing me with guidance and inspiration. His enthusiasm and optimism are contagious and I am very grateful for all the discussions for which he was always available. I express my gratitude to my thesis committee members Prof. Reinhard Schuh and Prof. Ahmed Mansouri for the helpful inputs and encouragement throughout the duration of my PhD. Special thanks goes to Georg Krohne who was a very kind and helpful collaborator. I am deeply indebted to all my past and present colleagues for building such a creative and helpful work culture in the lab. I would specifically like to thank Dr. Michaela Clever for insightful discussions and suggestions, Maria Kriebel for provision of a supportive figure and Franziska Winkler for helpful suggestions regarding the thesis. I am most grateful to Dr. Sreemukta Acharya for interesting discussions, suggestions with the thesis and constant support. Finally I would like to express my gratitude to the whole department of developmental biochemistry for creating a very pleasant and helpful working environment.

Abbreviations

C. elegans	Caenorhabditis elegans
CyO	Curly of Oster (balancer chromosome)
DAPI	4',6'-Diamino-2-phenylindole
Dm0	Lamin Dm0
DNA	deoxyribonucleic acid
Dr	Drop (marker gene)
EB(s)	enteroblast(s)
EC(s)	(absorptive) enterocyte(s)
ECM	extracellular matrix
EE(s)	(secretory) endocrine enterocyte(s)
ER	Endoplasmatic reticulum
GFP	green fluorescent protein
HGPS	Hutchinson-Gilford progeria syndrome
HP1	heterochromatin protein 1
ISC(s)	intestinal stem cell(s)
Kuk	Kugelkern
m	milli-
M	mol per liter
min	minute(s)
mRNA	messenger RNA

Mu	muscle cell
µ	micro-
n	nano-
NLS	nuclear localization signal
NURD	nucleosome remodeling and deacetylase (-complex)
PEV	position-effect variegation
RNA	ribonucleic acid
RNAi	RNA interference
SDS	sodiumdodecylsulphate
SDS-PAGE	SDS-polyacrylamide gel electrophoresis
Sp	Stenopleural (markergene)
TM3	Third-Multiple-3 (balancer chromosome)
Vm	Viceral muscle cells
WT	wild type
°C	degrees Celcius

Summary

The nuclear lamina is a protein meshwork at the inner side of the inner nuclear membrane and connects to essential cellular structures like chromatin, the nuclear pore complex and the cytoskeleton. The nuclear lamina is comprised of A-type lamins (lamin A, C and C2), B-type lamins (lamin B1, B2 and B3) and lamina associated proteins. Progerin is a altered form of Lamin A, which causes severe ageing-like effects of the Hutchinson-Gilford progeria syndrome. Progerin was also found in cells of normal aged individuals. Therefore, it is conceivable that the expression of Progerin is linked to the process of ageing and its effects. How the cellular effects of Progerin expression, like misfolded nuclei, decreased heterochromatin, increased apoptosis and increased DNA damage are mediated from the cellular to the organismic level is not well understood. It is conceivable however that stem cells play an important role in this process, since the early loss of hair is a typical symptom of HGPS and in HGPS-mouse-models a decrease of hair-follicle stem cell proliferation was reported. Also the loss of subcutaneous fat and reduced wound healing, found in HGPS patients and elderly people, indicates impairment of stem cell function. In *Drosophila* expression of the lamina proteins lamin Dm0 and Kugelkern induces effects similar to those observed in HGPS patients and HGPS-animal-models. In the course of this work, lamin Dm0 and Kugelkern were found to drastically reduce stem cell proliferation in the *Drosophila* midgut. Since the midgut is a relatively simple organ, with only 5 cell types and low degree of infoldings, it offers many benefits as a system to study stem cell behavior; and in this context, the effect of lamin Dm0 and Kugelkern on intestinal stem cells.
In this work the mechanism in which lamin Dm0 and Kugelkern act on intestinal stem cells was investigated. It is shown, that lamin Dm0 Kugelkern overexpression does not permanently damage intestinal stem cells or impair their function irreversibly. That the effects of lamin Dm0 and Kugelkern overexpression are likely not due to impaired nuclear transport. And that the inhibiting effect of lamin Dm0 on ISC proliferation is pinpointed to the impairment of the JAK/STAT signaling pathway on a transcriptional level.

1 Introduction

1.1 Nuclear lamina

The nucleus is a distinctive feature of eukaryotic cells and separates the chromatin from the cytoplasm via the nuclear envelope. The nuclear envelope of metazoans is comprised of three main elements: the nuclear pores, the nuclear membrane and the nuclear lamina [33] (Figure 1). The nuclear membrane consists of two lipid bilayers: the outer nuclear membrane (ONM) and the inner nuclear membrane (INM). The space between ONM and INM is called perinuclear space (PNS). The ONM and the PNS are continuous with the endoplasmatic reticulum (ER), while the INM associates with the nuclear lamina. The nuclear membrane is perforated by nuclear pore complexes (NPCs), which serve as gateways to regulate the transfer of macromolecules between nucleus and cytoplasm [35].

The nuclear lamina is a metazoan-specific protein meshwork located at the inner side of the INM. The lamina binds to the periphery of NPCs, to chromatin and is connected with the cytoskeleton and INM via a diverse set of lamina binding proteins and lamina associated proteins [1, 29, 31, 60, 72, 93]. The main structural component of the lamina are lamins, which are categorized as class V intermediate filaments [70] and are in fact the only nuclear intermediate filaments [84]. Based on sequence homology, lamins are categorized into A and B type lamins. Mammals have three A-type lamins (lamin A, C and C2, encoded by the *LMNA* gene) and three B-type lamins (lamin B1, encoded by *LMNB1* and lamin B2 and B3, encoded by *LMNB2*). As intermediate filaments, the lamin structure involves a head domain, an alpha-helical rod domain and a C-terminal tail domain. Additionally, they contain an immunoglobulin fold-like structure with β-sheets, a nuclear localization signal (NLS) in the tail domain and, except for Lamin C, they also contain a C-terminal CaaX motif (C = cysteine, a = aliphatic residues, X = any residue) [47, 84]. During the maturation of lamin A and B-type lamins, the CaaX motif undergoes a series of post-translational processing steps resulting in the addition of a farnesyl group at the last cysteine. The CaaX motif is considered to play a role in the targeting of lamins to the INM and in protein-protein interactions [76]. Lamin A and B are likely to interact with each other *in vitro* [32]. Also scanning electron microscopy images of nuclear envelopes of *Xenopus laevis* oocytes have shown an ordered meshwork of filaments [2]. However, little is known about the way in which lamins interact; whether they form a single

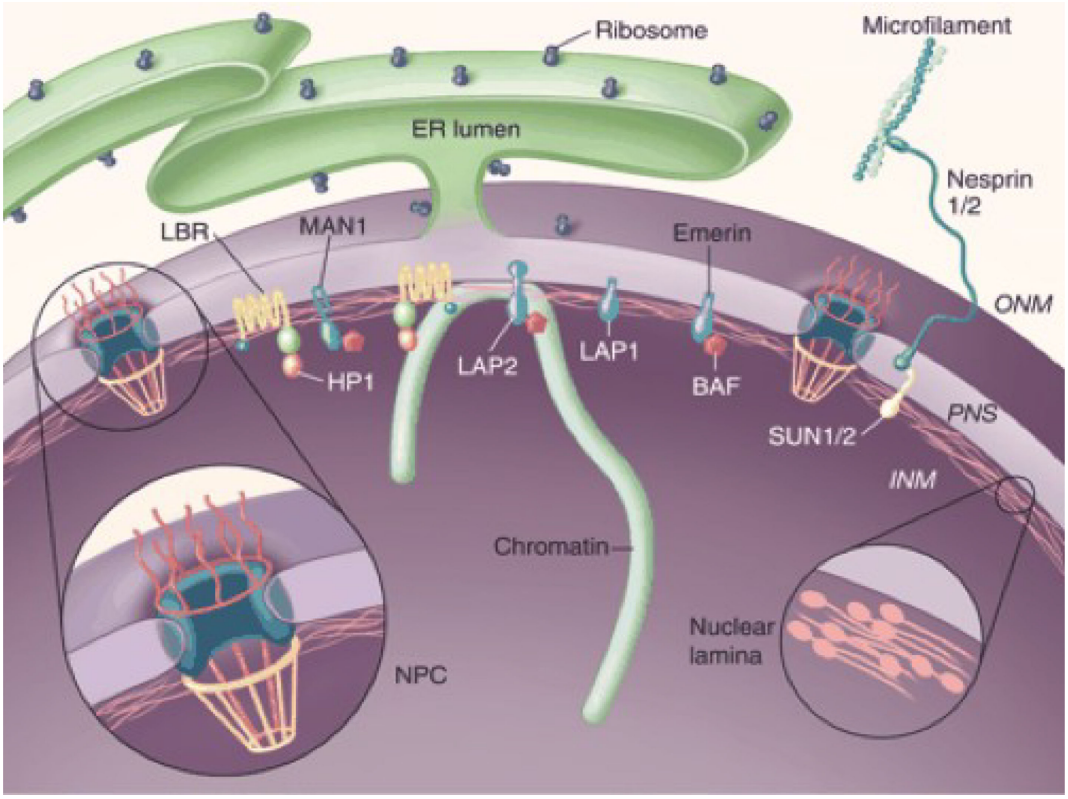

Figure 1: Nuclear Lamina
Schematic of the nuclear lamina, lamina proteins and associated cellular organelles. ER: Endoplasmatic reticulum, NPC: Nuclear pore complex, ONM:Outer nuclear membrane, PNS: Perinuclear space, INM: Inner nuclear membrane, Lamin binding proteins: LBR, LAP1, LAP2, Emerin, MAN1, SUN1/2, Lamina associated proteins: BAF, HP1, Nesprin. Adopted from [83].

interconnected network or layers of different types of lamins [90].

1.2 Laminopathies and HGPS

Since the discovery, in 1999, that autosomal dominant Emery-Dreifuss muscular dystrophy was caused by a mutation in the *LMNA* gene [10], many other diseases have been linked to heterozygous mutations in the same allele (Figure 2). These diseases are termed laminopathies and can be categorized into two main branches: "tissue-specific laminopathies" affecting muscle, fat or nerve tissue or "systemic laminopathies" like progeroid diseases affecting a wide range of tissues. Until now 464 different mutations have been found in the *LMNA* gene in a total of 2251 subjects. In contrast to this very few diseases are linked to mutations in LMNB1/B2. *LMNA* mutations leading to "tissue-specific laminopathies" are the most prominent (UMD-*LMNA* mutations database). However, the smaller set of "systemic laminopathies" contains a collection of premature ageing diseases which may help to understand the complex processes involved in ageing. One of the most prominent examples of this group is the Hutchinson-Gilford progeria syndrome (HGPS).

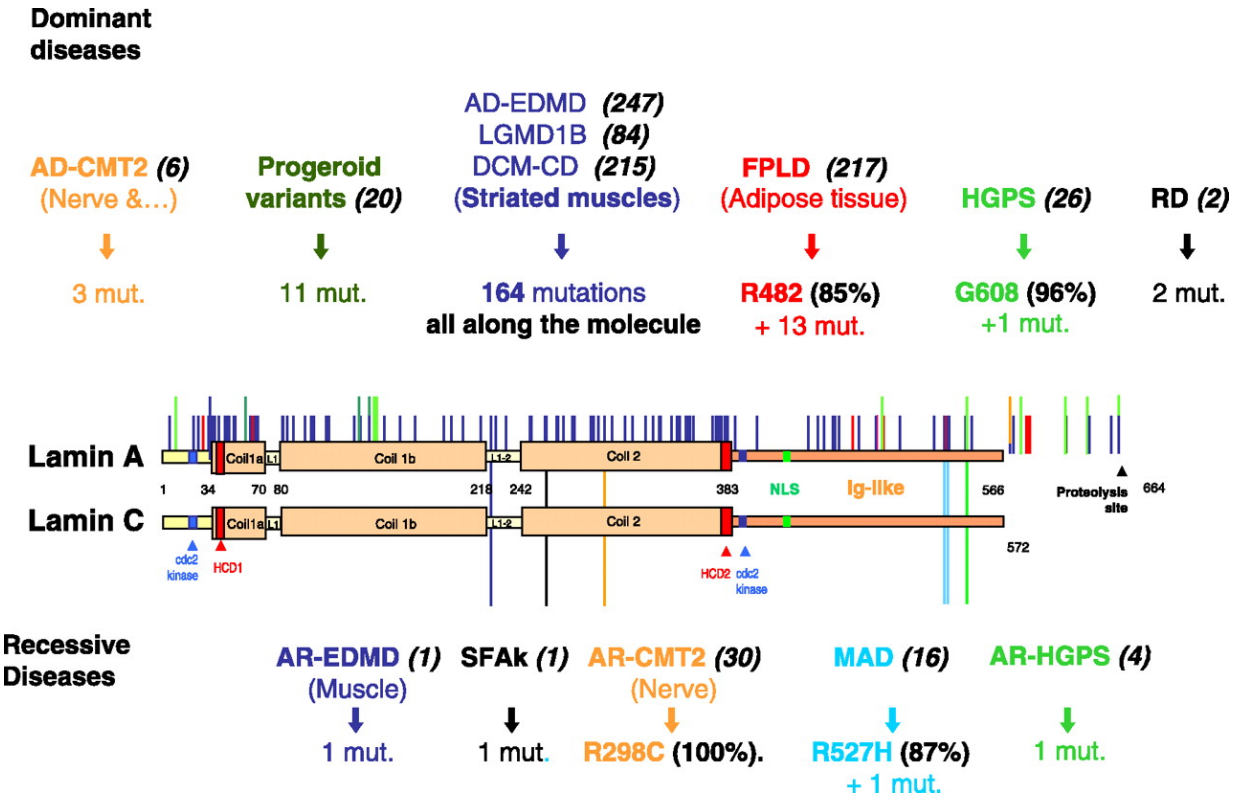

Figure 2: Laminopathies
Schematic of *LMNA* mutations that induce different types of laminopathies overlayed on the lamin A/C protein. Dominant disorders as a result of heterozygous *LMNA* mutations are depicted on the top of the protein scheme, whereas homozygous mutations, causing recessive laminopathies, are presented below. Numbers of people with the respective *LMNA* mutation and the corresponding phenotype are noted in parentheses close to each disease acronym (2006). cdc2: site of Cdc2 kinase, HDC: highly conserved domain, NLS: nuclear localization signal. Adopted from [15].

Hutchinson-Gilford progeria syndrome

HGPS is a rare genetic disease that starts affecting patients in early infancy, leading to several ageing associated phenotypes like growth retardation, premature atherosclerosis, loss of subcutaneous fat, altered pigmentation, decreased wound healing, osteolysis and loss of hair. While many phenotypic aspects of HGPS are also found in elderly people, some symptoms associated with "normal ageing", like neurodegeneration, type 2 diabetes, hyperlipidemia or cancer disposition, are absent in HGPS patients [23, 34, 42, 58, 77, 86]. HGPS can be subdivided into clasical HGPS and atypical HGPS. Atypical HGPS shares several of the phenotypes of classical HGPS but not all an with varying degree [42]. Atypical HGPS can be caused by a homozygous 1579C>T mutation in exon 9 of *LMNA* [42, 49].
The classical HGPS phenotype is generated in two main ways:

1. A silent G608G (GGC -> GGT) mutation within exon 11 of the *LMNA* gene (90% of patients) results in a constitutive activation of a cryptic splice site. This leads to a 50-amino acid deletion in Prelamin A (amino acids 607–656), thereby removing the recognition site for

the metalloproteinase ZMPSTE2 that normally cleaves off the last 15 C-terminal amino acids together with the farnesyl group [23, 27].

2. A mutation in the ZMPSTE2 gene locus itself resulting in a dysfunctional ZMPSTE2 protein [22].

In both cases the C-terminal part of Prelamin A with the farnesyl group is not cleaved off resulting in a truncated and permanently farnesylated form of prelamin A, termed Progerin. On a cellular level Progerin expression causes a multitude of harmful effects: nuclear abnormalities like blebs and invaginations, resulting in decreased nuclear stability [92], decreased heterochromatin [21], defective DNA repair, decreased genome stability and a chronic DNA-damage response [53, 54], reduced telomere length [24] and increased apoptosis [14].

Some evidence suggests that stem cells might play a role in HGPS. It was shown that stem cells from HGPS patients express Progerin [87] and that mesenchymal stem cells (MSC) have upregulated levels of Notch target genes [78]. This might indicate a loss of stem cell identity since Notch plays a crucial role in the Delta/Notch pathway, which is often necessary for stem cell/daughter cell fate determination. Another work in mice revealed that HGPS-model mice show decreased proliferation in hair follicle stem cells [28]. This result could indicate a similar mechanism in human HGPS patients since the early loss of hair is one of the hallmarks of HGPS. It might also indicate a connection to the loss of hair during normal ageing because it was found that expression of Progerin also occurs in normal individuals due to the sporadic use of a cryptic splice site (C1824T) that regulates the splicing outcome of the *LMNA* gene [68, 78]. This possibly establishes a direct link between the ageing-like phenotypes of HGPS and normal ageing.

HGPS model in *Drosophila*

In contrast to vertebrates, which have lamin A, C, B1 and B2*, Drosophila* only has one homologue of lamin C and one homologue of B-type lamins, termed Lamin Dm0 (*Drosophila melanogaster* 0*)*. It does not have a homologue of lamin A [37]. Interestingly, *Drosophila* encodes for another farnesylated lamina protein, Kugelkern (Kuk), termed after the embryonic phenotype of the mutant in which nuclei at the cellularization stage are round instead of elongated [13]. Kuk, similar to lamins, contains a putative coiled coil motif in its N terminus, a nuclear localization signal (NLS), and a CaaX motif in the C terminus (based on sequence prediction, Figure 3) [13]. In addition to the predicted structural similarities, Kuk also is likely to share functional similarities with Dm0, since overexpression of Kuk induces similar phenotypes as overexpression of Dm0. In this context it was also found that overexpression of Kuk and Dm0 induces ageing-like phenotypes and phenotypes typical for HGPS. Overexpression of both proteins in muscle cells induced nuclear abnormalities, reduced fitness, shortened lifespan, decreased heterochromatin and increased DNA damage [12]. These essential similarities justify the conclusion that overexpression of both Dm0 and Kuk can serve as an HGPS model

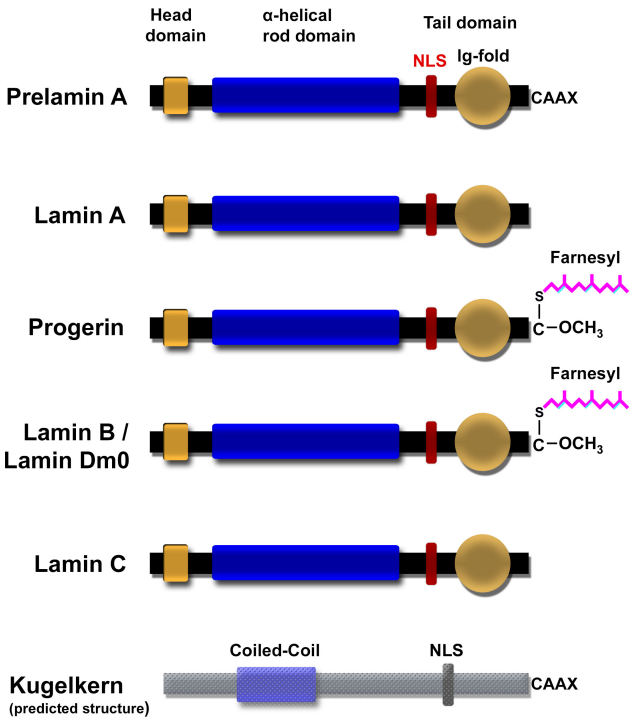

Figure 3: Lamins and Kugelkern
Scheme of *Drosophila* lamins (Lamin Dm0, Lamin C) and Kugelkern and human lamins (Prelamin A, Lamin A, Lamin B, Lamin C, Progerin). N-terminus on the left, C-terminus on the right. The structural information of displayed lamins is based on x-ray crystallography whereas the structure of Kugelkern is based on sequence prediction. The presence of a fanesyl-rest in Kugelkern was shown by western band shift and a Kuk mutant protein lacking the farnesylation site. NLS: Nuclear localization sequence. CAAX: Amino acid motif, necessary for farnesylation, with C = Cysteine, A = aliphatic amino acid, X = variable amino acid. C-OCH3: methylated C-terminus. Similar colored protein domains indicate structural (not sequential) similarity.

in flies. Interestingly ectopic expression of human lamin A and Progerin in developing and adult stages of *Drosophila* also did induce some of the effects typical for HGPS, such as nuclear deformations, reduced lifespan [70].

Dm0 function in adult flies

Dm0 plays an important role in *Drosophila* development. Several types of Dm0 null mutants have been generated. In the majority of cases only a small percentile of flies reaches the imago stage [62, 67]. Those "escapees" can not fly and walk like aged wildtype flies. This indicates that Dm0 plays an important role in neuromuscular function [62]. An additional function was found in *Drosophila* testes and ovaries, by using FLP/FRT-mediated mitotic recombination the authors generated Lam D395 mutant cyst stem cell clones and mutant follicle cells [18]. They found that Dm0 is essential in these cells to activate EGFR signaling, which is required for cyst stem cell proliferation and follicle cell function to define the AP polarity of the egg chamber [18, 63]. Another function was published in the following year by the same group. They

found that age related decline in Dm0 in fat bodies causes gut hyperplasia due to deregulated intestinal stem cell proliferation [19]. The fat body plays an important role as an immune organ, upon microbial infection it created a strong inflammatory response that helps to fend of invading microbes. However upon age related decline or knockout of Dm0 the fat body secretes peptidoglycan recognition proteins that suppress local intestinal immune deficiency signaling. Local intestinal immune deficiency signaling is known to negatively regulate excessive intestinal stem cell proliferation to maintain homeostasis [3, 17]. Therefore suppression of intestinal immune deficiency signaling by fat body secreted peptidoglycan recognition proteins causes loss of homeostasis.

Since Dm0 has an essential function in cyst stem cells of the testes, it is possible that Dm0 has similar functions in intestinal stem cells. The midgut, testes and ovaries are the only stem cell harboring organs in *Drosophila*. However, no such function has yet been reported, therefore it is plausible to test this hypothesis in this work.

1.3 Homeostasis and regeneration in the *Drosophila* midgut

Stem cells play a key role in regeneration and maintenance of tissues. They are undifferentiated cells that, depending on their hierarchy, form all other cells in a tissue, organ or organism [85]. Upon damage of a tissue, stem cells, regulated by signaling cues from the surrounding tissue, replace the damaged cells to maintain an equilibrium of newly formed and disposed cells. This process is termed homeostasis. Signaling cues are often also needed to maintain stem cells in their present number and location; in many tissues, specific cells in the vicinity of a stem cell remain in constant signaling crosstalk with it to achieve just that. Together they form a stem cell niche [82]. The decline of stem cell functionality is one of the hallmarks of the ageing process though it is often unclear whether this decline is caused by extrinsic (altered niche signaling) or intrinsic factors (decreased telomere length, increased number of mutations) [61]. Reduced regenerative capacity of tissues and organs and eventually functional failure is often cause of death in the elderly [44, 64, 75, 80, 79]. Therefore to study the ageing process and eventually ameliorate or reverse its harmful effects, proper understanding of stem cell function and regulation is necessary. However, since humans are difficult first hand research objects the use of model organisms to study stem cell behavior is a well established practice. In this work the *Drosophila* midgut is used as a model system to study stem cell regulation. This combines the powerful genetic tools of the *Drosophila* model-organism with a relatively simple system for stem cell regulation.

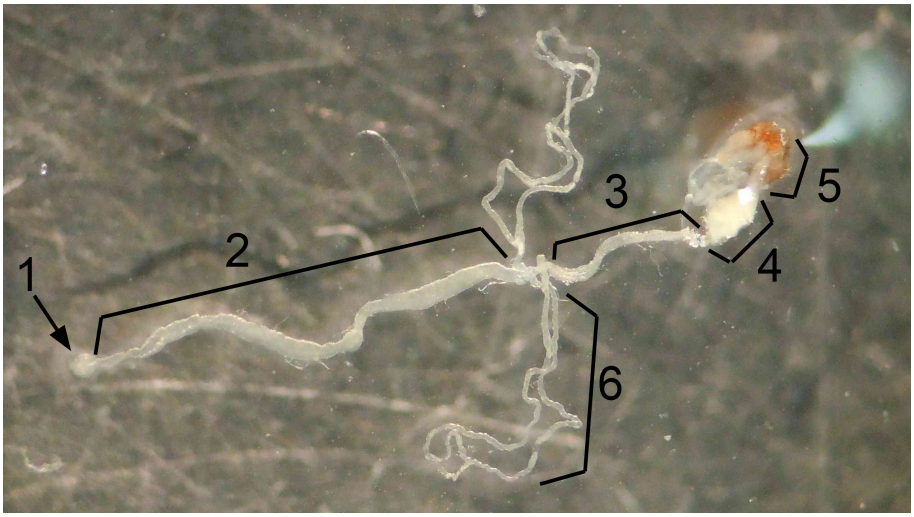

Figure 4: The *Drosophila* midgut
Dissected male gut with the following compartments: 1 proventriculus, 2 midgut, 3 hindgut, 4 rectum, 5 last abdominal segment and sexual organs, 6 malpighian tubules. (altered picture, diploma thesis, Roman Petrovsky)

The *Drosophila* midgut, a model system for stem cell behavior in vivo

The *Drosophila melanogaster* imago (adult stage) is a post-mitotic organism. Only two organ types are known to harbor stem cells in *Drosophila* imagos: the reproductive system and the midgut. This is plausible since in these systems the need for stem cell proliferation is highest; ovaries and testes constantly produce new germ cells and the midgut, due to its exposure to harmful agents in the food, needs to regenerate lost or damaged cells. The *Drosophila* midgut (Figure 4) has several advantages as a model system for stem cell behavior : It is a pseudostratified monolayered epithelium of cells without deep infoldings, simplifying imaging approaches (Figure 5 A). It is in direct contact to food, thereby giving direct access to the application of agents, altering stem cell behavior (i.e. bleomycin or *Pseudimonas entomophila*) It is a simple system to study stem cell behavior in vivo. The *Drosophila* midgut is comprised of only five cell types (Figure 5 B, 6): 1. Intestinal stem cells (ISCs) are the only cells that undergo division and thereby regenerate damaged cells [59, 65], 2. Absorptive enterocytes (ECs) are polyploid and form the majority of the gut mass, 3. Secretory enteroendocrine cells (EEs) secrete digestive enzymes [59, 65], 4. Enteroblasts (EBs) are post-mitotic progenitor cells for ECs and EEs, 5. Viceral muscle cells regulate maintenance of the stem cell pool and give stability to the gut and promote movement of the food through the intestine [51, 66].

Signaling and homeostasis in the *Drosophila* midgut

The ordered replacement of damaged cells is one of the challenges of tissues to maintain homeostasis. Therefore, a well balanced signaling system is needed to regulate the proliferation of stem cells and differentiation of progenitor cells. In the *Drosophila* midgut, a set of six signaling

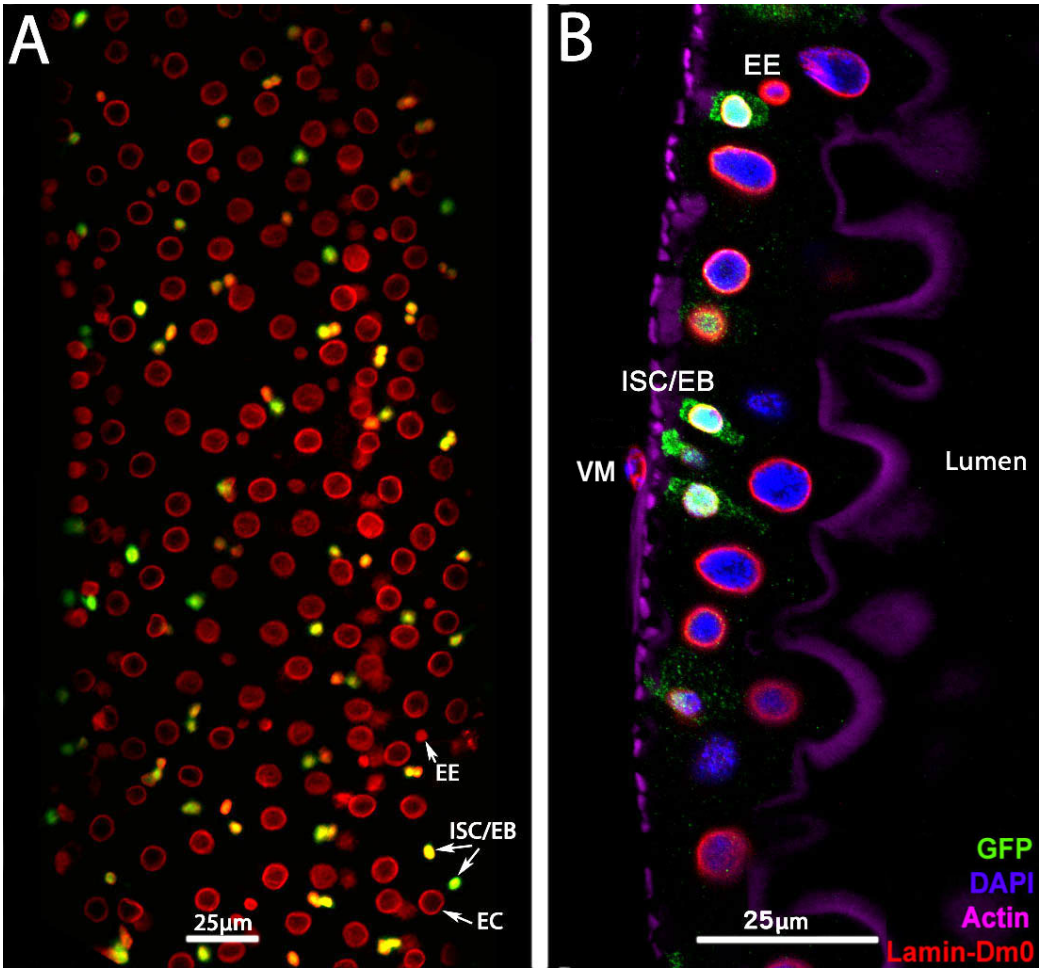

Figure 5: Cell types of the *Drosophila* midgut
(A) Onview of the *Drosophila* midgut. Immunostaining with merged channels of GFP (marking ISCs/EBs), and Lamin-Dm0. ISC/EB: intestinal stem cell/enteroblast, EE: secretory enteroendocrine cell, EC: enterocyte. (B) Sideview of the *Drosophila* midgut. Immunostaining with merged channels of GFP (marking ISCs/EBs), DAPI, Lamin-Dm0 and actin (stained by phalloidin). ISC/EB: Intestinal stem cell (ISC, precurser for EBs)/enteroblast (EB, precursor cell for EEs and ECs). Both marked by GFP. EE: Enteroendocrine cell (secretory cell). EC: Enterocyte (absorbtive cell), VM: Viceral muscle cell.

pathways is reported to regulate the proliferation of ISCs and differentiation of EBs into EEs and ECs: Upon damage the Jun N-terminal kinase (JNK) signaling pathway is activated in ECs, which leads to the secretion of cytokines (Unpaired 1, 2, 3) and mitogens (EGFs) that in turn lead to secretion of Vn and EGFs from EBs and the visceral muscle. This leads to the activation of EGFR/Ras/MAPK, JAK/STAT and Wg/Wnt signaling in the ISCs [8, 9, 16, 43]. The Hippo pathway serves as an additional stress sensor; inactivation in ISCs induces their proliferation while inactivation in ECs leads to secretion of cytokines, which in turn induce ISC proliferation [81]. However, Hippo pathway induced proliferation was found to be dependent on a basic level of JAK/STAT pathway activity [45]. All these pathways can substitute each other but silencing of all leads to a constant decline of the stem cell population. After a regenerative proliferation event the injury-induced BMP/Dpp pathway can downregulate ISC proliferation

to reach maintenance levels [40].

For long term maintenance of ISCs the visceral muscle cells secrete the signaling ligands Wingless (Wg), Unpaired (UPD) and Vein (Vn), which activate the canonical Wnt, JAK/STAT and EGFR signaling pathways respectively in ISCs in cooperation with signals from the epithelium [50, 51, 52, 89]. Additionally insulin signaling from the muscle cells induces ISC proliferation and consequently increase of the gut size, forming a mechanism to react to increased food uptake [20].

ISC and EB identity is regulated by the Delta/Notch signaling pathway. Delta and Notch are plasma membrane-localized ligands that are expressed differently in ISCs and EBs. ISCs express higher levels of Delta, which activates Notch, that is expressed in higher levels by EBs (Figure 6) [59, 65, 66]. A major target of Notch signaling in EBs are 'enhancer of split complex' target genes. ISCs are kept in an undifferentiated state by repression of the split complex through a hairless-suppressor of hairless complex [5].

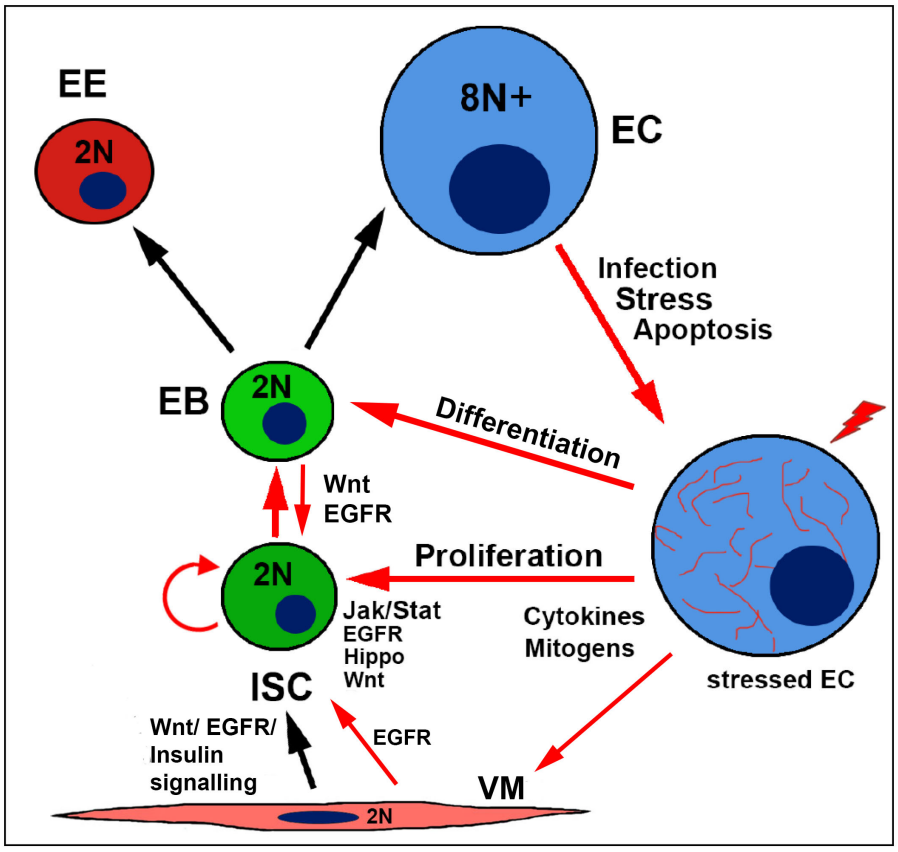

Figure 6: Mechanism of *Drosophila* midgut regeneration

Cell types and signaling pathways involved in homeostatic regulation of the *Drosophila* midgut. ISC maintenance is controlled by Wnt and EGFR signaling from the visceral muscle cells (VMs). Upon damage ECs secrete cytokines and mitogens which induce Wnt, EGFR, Hippo and JAK/STAT-signaling in ISCs, promoting their proliferation. Cytokines from ECs also induce differentiation of EBs into ECs or EEs. Additionally mitogens from ECs induce the secretion of mitogens from VMs and EBs , which induce EGFR and Wnt signaling in ISCs. Insulin signaling from the VMs induces ISC proliferation in reaction to food intake.

1.4 Aim of the work

Overexpression of Lamin Dm0 and Kugelkern in *Drosophila* leads to several cellular and organismic effects that are related to symptoms of HGPS patients or phenotypes of other animal models. One of these effects is the loss of homeostasis due to impaired stem cell function. Since decline of stem cell function also plays a key role in normal ageing the question how this effect is mediated is of high significance. In this work, the effects of Lamin Dm0 and Kugelkern were analyzed in *Drosophila* intestinal stem cells with the aim to find underlying molecular mechanisms that are causing the inhibition of stem cell function and loss of homeostasis.

2 Materials and Methods

2.1 Materials

2.1.1 Buffers and Solutions

Table 1: List of Buffers and Solutions

Agent	Ingredients
Laemmli buffer	2x 0.09 M Tris-HCl [pH 6.8], 6% SDS, 0.6% bromophenol blue, 20% Glycerol, 6% β-mercaptoethanol
10x SDS-PAGE buffer	(1L) 150 g Glycine, 10 g SDS, 32.8 g Tris base filled up with H_2O
1x transfer buffer	(1L) 14.4g Glycine , 2.03g Tris, 200ml Methanol filled up with H_2O
50x TAE buffer:	2M Tris/HCL [pH 8,5], 0.05M EDTA, 1M acetic acid filled up with H_2O
PBS	(1L) 8g NaCl 0.2g KCl, 1.15g Na_2HPO_4, 0.2g KH_2PO_4, 0.1g $MgCl_2$*$6H_2O$, 0.1g $CaCl_2$ filled up with H_2O
PBS-T 0,1%	PBS, 0.1 % Tween-20
Fixation mix	0.2% Tween-20, 0.5% Nonidet P40, 8% Formaldehyde, in PBS
EM fixation mix	2.5% Glutaraldehyde, 50 mM Natrium-Cacodylate pH 7.2, 50 mM KCl, 2.5 mM MgCl2 in H_2O
Permeabilization mix	0.5% Saponin, 0.5% Triton-X100, in PBS
Blocking solution	5% BSA in PBS-T
Mounting medium	47.5% glycerol, 47.5% PBS, 5% DABCO
Elastase solution	4 mg/ml Elastase in dissociation buffer

2.1.2 Chemicals and substances

All standard chemicals were purchased from AppliChem GmbH (Darmstadt), Invitrogen (Carlsbad, USA), Merck (Darmstadt), Roth (Karlsruhe), Sigma-Aldrich (St. Louis, USA) and Gibco BRL(Eggenstein) unless mentioned below.

- milk powder: Magermilchpulver (SUCOFIN)
- Dissociation buffer (Sigma Aldrich)
- Rifampicin (Sigma Aldrich)
- ABT100 (MedKoo)
- Aquapolymount (Polysciences, Inc.)
- 10S and 3S VoltaLef Halocarbon oil (Lehmann & Voss & Co.)

2.1.3 Enzymes

All restriction enzymes were obtained either from Thermo Scientific (St. Leon-Rot) or New England Biolabs (Ipswich, USA) unless mentioned below.

- Taq Polymerase (expressed and purified in the lab)
- Pfu DNA Polymerase (expressed and purified in the lab)
- T7 RNA Polymerase (expressed and purified in the lab)
- DnaseI (Roche)
- Elastase (Sigma Aldrich)

2.1.4 Bacteria

- *E.coli* DH5-α for molecular cloning: F-, ø80dlacZΔM15, Δ(lacZYA-argF)U169, deoR, recA1, endA1, hsdR17(rK –, mK+), phoA, supE44, λ–,thi-1, gyrA96, relA1
- *E.coli* BL21DE for protein expression: F-, dcm, ompT, hsdS(rB -mB -), gal l(DE3).
- *Pseudomonas entomophila*

2.1.5 Cell lines

- S2 (*Drosophila* genomics Research Center)
- Kc167 (*Drosophila* genomics Research Center)

2.1.6 Oligonucleotides

Table 2: Oligonucleotides used in this study

Name	Sequence	Direction	Ta °C	Description
RP1	gagagatctatggagaccc cgtcccag	sense	55	amplification of lamDelta50, introducing a BglII site
RP2	tgatcagttatctagatccgg	anti-sense	55	amplification of lamDelta50 from pYFP-lamDelta50, including a XbaI site
RP3	gccctacctcgcagcgc	sense	57	Sequencing primer for lamin Delta50 (Progerin)
RP4	cagccttcagggtgaacttt	antisense	52	Sequencing primer for lamin Delta50 (Progerin)
RP5	tgcagcgcatccgccagc	antisense	61	Sequencing primer for lamin Delta50 (Progerin)
RP12	ccgggtcgacggatccca ctcgcccagctcg	sense	52	In-Fusion primer for cloning of "Lipin b" (lipin-A-mRNA bp 2063-3743) into QE80ZZtev
RP13	gatgagatctggatccgga attaatccacttgggaggc	antisense	53	In-Fusion primer for cloning of "Lipin b" (lipin-A-mRNA bp 2063-3743) into QE80ZZtev
RP16	tttcattcatgccctccttga gg	antisense	55.9	seq primer for Lipin b QE80ZZtev antisense from bp1254
RP17	gcaaggatgagaaagatg gtgatc	sense	55.2	seq primer for Lipin b QE80ZZtev sense from bp1039
UASt 1	gttttatttttaataatttgcga gtacgca	sense	56.1	For sequencing transgenes in the MCS of the UASt vector
UASt 2	cacagaagtaaggttcctt cacaaag	anti-sense	56.1	For sequencing transgenes in the MCS of the UASt vector

2.1.7 Plasmids

Table 3: Plasmids constructed in this study

Name	Description
QE80ZZtev Lipin B	In-Fusion cloning of Lipin B (bp 1587-3267, transcript variant A) into the pQE80ZZtev vector for protein expression: In-Fusion primers (RP13/RP13) were used to obtain the Lipin B PCR product from the Ovo Ib library (created by Jörg Grosshans). The PCR product was recombined into a unique BamHI site of the pQE80ZZtev vector.
pUASt-Kuk	Kuk sequence from pMT-Kuk vector (NotI /EcoRI) inserted into pUASt vector (NotI /EcoRI)
UASp-LaminΔ15	PCR construct of LaminΔ15 (RP1/RP2) from pEYFP vector inserted into pUASt vektor (BglII/XbaI)
UASp-mCherry-Kuk	PCR construct of mCherry (RP8/RP9) from pMT-vector: SpeI site is added at the beginning of the mCherry sequence, a c/g pair is removed at the end of the sequence to prevent frameshift. GFP sequence is removed from UASp-GFP-Kuk vector (SpeI) and replaced by mCherry (SpeI)

Table 4: Plasmids provided by others

Name	Source
QE80ZZtev	provided by D. Görlich
pCS2-eGFP	Constructed by Maria Polychronidou
pCS2-HA-Kuk	Constructed by Y. Kussler-Schneider
1xGFP	provided by M. Fornerod
2xGFP	provided by M. Fornerod
5xGFP	provided by M. Fornerod
10xGFP	provided by M. Fornerod

2.1.8 Antibodies

Table 5: Antibodies used in this work

Antibody	Source	Dilution
Primary antibodies		
rabbit-α-Caspase 3	Abcam	1:500
rabbit-α-dMyc(d1-717)	Santa Cruz	1:100
rabbit-α-GFP	Torrey-Pines-Biolabs	1:3000
mouse-α-HP1 (*Drosophila* HP1)	Developmental Studies Hybridoma Bank	1:1000
mouse-α-Lamin Dm0	provided by H. Saumweber	1:1000
mouse-α-Lamin C	Developmental Studies Hybridoma Bank	1:1000
mouse-α-Prospero	Developmental Studies Hybridoma Bank	1:100
rabbit-α-Kuk	Brandt *et al.*, 2006	1:1000
guinea-pig-α-Lamin Dm0 C-terminus	provided by G. Krohne	1:250
rabbit-α-Stat92E	provided by Steven X. Hou	1:1000
mouse-α-pStat92E	provided by Xinhua Lin	1:2000
rabbit-α-PH3	Millipore-Upstate	1:4000
mouse-α-PH3	Millipore-Upstate	1:1000
rabbit-α-Tribbles	Jörg Großhans	1:500
rabbit-α-String	Glover	1:500
rabbit-α-Frühstart	Jörg Großhans	1:500
guinea-pig-α-Lipin	this work	1.1000
rat-α-Lipin	this work	1.1000
Secondary antibodies		
Alexa-coupled antibodies used for immunofluorescence		
goat-α-mouse	Invitrogen	1:500
goat-α-rabbit	Invitrogen	1:500
goat-α-guinea-pig	Invitrogen	1:500
Horseradish peroxidase coupled antibodies used for imunoblotting		
goat-α-mouse	Sigma-Aldrich	1:10.000
goat-α-rabbit	Sigma-Aldrich	1:10.000
goat-α-guinea-pig	Sigma-Aldrich	1:10.000

2.1.9 Other reagents used in immunostainings

- DAPI (4',6'-Diamino-2-phenylindole) from (Sigma-Aldrich): used for DNA staining, in a final concentration of 0,05 µg/ml
- Alexa-coupled Phalloidin (Molecular Probes): used for actin staining, in a final concentration of 6 nM

2.1.10 *Drosophila* stocks

EsgTS: $\frac{Esg{-}Gal4, tub{-}GAL80^{\mathrm{TS}}, UAS{-}nlsGFP}{CyO}$

Source: Bruce Edgar lab

Esg; TS: $\frac{Esg{-}Gal4}{CyO}$; $\frac{tub{-}GAL80^{\mathrm{TS}}, UAS{-}nlsGFP}{tub{-}GAL80^{\mathrm{TS}}, UAS{-}nlsGFP}$

Source: Bruce Edgar lab

Esg; TS (-GFP): $\frac{Esg{-}Gal4}{CyO}$; $\frac{tub{-}GAL80^{\mathrm{TS}}}{TM6b}$

Source: Bruce Edgar lab

Myo; TS: $\frac{Myo{-}Gal4}{Myo{-}Gal4}$; $\frac{tub{-}GAL80^{\mathrm{TS}}, UAS{-}nlsGFP}{TM6b}$

Source: Bruce Edgar lab

EsgTS; F/O: $\frac{Esg{-}Gal4, tub{-}Gal80TS, UAS{-}nlsGFP}{CyO}$; $\frac{act>CD2>Gal4, UAS{-}flippase}{act>CD2>Gal4, UAS{-}flippase}$

Source: Bruce Edgar lab

UAS-UPD (UPD1): $\frac{UAS{-}UPD26.2}{CyO}$

Source: Bruce Edgar lab

UASt-Dm0: $\frac{UASt{-}Lamin\ DmO}{Tm3}$

Source: EDRC (45635)

UAS-UPD; UASt-Dm0: $\frac{UAS-UPD26.2}{CyO}$; $\frac{UASt-Lamin\ DmO}{Tm3}$

Source: this work

UASt-Lamin C CaaX: $\frac{UASt-Lamin\ C\ CaaX}{Tm3}$

Source: Georg Krohne

MARCM: $\frac{hsFLP,UAS-CD8-GFP}{hsFLP,UAS-CD8-GFP}$; $\frac{tub-Gal80FRT2L}{tub-Gal80FRT2L}$; $\frac{tub-Gal4}{tub-Gal4}$

Source: Bloomington *Drosophila* Stock Center

FRT40A Lam D395/CyO: $\frac{FRT40A::LamD395}{CyO}$

Source: Yixian Zheng

UAS-FUCCI: $\frac{UASp-GFP-E2F1, UAS-mRFP1-NLS-CycB}{CyO,\ wg-lacZ}$

Source: Bloomington *Drosophila* Stock Center

UASt-Progerin: $\frac{UASt-Progerin}{Tm3}$

Source: this work

UASt-Kuk: $\frac{UASt-Kugelkern}{Tm3}$

Source: this work

2.1.11 Media

LB Medium

10g Bactotryptone, 5g Yeast extract, 10g NaCl in 1000ml ddH20

Drosophila food

20 l of H_2O were cooked for 2 h with 160 g thread agar. After 2 h, 500 g fresh baker yeast, 200 g soja bean meal and 440 g molasses were added and cooked another 2 h. After 2 h cooking

1,6 kg malt extract, 1,6 kg corn meal and 120 ml of propionic acid were added, mixed and the food was filled in vials.

Apple juice plates

100g sugar was dissolved into 1 l of organic apple juice and kept in a 60 °C water-bath. 40ml Nipagin solution (15% Nipagin in ethanol) was added to the apple juice. 70g agar was dissolved into 3 l water and to this, the apple juice mixture was added, mixed and allowed to cool down to 60 °C. The apple juice agar was poured into Petri dishes and stored at 4 °C.

ABT100, RU486 food plates

Normal *Drosophila* food was heated in the microwave until it reached a liquid state. The food was cooled down to 60 °C and the respective amount of ABT100/RU486 was added to reach the desired end concentrations. The mix was stirred, poured into agar food plates and cooled at room temperature.

2.1.12 Equipment

- Forceps
- Antibody staining tubes
- Pipettes: 0.2-2 µl, 2-20 µl, 50-200 µl, 200-1000 µl Pipetman (Gilson)
- Microliter syringe: 50 µl (HAMILTON)
- micro-scissors (Tiemann)
- Eppendorf tubes: 1.5 ml, 2 ml, 5 ml (Eppendorf)
- Falcon tubes: 15 ml, 50 ml (BD Falcon)
- PCR tubes (Brand, Wertheim)
- Fly vials (Greiner)
- Glass pipettes: 5 ml, 10 ml, 20 ml, 25 ml (Silber Brandt)
- Plastic sterile pipettes 1 ml, 5 ml, 10 ml, 25 ml (Sarstedt)
- Cover slips (Menzel)
- Glass slides (Menzel)
- Parafilm ”M” (Bewis)

- Western transfer cell: Trans-Blot SD semi-dry transfer cell (Bio-Rad)
- Pipetman: Pipetboy acu (Integra Biosciences)
- Develloper: Typ TR (Optimax)
- Developping casett
- Heater: DRI-BLOCK DB-2D (Techne)
- Centrifuges: 5415 D (Eppendorf), SS-34 (Sorvall), #3057 (Heraeus)
- Scanner: Perfection 4990 Photo (Epson)
- SDS gel electrophoresis power supply: Electrophoresis constant power supply ECPS 3000/150 (Pharmacia Fine Chemicals)
- Nitrocellulose transfer membrane: Protran (Whatman)
- medical x-ray film: Super RX, Fudji Medical X-Ray Film 100NIF 13x18 (Fujifilm)
- Scale: BP 2100 S (Satorius)
- Eppendorf Thermomixer comfort
- Fluorescence microscope: Axioplan, ZEISS Axioplan 2 (Zeiss)
- Confocal microscope: LSM 510 META (Zeiss)
- Microinjection microscope (Zeiss)

2.1.13 Kits

- MiniElute Gel extraction Kit (Qiagen)
- Plasmid Midi Kit Nucleobond AX (Macherey-Nagel)
- In-fusion HD cloning kit (Clontech)
- Arcturus PicoPure RNA Isolation Kit (Applied Biosystems, Life technologies)

2.1.14 Software

- Lyx (LyX Team)
- Microsoft excel (Microsoft)
- Microsoft word (Microsoft)
- Adobe Photoshop CS6 (Adobe)
- Adobe Illustrator CS6 (Adobe)
- Adobe Reader (Adobe)
- FIJI (NIH)
- Zen 2012 (Carl Zeiss)
- Lasergene (GATC biotech)
- Zotero (Roy Rosenzweig Center for History and New Media)

2.2 Methods

2.2.1 Molecular cloning

All methods used for molecular cloning were carried out according to Sambrook and Russel, 2001 [39], unless otherwise stated.

2.2.2 PCR

Dependent on the purpose of the PCR either Taq or Pfu DNA polymerase was used. The following agents were used: 50-1000 ng template DNA template (high concentrations needed for DNA-library), 0.5 µM forward and reverse primers, 50 µM dNTP (each), 10X PCR buffer, 1-2 units (per 50 µl of reaction) Taq or Pfu polymerase. The PCR reaction was run in a thermocycler with the following protocol:
Step 1 (Initial denaturation): 94 °C - 2 min
Step 2 (Denaturation): 94 °C - 30 sec
Step 3 (Annealing): 50-62 °C - 30 sec (depending on the annealing temperatures of the primers)
Step 4 (Elongation): 72 °C - Pfu: 2 min/1000bp Taq: 1 min/1000bp
Step 5 (Repetition of cycles) Steps 2 to 4 - 20-30 cycles
Step 6 (Final elongation) 72 °C - 10 min
Step 7 (Hold) 4 °C - ∞

2.2.3 DNA sequencing

Sequencing was either performed by the SeqLab company or by a Sequencing service provided by the Department of Developmental biochemistry.

2.2.4 Generation of transgenic flies

1. 3 µg of plasmid, containing the transgene with a 5'P and 3'P P-Element element (CaSpeR), and 1µg of Delta2-3turbo (transposase) DNA were precipitated and dissolved in H2O to a concentration of 0,1-0,5 µg/µl.

2. Embryos were dechorionated, dried in a desiccation chamber for 8-10 min and covered with halocarbon oil.

3. The prepared DNA mix was injected into the pole plasma at the posterior tip of the embryo, pior to pole cell formation.

4. The hatching larva (G0 generation) were transfered to a new food vial and the adult flies crossed with the yw line.

5. The offspring (G1) was screened for yellow to red eyes and one male selected for each grade of eye color. The male is crossed with the w; Sp/CyO; Dr/TM3, Sb double balancer line.

6. Hatching males (G2) w; + /CyO; + /TM3, Sb were recrossed with the w; Sp /CyO; Dr /TM3, Sb double balancer line to test for the chromosome of integration.

2.2.5 Western blotting

Dissected guts of the respective genotype were transferred into a 2 ml eppendorf tube, covered with Laemmli buffer and ground using a grinding stick. The mix was transferred to an 1.5 ml eppendorf tube (2 ml eppendorf vials wouldn not fit in the heating block) placed into a heater and heated at 98 °C for 4 min. Afterwards the mix was centrifuged at 10000 g for 1 min.
The following steps: SDS-page, transfer and antibody incubation were performed according to standard protocol [39]. Whatman paper and Whatman nitrocellulose transfer membrane were used for transfer. Secondary antibodys were Horseradish Peroxidase-Conjugated.

Development

Incubated with a mix of solution A and B of the GE Healthcare development kit for one minute. Put into a plastic foil and taped into a developing cassette. In the darkroom a medical x-ray film was put into the developing cassette and exposed to the membrane for 30 seconds. Then the medical x-ray film was put into the developer. Depending on the strength of the reaction

and thereby the intensity of the bands on the film a second film was exposed to the membrane either in a shorter or longer time period.

2.2.6 Induction of clones

Flipout clones were induced by keeping flies at 29 °C, 3-6 days after eclosion.

MARCM clones were induced on three consecutive days for 1 h at 37 °C, 3-6 days after eclosion.

2.2.7 RNAseq

Four phenotypes were compared in this experiment: 1. EsgTS/CyO; Dr/TM3 (control) 2. EsgTS; Dm0/(Dr/TM3) (Dm0 overexpression) 3. EsgTS/UPD; +/(Dr/TM3) (UPD expression, induction of ISC proliferation) 4. EsgTS/UPD; Dm0/(Dr/TM3) (UPD expression together with Dm0 overexpression). From each phenotype 100-150 guts were dissected and the intestinal cells dissociated by elastase treatment and agitation. The dissociated cells were transported to the FACS facility and GFP positive cells sorted directly into RNA extraction buffer. The mix was transported back to the lab, the RNA extracted and frozen. Each genotype was processed 3 times in this manor (3x 100-150 guts) on different days. In the end three samples of extracted RNA per phenotype (12 samples) were given to the „Microarray Core Facility" for analysis.

Dissociation of *Drosophila* guts

100 to 150 guts, for each genotype, were dissected and transferred to a 1.5 ml Eppendorf tube containing 400 µl of PBS. 100 µl of Elastase solution was added to reach a final concentration of 0.8 mg/ml. The guts were incubated for 1 hour at 27 °C and agitated every 15 minutes, by pipetting up and down about 40 times. Afterwards the mixture was centrifuged for 10 min at 600 g at 4 °C and the pellet resuspended in 500 µl PBS.

FACS

FACS was performed in the Scientific Flow Cytometry Facility of the University Medical Center Göttingen (UMG), affiliated with the Department of Hematology and Oncology. The dissociated gut cells were applied to a 50 µm cell-sieve, removing enterocytes and cellular debris from the solution. The remaining cells were sorted for granularity, excluding damaged or clumped cells, and the presence of GFP, specific for ISCs and EBs. The cells were sorted directly into RNA extraction buffer (PicoPure RNA isolation kit).

RNA extraction

For the following procedure all reagents used were part of the Arcturus PicoPure RNA isolation kit.
After FACS, the sorted cells, in RNA extraction buffer, were incubated in a thermomixer at 42 °C for 1 h. Then 500 µl 70% RNAse free Ethanol was added, mixed well and the solution was applied to two extraction columns in volumes of 270 µl. The columns were centrifuged 2 min at 100 g, to bind the RNA, followed by 30 s at 16000g. The flow-through was discarded, 100 µl Wash buffer 1 applied to each column followed by 1 min centrifugation at 8000 g.

Total RNA sequencing

The total RNA sequencing procedures were performed by the „Microarray Core Facility". Medizinische Fakultät Georg-August-Universität Göttingen, using the Illumina "sequencing-by-synthesis" technology.

2.2.8 Maintenance of *Drosophila* flies

Drosophila stocks were maintained at 21 °C and flipped (transfer of flies into new vials) weekly.

2.2.9 Dissection of *Drosophila* guts

The flies were anesthetized with CO_2 and beheaded. Then the beheaded flies were transferred on a glass slide with a brush and several drops of PBS-T 0.1% were added on the flies and a free part of the glass slide on the right of the flies. For dissection each fly was transferred to the PBS-T 1% covered area on the right. Then the flies were pulled with two precision forceps between the last abdominal segment and the thorax until the last segment loosens and the gut, mostly together with the malpighian tubules, comes out to about half of its length. To prevent rupture of the gut by further pulling, the thorax and the first abdominal segment were pulled apart revealing the fore-gut and sometimes also the crop. The crop, if pulled out, would be removed and the gut pulled through the abdomen by pulling of the last abdominal segment. The obtained gut consists of foregut (together with the proventriculus), midgut and hindgut (together with the last abdominal segment). The guts were transferred onto the antibody staining container (Figure 7) using a cut pipette tip preincubated with BSA to prevent sticking of the guts to the tip. The staining container, consists of the upper part of a MinElute purification column with the DNA/RNA filter part removed. A metal net was attached to the bottom by carefully pressing the cut column onto the heated metal net (on a heating block covered with aluminum foil). The contraption was finally placed into a cut cryo tube and labeled. The system was developed during the diploma thesis, Roman Petrovsky.

Figure 7: Staining container
Antibody staining container consisting of a cut MinElute purification column, melted together with a metal net and a cut cryo tube. (altered picture, diploma thesis, Roman Petrovsky)

2.2.10 Antibody staining of *Drosophila* guts

For each genotype about 10 guts were dissected and processed according to the following manual by transfering the guts, in the staining container, from one solution into the next.

- Fixation: 40 min in 0.2% Tween-20, 0.5% Nonidet P40, 8 % Formaldehyde, in PBS
- 1x quick wash in PBS-T
- Permeabilization : over night in 0.5% Saponin, 0.5% Triton-X100, in PBS
- 1x quick wash in PBS-T
- Blocking: 40 min with 5 % BSA in PBS-T
- First antibody: 2 hours or over night, antibody diluted in PBS-T
- 3x quick wash in PBS-T
- 1 hour wash in PBS-T
- Secondary antibody: 2 hours or over night, antibody diluted in PBS-T
- 3x quick wash in PBS-T
- 1 hour wash in PBS-T

2.2.11 Mounting of *Drosophila* guts

Using a BSA coated pipet tip, guts were transferred on a glass slide and arranged into two groups of five, top and bottom with the rectum facing upwards /downwards. The PBS-T was carefully removed and replaced with 20 µl of mounting medium (47,5 % glycerol, 47,5 % PBS, 5 % DABCO). A cover slip (18x18 mm) with 4 spacers of modeling clay, one on each corner, was placed over the guts and carefully pressed down making contact with the mounting medium. Controlled doses of pressure were applied onto the four corners, compressing the modeling clay spacers and equally distributing the mounting medium under the glass slide. To prevent

evaporation of mounting medium and provide stability, the borders of the cover slip were sealed by nail polish.

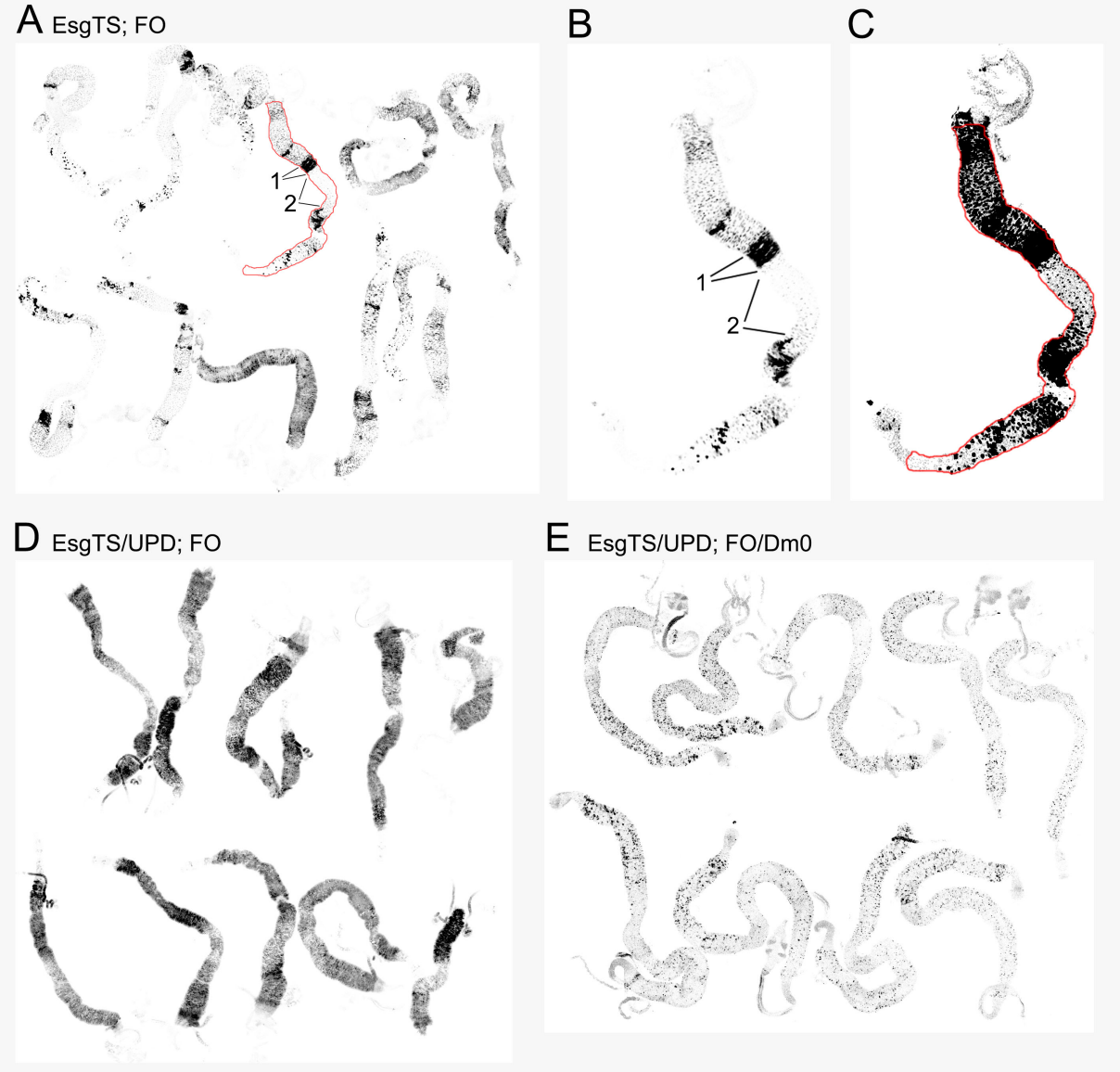

Figure 8: Quantification of midgut stem cell proliferation
All images show inversed gray values of GFP fluorescence aquired by confocal tile scans. Proliferation marked by GFP positive "flipout" clones. A: Control with patches of strong (1) and mild to no proliferation (2). B: control gut, 2 fold magnification, C: Control gut, increased gray values to visualize the structure of the gut. Red outline marks selected area quantified by mean fluorescence. D: Induced stem cell proliferation activation leads to near complete population of the gut by GFP positive cells. E: Repression of induced stem cell proliferation, little to no patches, mostly singe cells.

2.2.12 Quantification of stem cell proliferation

Stem cell proliferation was quantified by measuring the mean GFP fluorescence per gut area. Tile scans of the respective guts were acquired by confocal imaging. The area of each gut was outlined using the Fiji "freehand selection tool",(Figure 8A, B, C), and the mean fluorescence of

the selected area determined using the Fiji ”measure” function. Two phenotypes, with varying amounts of GFP+ cells, were selected to display differences in GFP mean fluorescence values (Figure 8D and E).

2.2.13 Purification and antibody generaion of Lipin B

The QE80ZZtev Lipin B construct (Table 3) was transformed into BL21. Expression was induced by 0.5 mM IPTG for 2h at 37 °C. Cells were harvested by centrifugation with 5000 rpm (Heraeus #3057) for 20 min at 4 °C and lysed by microfluidizer. The lysate was centrifuged at 15000 rpm (Sorvall SS-34) for 15 min and the Supernatant loaded on a His-trap column. Elution fractions 2-4 were pooled and loaded on a PD-10 desalting column. Desalting fractions 1, 2 and 3 were pooled (2.8 mg/ml protein concentration) and send to ”Charles River” for generation of antibodies. The received serum was successfully tested for specificity in Flipout clones expressing *Lipin* RNAi (Figure44B). During the purification samples from all significant steps were taken (Figure 9).

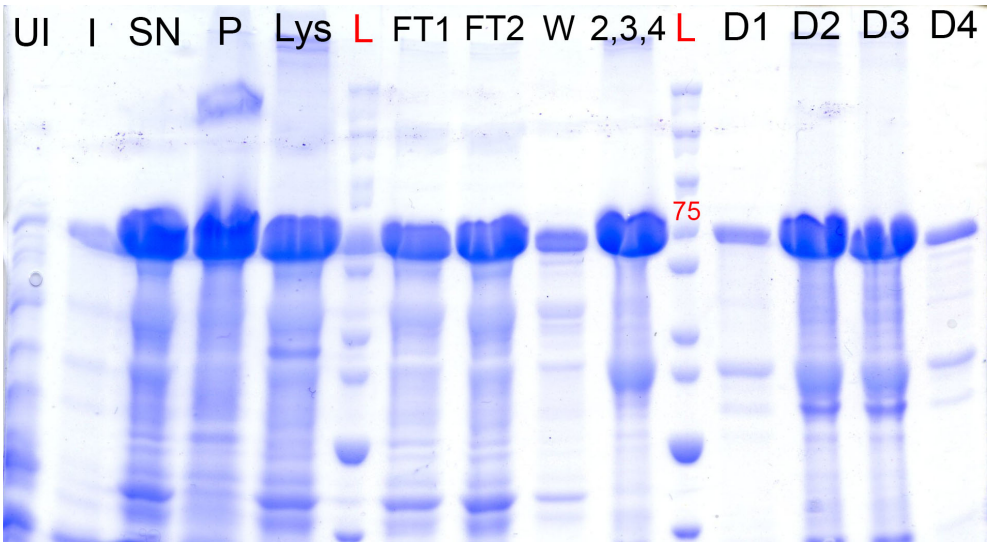

Figure 9: Lipin B purification
Scanned SDS-gel of purification samples. Thick band at about 75 kDa marks the expressed Lipin construct. UI: Uninduced, I: Induced, SN:Supernatant, P: Pellet, Lys: Lysate, FT1/FT2: Flowthrough W: Wash L: Ladder, (2,3,4): pooled elution fractions, (D1, D2, D3, D4): Desalting fractions

2.2.14 *Pseudomonas entomophila* infection

100 ml LB-medium + 100 µl Rifampicin were inoculated with *Pseudomonas entomophila* (P.e.) bacteria and incubated at 30 °C, over night. The culture was centrifuged at 3466 g for 15 min and the pellet resuspended in 5 ml PBS + 5 % Sucrose. A small empty fly vial was filled with a 1 cm layer of small LB-Agar crumbs and about 1,5 ml of P.e./Sucrose solution was pipetted onto the LB-agar layer, completely covering the Agar pieces. Subsequently a portion

of the solution was removed, the remaining solution covering only lower levels of the agar layer but still being accessible to the flies. The upper level of the agar layer was thereby forming a platform for flies to stand and drink the P.e./Sucrose solution, whilst still being covered by a layer of P.e., depriving the flies access to a P.e. free source of liquid. A piece of filter paper also inserted into the vial and attached above the agar layer, without making contact, forming a platform for flies to rest and clean. To facilitate proper uptake of the solution the flies were kept without food and water for 16 hours, before being transferred to the prepared vial.

2.2.15 ABT100 treatment

ABT100 was added directly to the cell medium in varying concentrations. Cells were grown on cover slips and treated with ABT100 for 3 days. ABT100 was added to preheated fly food in varying concentrations and for different timescales.

2.2.16 Lifespan

Three times 100 flies per genotype (each in a separate small fly cage) were kept in a separate incubator. Food plates contained either normal fly food or fly food with ABT100, Ru486 or both. The plates were changed every second day, during the change number of dead flies on the old plates was noted.

2.2.17 Electron microscopy

To fixate the gut in its natural environment the abdomen of the fly was cut off of the thorax by use of a micro-scissor and carefully torn on several places to give better access to the fixation solution. About 8 abdomen were processed in this manner and collected in a 1.5 ml Eppendorf tube, filled with PBS. The PBS was removed and replaced by fixation solution. The Eppendorf tube was sealed with parafilm and send to our collaborator, Prof. Georg Krohne, on the same day.
Subsequent steps were performed by Prof. Georg Krohne, Universität Würzburg, Division of Electron Microscopy.

3 Results

3.1 Lamin Dm0

3.1.1 Role of Dm0 in stem cell signaling

HGPS is a gain-of-function disease caused by the overexpression of a permanently farnesylated form of Lamin A. As mentioned in section 1.2, among the symptoms of HGPS are a drastically reduced life span and reduced physical fitness. On a cellular level nuclei of HGPS patients show nuclear deformations, increased DNA damage and reduced heterochromatin. The Großhans lab has established a model of HGPS in *Drosophila* fruit flies. By overexpression of the permanently farnesylated Lamin Dm0 all of the above mentioned symptoms of HGPS can be observed in *Drosophila.* Overexpression of Dm0 in *Drosophila* midguts reduced the proliferation of ISCs (Henrick Steffen, bachelor thesis). This result falls into line with the work of other groups, claiming an involvement of impaired stem cell function in HGPS and ageing [28, 78].

Lamina protein dynamics in the *Drosophila* midgut

The lamina proteins Dm0, Lamin C and Kugelkern show a distinct dynamics in the *Drosophila* midgut. In smaller cell types (ISCs, EBs, EEs) Lamin Dm0 and Kuk show a stronger staining in comparison to big cell types (ECs). In contrast, lamin C shows weaker staining in small cell types compared to ECs. Other nucleoplasmic/chromatin bound proteins, like HP1 or nuclear pore proteins have similar levels in small and big cell types (Figure 10). This difference could indicate a functional difference in case of Lamin C compared to Dm0/Kuk or redundancy, in case of Dm0 and Kuk. Since Kuk staining in wildtype flies did show localization at the nuclear envelope and inside the nucleus at a distinct area, Kuk staining was repeated with a Kuk deficiency line (pictures right of wildtype Kuk pictures). In the deficiency line the staining at the nuclear envelope was lost while the staining inside the nucleus remained, proving this type of staining to be unspecific.

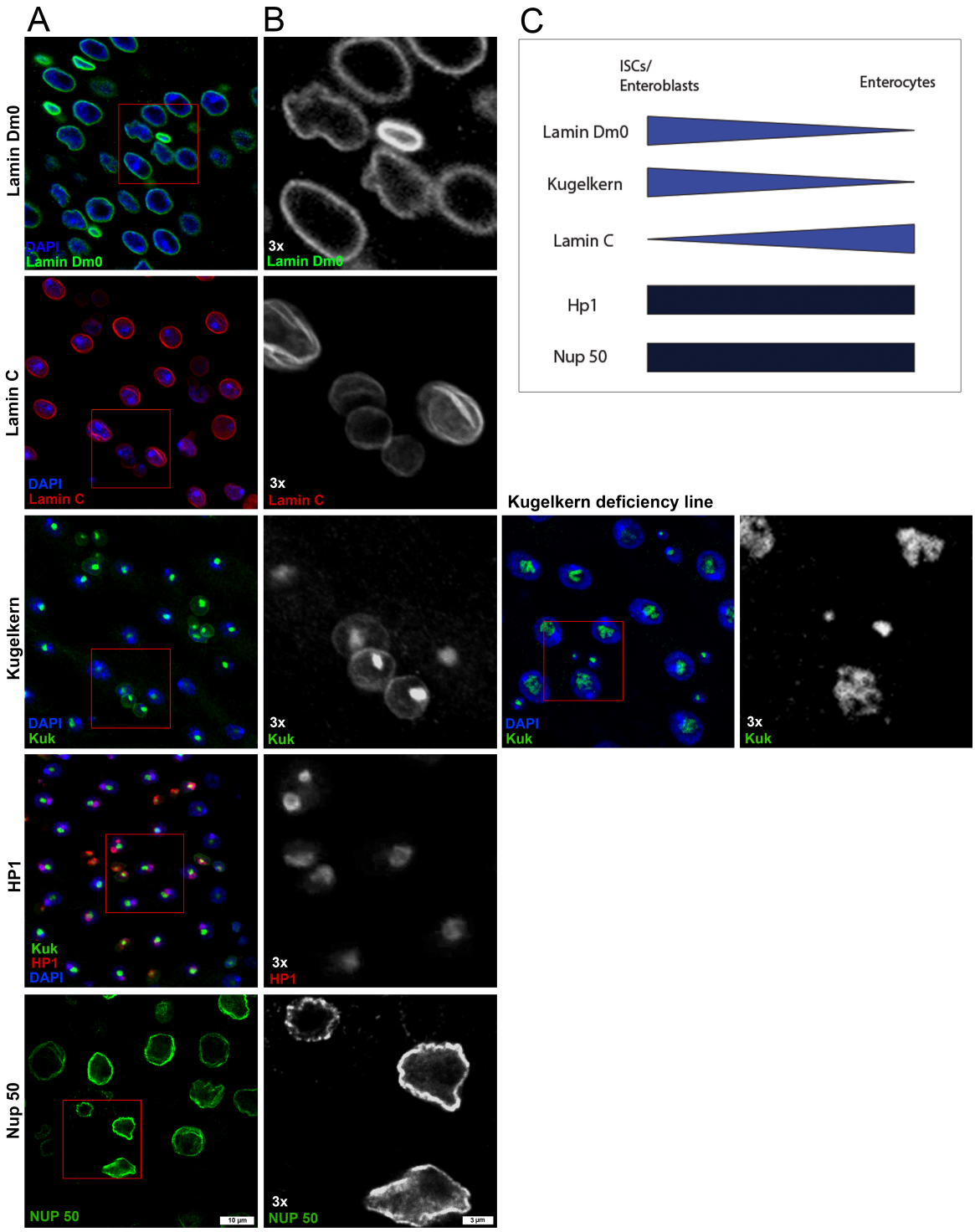

Figure 10: Dynamics of selected Lamina proteins
A: Overlay of DAPI and a respective lamina protein. Red box marks magnified selection. B: Magnified selection of the respective lamina protein from A C: Schematic of the dynamics of the respective lamina protein, comparing protein levels in ISC/EBs and ECs. Kugelkern staining shows localization at the nuclear envelope and at a distinct area inside the nucleus. Kuk staining in the Kuk deficiency line (pictures on the right of Kuk wildtype stainings) shows that this is unspecific staining of the Kuk antibody.

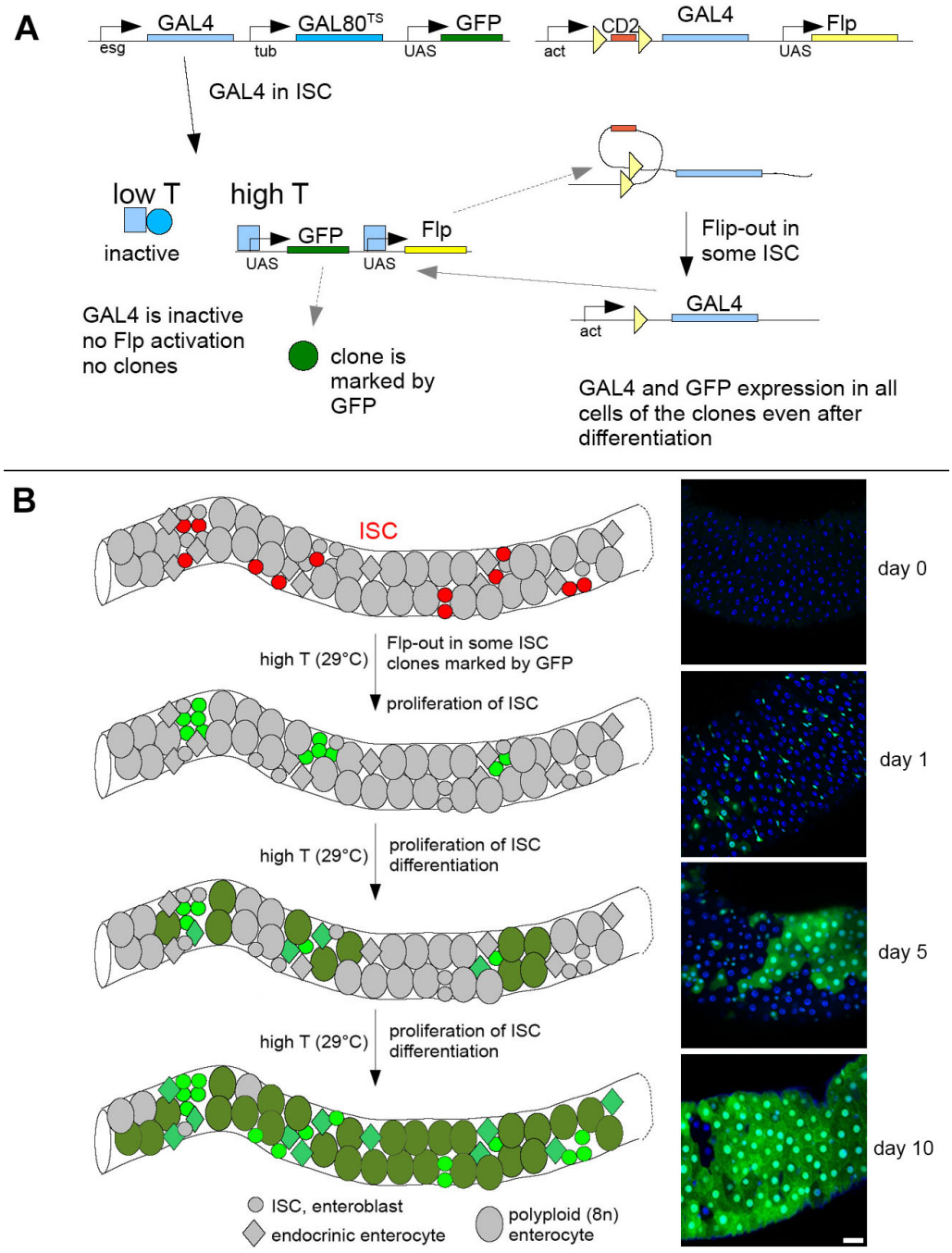

Figure 11: Flipout clonal system

A: Schematic depiction of the genetic mechanism used for "flipout clones". Gal4 is expressed under the control of the ISC/EB specific Esg promoter and is repressed by Gal80TS, under the control of the tubulin promoter. At 29 °C (high T) Gal80TS is denatured, Gal4 binds to UAS and induces expression of GFP and flippase. Flippase induces recombinatory flip-out of CD2 thereby putting a second Gal4 allele under the control of the actin promotor. All daughter cells of the ISC with this recombination event will continue to express Gal4 and thereby GFP. B: Scheme of flipout-clone induction with confocal images respective to the depicted state of induction, right. After clonal induction, by shifting flies to 29 °C, only ISCs/EBs are marked by GFP. With longer time at 29 °C also their daughter cells are marked with GFP and form clones. Altered scheme, initially created by Jörg Großhans. Scale bar: 25 µm

Overexpression of Lamin Dm0 has an inhibitory effect on native ISC proliferation

To study the effects of overexpressed Lamina proteins on intestinal stem cell proliferation, the flipout clonal system [43] was used as a tool to visualize stem cell proliferation over time (Figure 11 A and B). By shifting the flies to 29 °C the temperature-sensitive protein Gal80TS, which binds and represses Gal4, changes conformation and loses its repressive function. Gal4 is under the control of the Escargot promoter (Esg), which is specific for ISCs and EBs.
Due to the inhibition of Gal80TS by tempereture shift to 29 °C, Gal4 can bind to Upstream Activating Sequences (UAS) which induce expression of GFP and flippase. The expressed flippase induces recombinatory flip-out of CD2, a gene introduced as a block between the actin promoter and a second Gal4 transgene. With the absence of CD2 and its stop codon, Gal4 is now additionally expressed under the control of the actin promoter. This marks the time-point of clonal induction as henceforth not only ISCs and EBs express GFP but also their progeny. The flip-out system, as described here, is shortened by the term "EsgTS; FO" where the Escargot-promoter and the temperature-dependent elements, located on the second chromosome, are termed "EsgTS" and the clone-inducing elements on the third chromosome "FO", for flip-out. In addition to GFP, other UAS transgenes can be crossed into the EsgTS; FO background and will be expressed in the clonal cells. The size of the clonal area can be controlled by the time the flies are kept on 29 °C (Figure 11 B).
The *Drosophila* midgut has a natural turnover of about 12 days in females and about 3 weeks in males [43]. The native proliferative behavior of *Drosophila* midguts varies strongly in individual flies. Sex, age and quality of food play a decisive role. However, after excluding these factors a distinctive variability remains.
To reproduce and quantify previous results, flip-out clones with and without Dm0 overexpression, were induced in *Drosophila* midgut for five days. ISCs in flies expressing Dm0 showed a strong reduction in clonal area (Figure 12 B) compared to control flies (Figure 12 A). Quantification of mean fluorescence intensity of GFP per gut, indicating the amount of proliferation (described in subsection 2.2.12) shows a significant reduction in guts overexpressing Dm0 (Figure 12 C). The level of Dm0 expression was tested by expression in ECs using the EC-specific Myo promoter to drive Gal4 (Figure 13). Dm0 levels are already significantly increased after one day of expression,compared to wildtype, and continue to be so after 3 days of expression.
It can be concluded that Dm0 expression was successfully induced in flipout-clones and lead to a drastic decline in ISC proliferation.

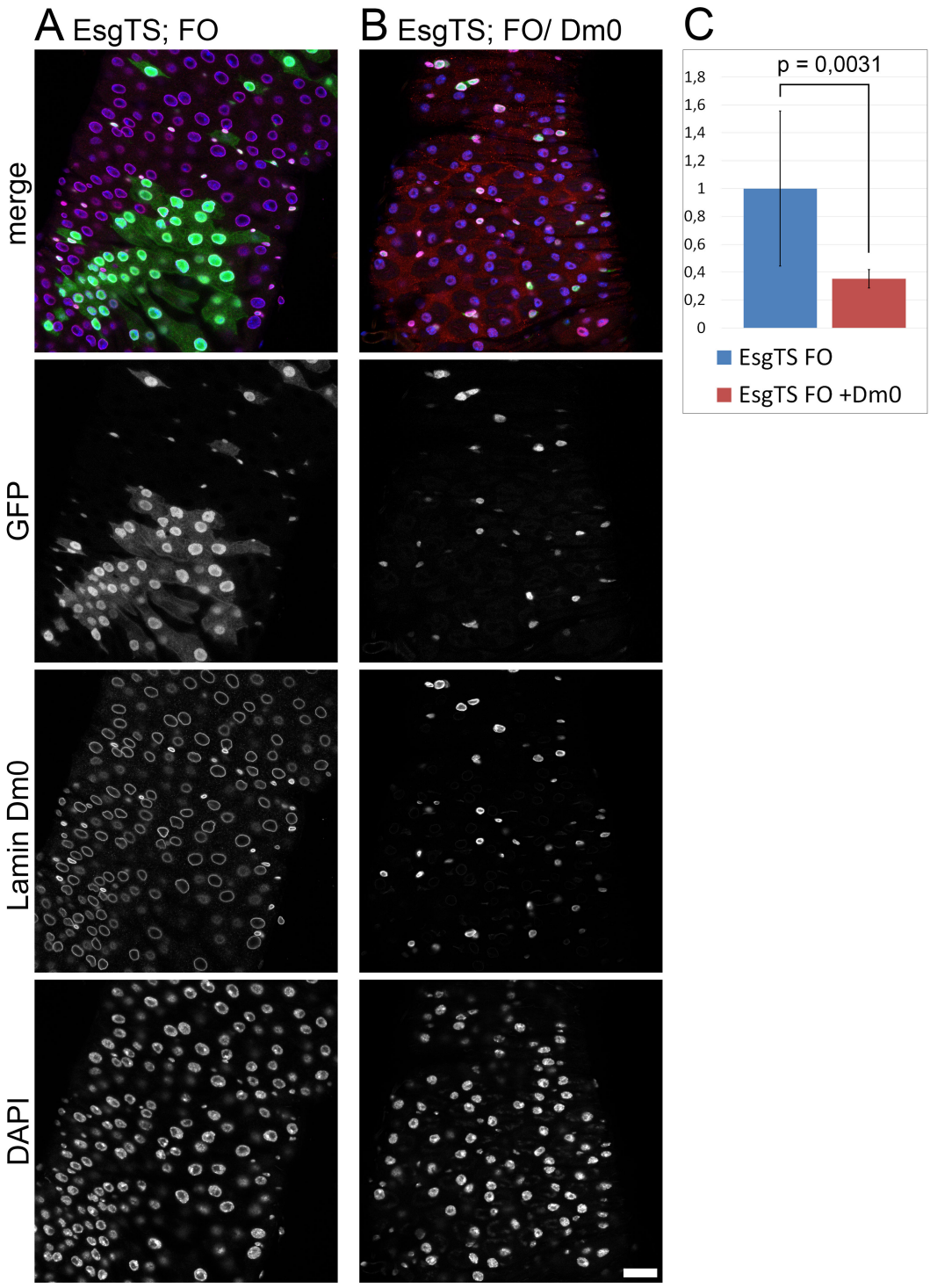

Figure 12: Dm0 suppresses native proliferation

A: (EsgTS/(Sp/CyO); FO/(Dr/TM3)) Control with about 40 % clonal gut epithelium on average. B: (EsgTS/(Sp/CyO); FO/UASt-Lamin Dm0) Lamin Dm0 overexpression leads to a strong reduction of stem cell proliferation. Due to the strong increase of Dm0 staining in Dm0 overexpressing cells other cells are not visible in the Dm0 channel. C: Quantification of stem cell proliferation by mean fluorescence/gut, normalized to control. Clonal induction for 5 days. Scale bar: 25 µm

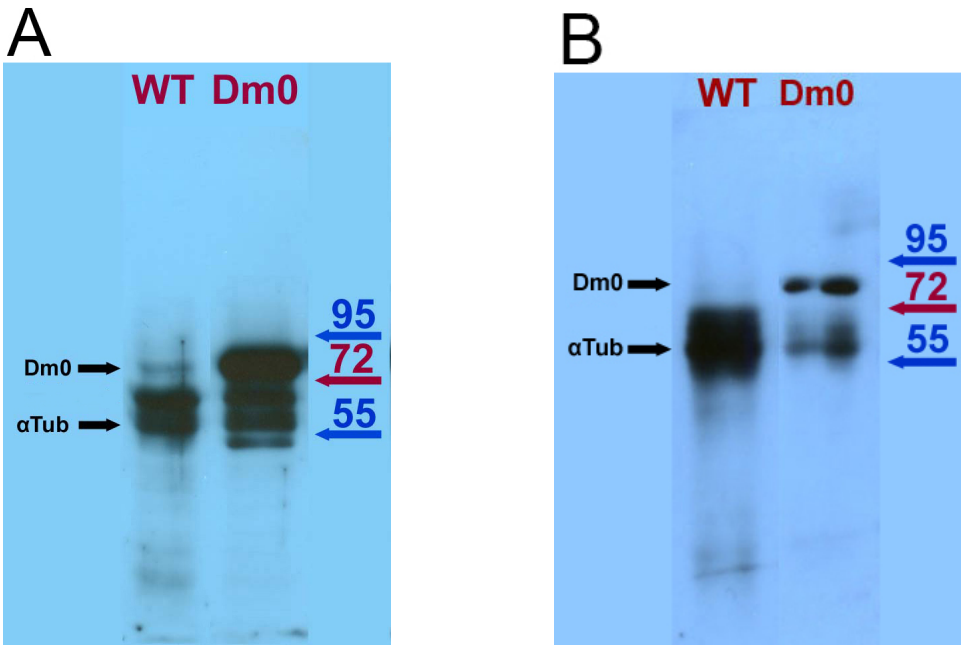

Figure 13: Western blot of 1 and 3 day induced myo-Gal^{TS} x UAS-Lamin DmO and OrigonR(wildtype) with Dm0 and α-tubulin costaining
A: 1 day of induction. In the Lamin Dm0 trace a strong additional band can be seen at about (76 KDa), in comparison to the wildtype (OrR). Another band is in the range of α-tubulin (50 kDa).
B: 3 days of induction. In the Lamin Dm0 trace a clear additional band can be seen at about (76 KDa) and a band in the range of α-tubulin. The WT trace shows no band in the range of Lamin Dm0 and a strong band in the range of α-tubulin in an area of indistinct staining. (diploma thesis, Roman Petrovsky)

Lamin Dm0 overexpression does not induce apptosis

To test whether the lack of stem cell proliferation in Dm0 overexpressing guts was due to induced apoptosis in stem cells, control (Figure 14 A) and Dm0 overexpressing (Figure 14 B) guts were stained with Caspase-3 antibody. The Caspase-3 antibody provided was later reported to stain the active form and the inactive procaspase (zymogen) form. The staining proved to be variable in small and big cell types. In both genotypes small cells with (Figure 14-2) and without (Figure 14-1) measurable Caspase levels were present and Caspase levels had not changed. To test whether the antibody shows a stronger affinity to the active Caspase form, Maria Kriebel, a PhD student of the Grosshans lab, tested the antibody in wing-imaginal disks (Figure 14 C and D). In comparison to the control (Figure 14 C), induced apoptosis by expression of the Reaper protein (Figure 14 D) proved to significantly increase levels of Caspase 3 staining, compared to the control. Additionally a western blot, provided by the supplier (Abcam), with the human active form in Lane 1 and the inactive procaspase form in Lane 2 clearly shows a stronger affinity of the antibody to the active form. Changes in the size of cells and stained areas are due to natural fluctuations in gut composition, in Caspase low level background activity and possibly in background activity of the antibody. So it can be argued, that since Caspase-3 staining of intestinal cells elicits no change in Caspase-3 levels, no

significant alteration of Caspase function was induced by Lamin Dm0.

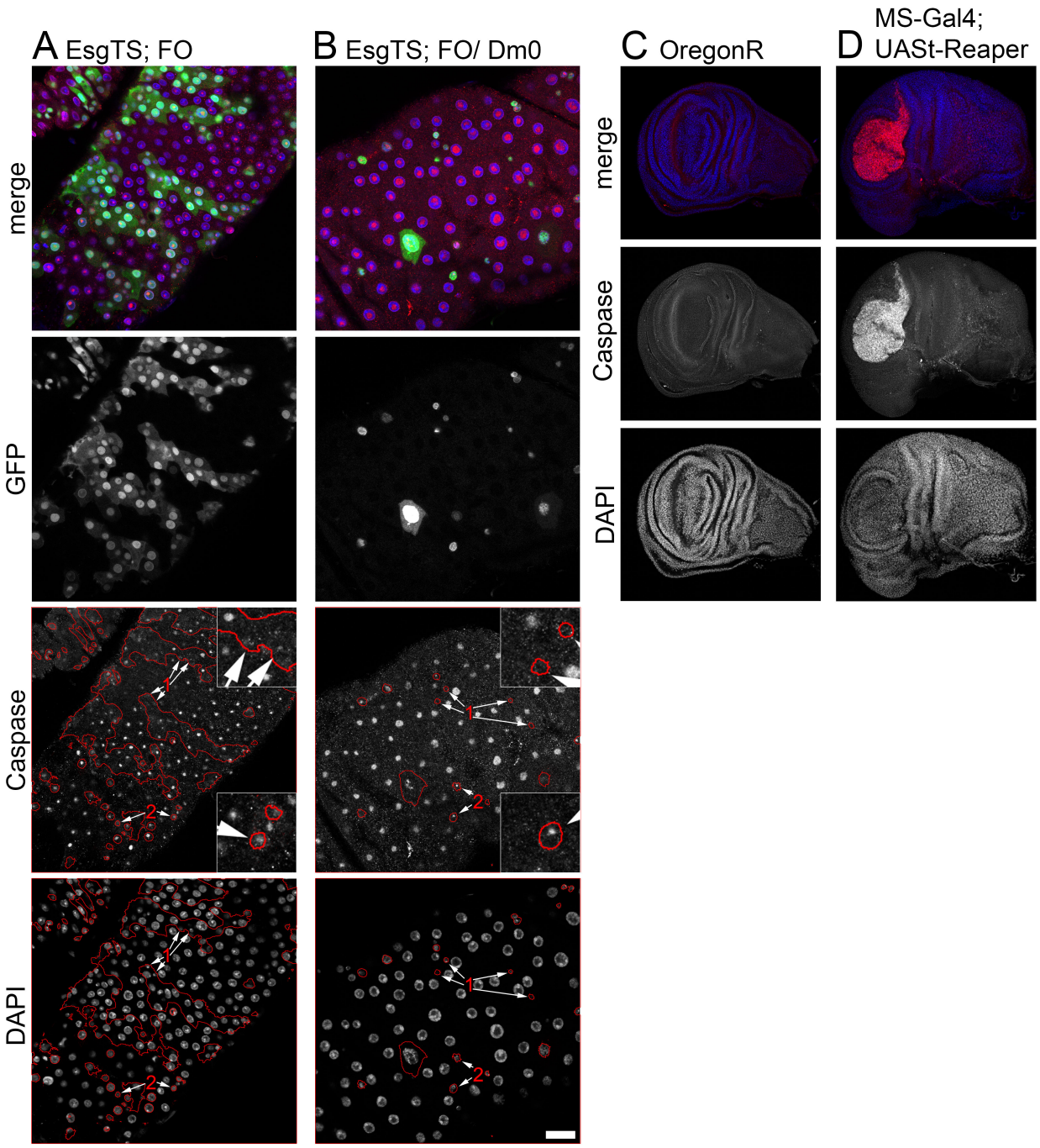

Figure 14: Caspase levels are not altered by Lamin Dm0 overexpression

A: (EsgTS/(Sp/CyO); FO/(Dr/TM3)) Control, (1) marks small cells with no Caspase staining, (2) marks small cells with Caspase staining. B: (EsgTS/(Sp/CyO); FO/UASt-Lamin Dm0) Dm0 overexpression with similar Caspase distributions as control. (1) marks small cells with no Caspase staining, (2) marks small cells with Caspase staining. 3x enlarged detail of gut-cells in the top (for 1) and bottom right (for 2) of Caspasauthore channel pictures. C: Oregon R (control) staining of Caspase 3 antibody in wing imaginal disk (courtesy: Maria Kriebel). D: (MS1096-Gal4; UASt-Reaper) Levels of Caspase 3 staining clearly increase in areas of induced apoptosis in wing imaginal disks. (courtesy: Maria Kriebel). Clonal induction for 5 days. Scale bar: 25µm

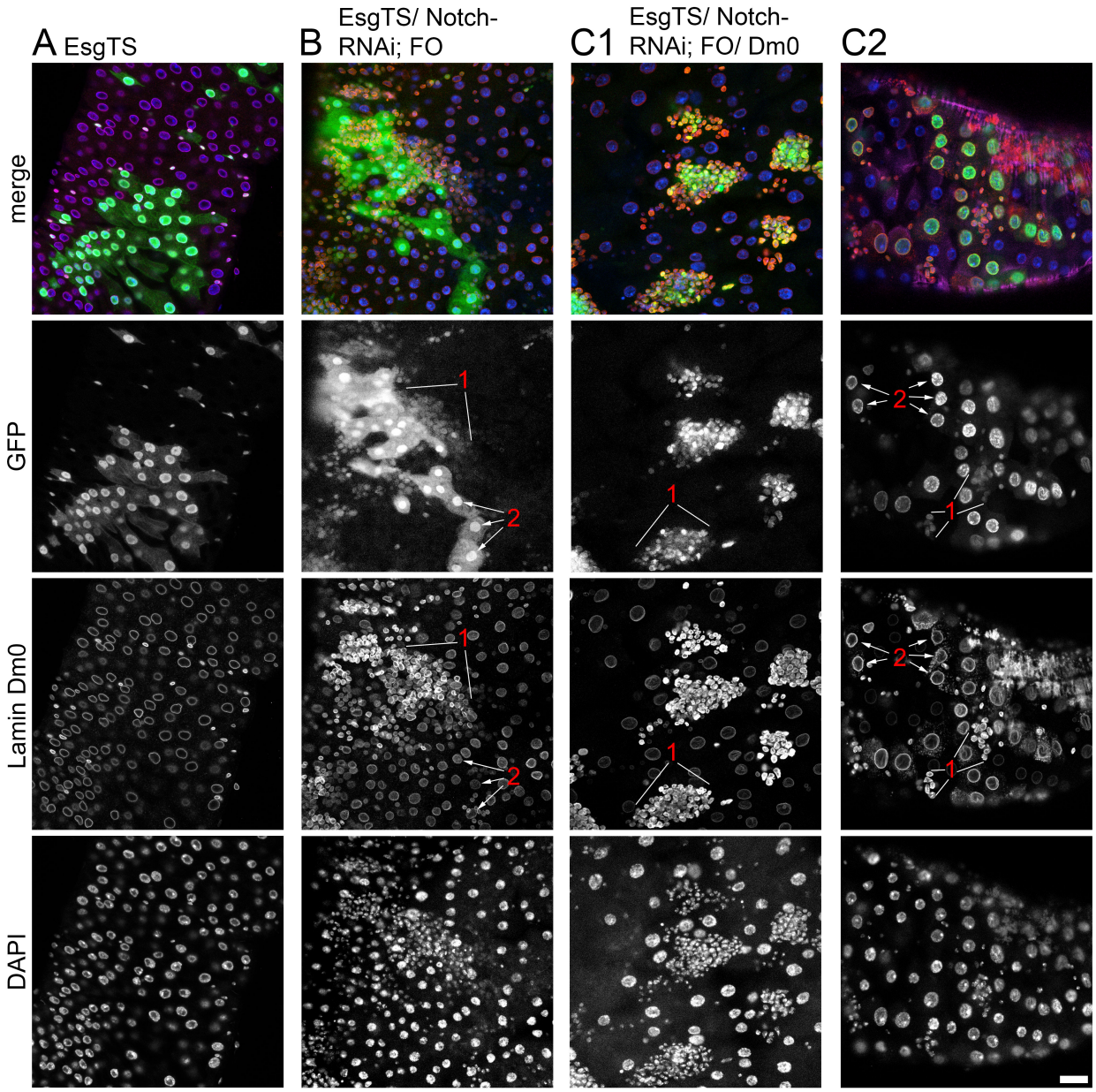

Figure 15: *Notch* RNAi overrules inhibition of stem cell proliferation, induced by Lamin Dm0
A: (EsgTS/(Sp/CyO); FO/(Dr/TM3)) Control, B: (EsgTS/*Notch*-RNAi; FO/(Dr/TM3)) Expression of *Notch* RNAi induces strong proliferation of ISCs. Dm0 and DAPI staining shows a dense population of small cell types. C: (EsgTS/*Notch*-RNAi; FO/UASt-Lamin Dm0) Overexpression of Lamin Dm0 together with *Notch* RNAi does not inhibit stem cell proliferation (C1/C2, 1) or EB differentiation (C2, 2). Clonal induction for 5 days. Scale bar: 25µm

Expression of *Notch* RNAi can overrule the inhibitory effect of Lamin Dm0

To investigate whether overexpressed Lamin Dm0 permanently inhibits stem cell function, several ways of inducing proliferation were tested in the Lamin Dm0 overexpression background. Two ways proved to be successful: the expression of *Delta* RNAi and *Notch* RNAi. Both are

known to induce strong overproliferation in ISCs leading to condensed local accumulations of small cell types, often referred to as Notch-tumors. The Delta/Notch signaling pathway controls the identity of ISCs and EBs. Furthermore, it regulates the replenishment of EBs in case of damage or depletion. ISCs and EBs are known to stay in proximity to each other forming ISC/EB pairs, with ISCs retainig higher Delta levels, and EB retaining higher Notch levels. If the ISC senses a reduction of Delta/Notch signaling from its EB partner it will start to proliferate to replenish the EB until Delta/Notch signaling is reestablished [65, 66]. So if Delta or Notch are knocked down in ISCs a loss of its EB partner is simulated, inducing continuous ISC proliferation. This proliferation is known to be mediated by autocrine EGFR signaling in the initial stage of the tumor and it is further increased when the proliferating ISCs push ECs out of the epithelium and induce their apoptosis. ECs then secrete cytokines which induce JAK/STAT signaling in ISCs increasing their proliferation [71]. By expressing *Notch* RNAi in flip-out clones the described effect was reproduced (Figure 15 B). DAPI and Lamin Dm0 channels show a dense accumulation of small cell types (Figure 15 B1). However clones also were comprised of differentiated ECs (Figure 15 B, 2). By overexpressing Lamin Dm0 in the background of *Notch* RNAi induced proliferation, a mild reduction of proliferation was observed (Figure 15 C1 and C2). Guts still harbour pockets of intense local proliferation (Figure 15 C1/C2, 1) but also show differentiated ECs (Figure 15 C2, 2); so the ability of enteroblasts to differentiate was not altered by Dm0 overexpression. The reduction in proliferation could possible result from inhibition JAK/STAT signaling since initial proliferation of ISCs in Notch-tumors requires autocrine EGFR signaling and the occurrence of tumors was not noticeable reduced but rather their size. However quantification of this effect is difficult since tumors of a certain size would naturally merge and thereby render indistinguishable. Since wildtype Notch-tumors are bigger they would more often form islands of GFP positive cells likely formed of several initial Notch-tumors.
The results indicate that Dm0 expression does not permanently harm ISCs or inhibit their proliferative function. Nor does Dm0 permanently inhibit differentiation.

Tested signaling pathways

As ISC proliferation is dependent on a set of signaling pathways [48, 43, 81, 89] it is conceivable that Dm0 might elicit its repressive effect on ISC proliferation by negatively affecting signaling pathway components. Activating each signaling pathway and coexpressing the activator with Dm0 could reveal which pathway would be affected by Dm0 overexpression. Several known activators of ISC proliferation were expressed in flip-out clones and their potential to induce ISC proliferation was assessed (Figure 16). The expression of a constitutively active form of Hopscotch (Hop^{Tuml}) or UPD (both activators of the JAK/STAT signaling pathway) and induction of *Warts* RNAi (activating the Hippo pathway) showed a significant increase in ISC proliferation and will be addressed in following chapters.

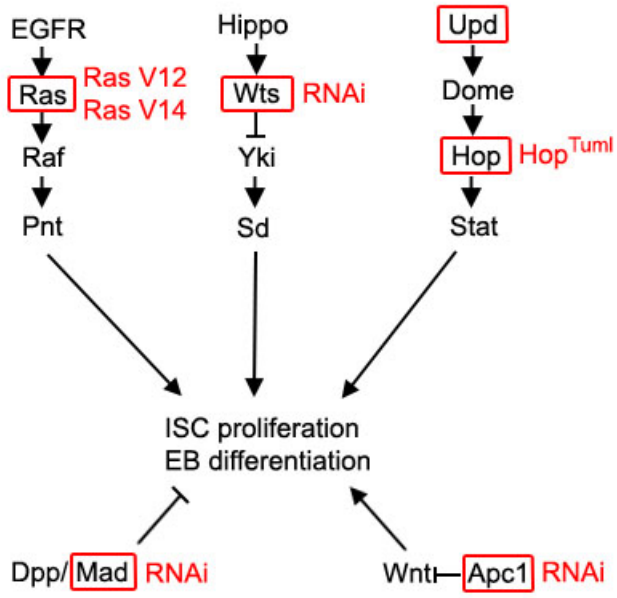

Figure 16: Tested activators of signaling pathways involved in ISC proliferation
Scheme lists known signaling pathways involved in ISC proliferation and highlights pathway activators (red box and text) that were tested in flipout clones. Tested pathways (simplified) from left to right: EGF/EGFR, Hippo, Jak/Stat, Dpp (BMP), Wnt (canonical).

Induction of *Mad* RNAi (leading to downregulation of the BMP pathway that inhibits ISC proliferation) and *APC1* RNAi (activating Wnt signaling) did not result in a significant increase in ISC proliferation (Figure 16, Figure 17 B and C). Therefore, since activation of the DPP and Wnt pathway was unsuccessful, a potential effect of Dm0 on these pathways could not be tested. However since all mentioned pathways are reported to drive native ISC proliferation it can be argued that Dm0 is at least able to inhibit Dpp and Wnt-induced proliferation in an unchallenged situation (Figure 12). Expression of Hop^{Tuml} lead to a significant increase in ISC proliferation (Figure 17 D) but could not be utilized to test for the inhibitory effect of Dm0 because a fly stock with Hop^{Tuml} and Lamin Dm0 transgenes was lethal at the larval stage.

Lamin Dm0 inhibits *Warts* RNAi induced stem cell proliferation

Warts RNAi was induced in flip-out clones without and with Dm0 coexpression (Figure 18 B/C). *Warts* RNAi alone lead to a significant increase in proliferation (Figure 18 B) and increase in small cell types (Figure 18 B, 1). However, the effect was not as strong as UPD-induced proliferation (shown later). Co-induction of *Warts* RNAi with Dm0 lead to a drastic decrease of clonal ISC proliferation (Figure 18 C). Quantification shows that *Warts* RNAi induced increase in proliferation and its suppression by Dm0 coexpression is significant. (Figure 18 D).

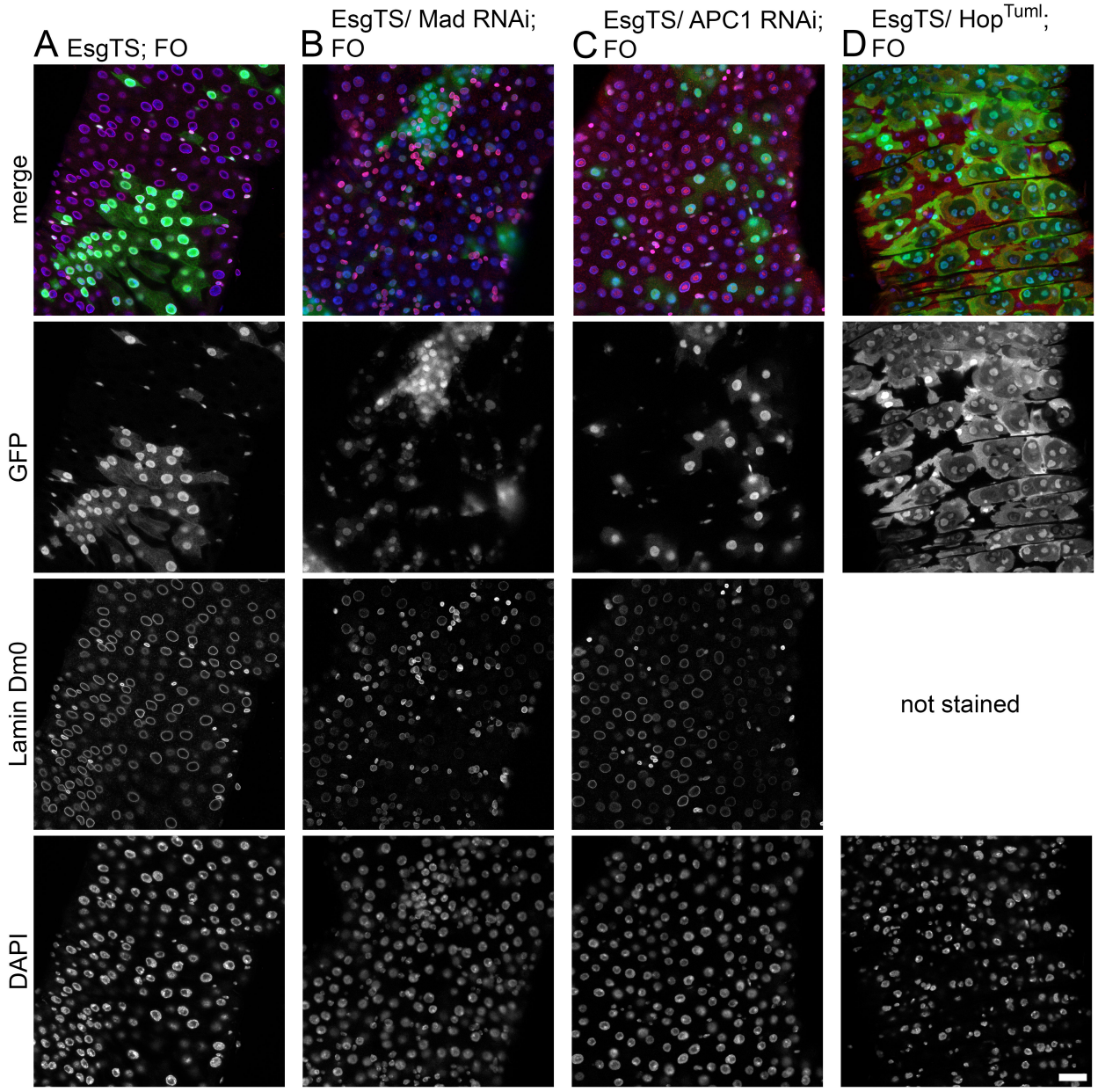

Figure 17: Tested signaling pathway activators
A: (EsgTS/(Sp/CyO); FO/(Dr/TM3)) Control, B: (EsgTS/*Mad*-RNAi; FO/+) No significant increase in proliferation compared to control. C: (EsgTS/*APC1*-RNAi; FO/+). No significant increase in proliferation compared to control. D: (EsgTS/Hop$^{\text{Tuml}}$; FO/+). Significant increase in proliferation after 4 days of proliferation compared to control. Clonal induction for 5 days for A, B, C. Scale bar: 25µm

Lamin Dm0 inhibits UPD-induced stem cell proliferation

Expression of UPD in flipout clones lead to a strong over-proliferation event with nearly complete coverage of gut area by clonal cells within 5 days (Figure 19 B). Dm0 and DAPI staining also shows an increased number of small cell types (Figure 19 B, 1) and higher cellular density.

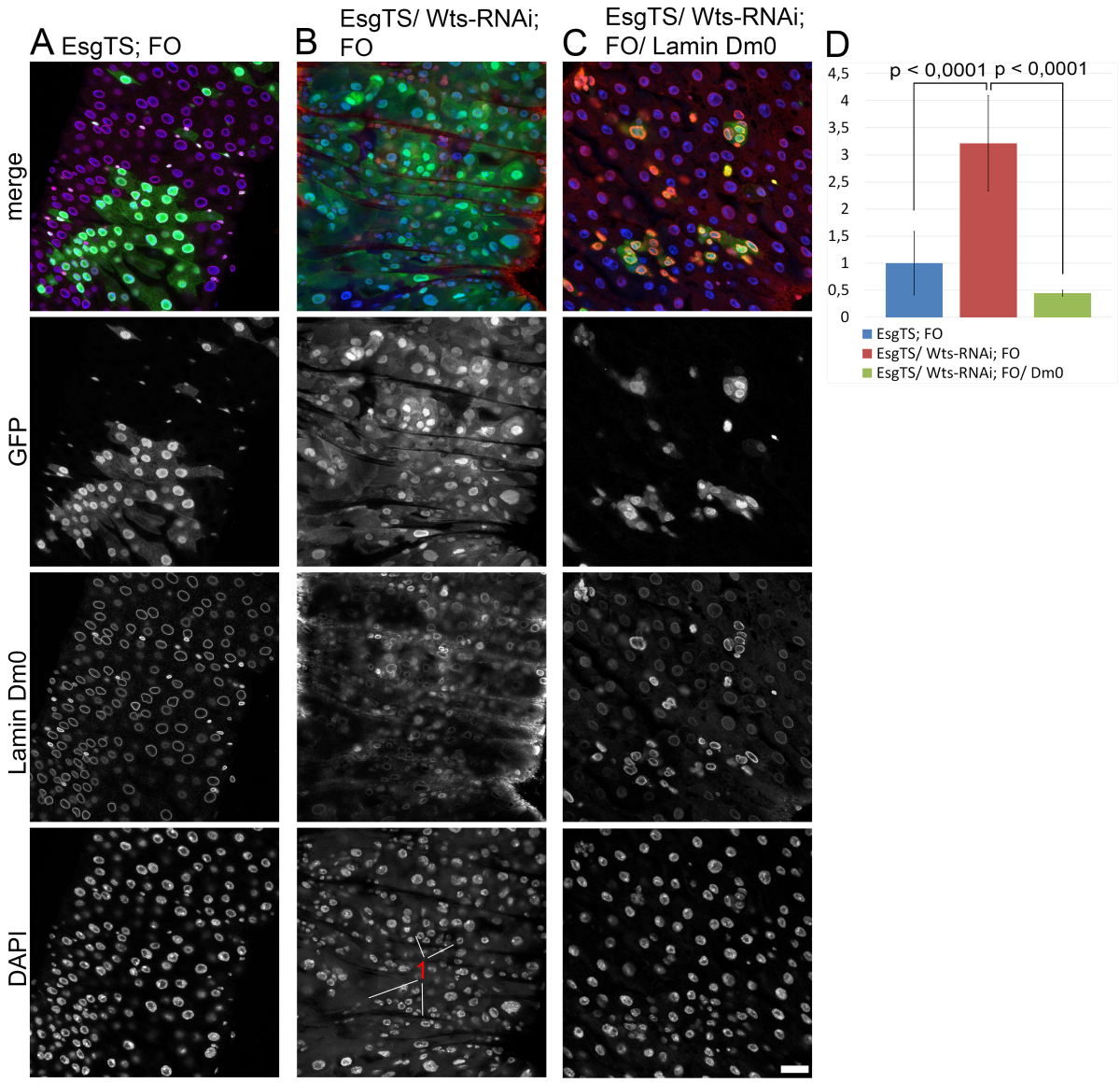

Figure 18: Dm0 suppresses *Wts* RNAi induced proliferation
A: (EsgTS/(Sp/CyO); FO/(Dr/TM3)) wildtype, B: (EsgTS/UAS-*Warts*-RNAi; FO/(Dr/TM3)) Expression of *Warts*-RNAi greatly increases ISC proliferation and leads to an increased number of small cell types (1) C: (EsgTS/ *Warts*-RNAi; FO/UASt-Lamin Dm0) Dm0 coexpression with *Warts* RNAi overrules the proliferation signal and reduces ISC proliferation to about 50% of WT-levels. D: Quantification of stem cell proliferation by mean fluorescence/gut, normalized to control. Clonal induction for 5 days. Scale bar: 25µm

Upon Dm0 overexpression UPD-induced proliferation was reduced drastically (Figure 19 C) similar to levels present in sole Dm0 overexpression (Figure 19 D). Detail box in Dm0 and GFP staining pictures shows increased Dm0 staining in clonal cells versus non clonal cells upon UPD and Dm0 overexpression (Figure 19 C) and very strong Dm0 staining in clonal cells versus non clonal cells upon overexpression of Dm0 (Figure 19 D), compared to wildtype and UPD overexpressing cells (Figure 19 A and B). Quantification shows that the UPD induced increase in proliferation is highly significant. Also reduction of proliferation upon coexpression of Dm0

and UPD is highly significant and similar in strength as Dm0 expression alone (Figure 20).

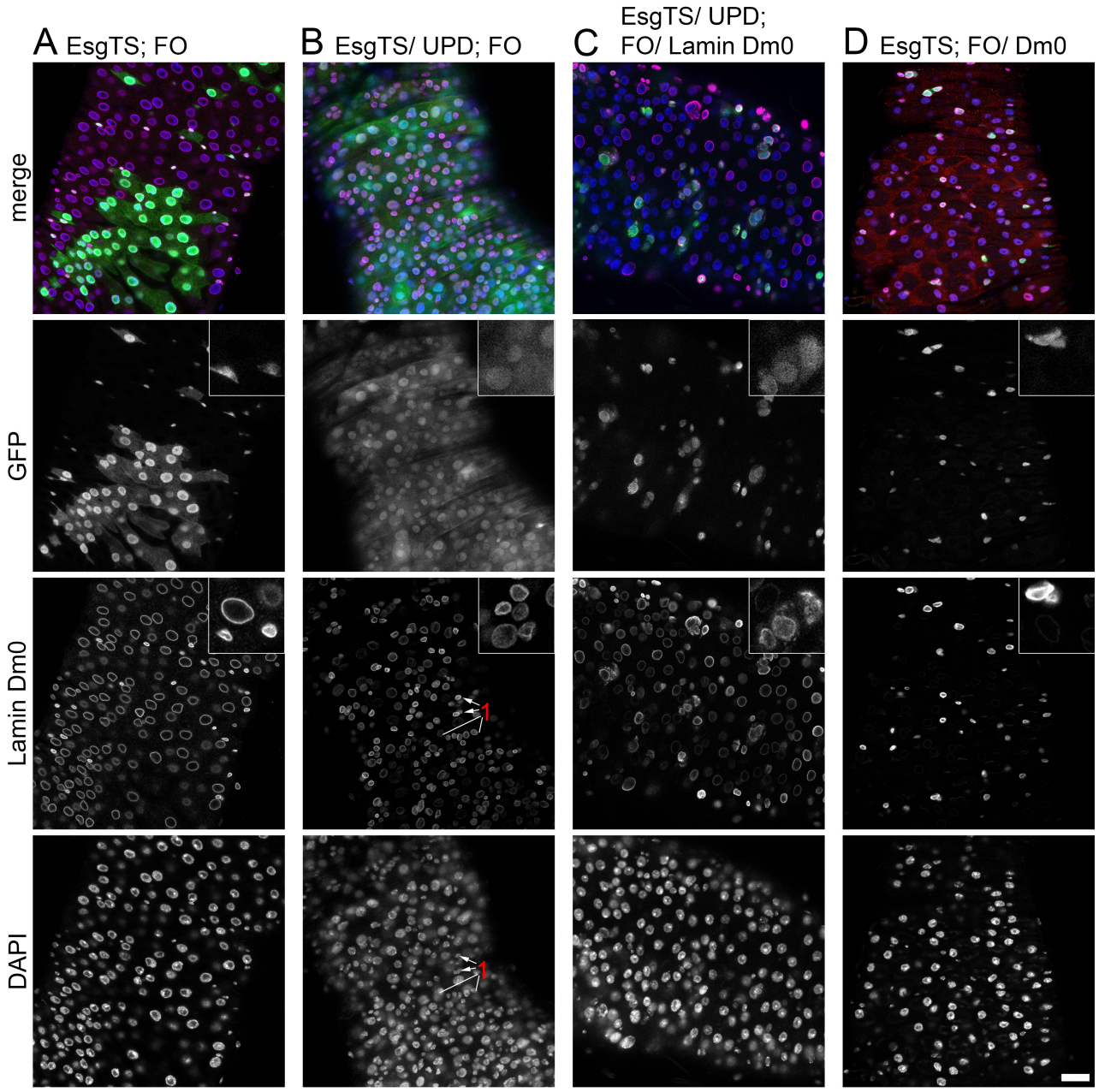

Figure 19: Dm0 suppresses UPD induced stem cell proliferation
A: (EsgTS/(Sp/CyO); FO/(Dr/TM3)) Wildtype, B: (EsgTS/UASt-UPD; FO/(Dr/TM3)) Expression of UPD leads to a strong overproliferation event with increased numbers of small cell types (1) and cellular density. C: (EsgTS/UASt-UPD; FO/UASt-Lamin Dm0) In coexpression with UPD Dm0 inhibits ISC proliferation similar to levels present in sole Dm0 overexpression (D). D: (EsgTS/(Sp/CyO); FO/UASt-Lamin Dm0) Lamin Dm0 overexpression leads to a strong reduction of stem cell proliferation. 3x enlarged detail of gut-cells in the top right of Dm0 staining pictures shows clonal and non clonal cells with varying degree of Dm0 staining. Clonal induction for 5 days. Scale bar: 25µm

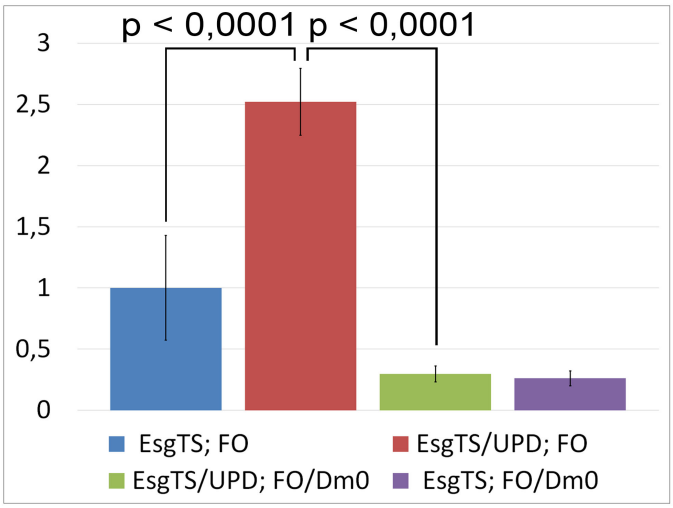

Figure 20: Dm0 supresses UPD induced stem cell proliferation
Quantification of A, B, C, D. Increase in proliferation upon UPD expression and decrease of proliferation upon Dm0 overexpression are significant (p-value $< 0{,}0001$).

Lamin Dm0 and Stat levels are anti-correlated in enterocytes

To test whether Dm0 directly or indirectly affects the JAK/STAT pathway or whether it inhibits proliferation pathway independently, antibody staining against the active form of Stat (pStat) was applied to previously processed phenotypes. Increased Stat staining in wildtype applies mostly to patches of cells which do not stringently correlate with clones. Overexpression of UPD-expressing clones clearly correlates with an increase in pStat levels compared to non clonal areas (Figure 21 B). Coexpression of Dm0 with UPD reduces stat levels in nearly all clonal cells (Figure 21 C, 1) while non clonal cells show an increase in Stat levels. In clones with sole Lamin Dm0 expression pStat staining is absent in the majority of cells (Figure 21 D, 1) but still present in far more cells (Figure 21 D, 2) as in UPD/Dm0 co-expressing clones.
To test whether Lamin Dm0 acts differently on Stat than on pStat levels, a co-staining with both antibodies was made (Figure 22). Both antibodies showed a high similarity in their specificity in clonal and non clonal cells. Increase in Stat levels in a particular cell did directly translate into increased pStat levels.
The pStat reducing effect of Dm0 in clones co-expressing UPD could be reproduced with Stat staining and was quantified (Figure 23). Overlay of Dm0 and GFP staining serves as a control (Figure 23 A). Quantification of nuclei with high GFP staining vs. nuclei with high Dm0 staining shows a positive correlation as cells with GFP also overexpressed Dm0 (Figure 23 D). Fluorescence levels of Dm0 and Stat staining however are anti-correlated (Figure 23 C) indicating a direct or indirect effect of Dm0 on Stat levels.

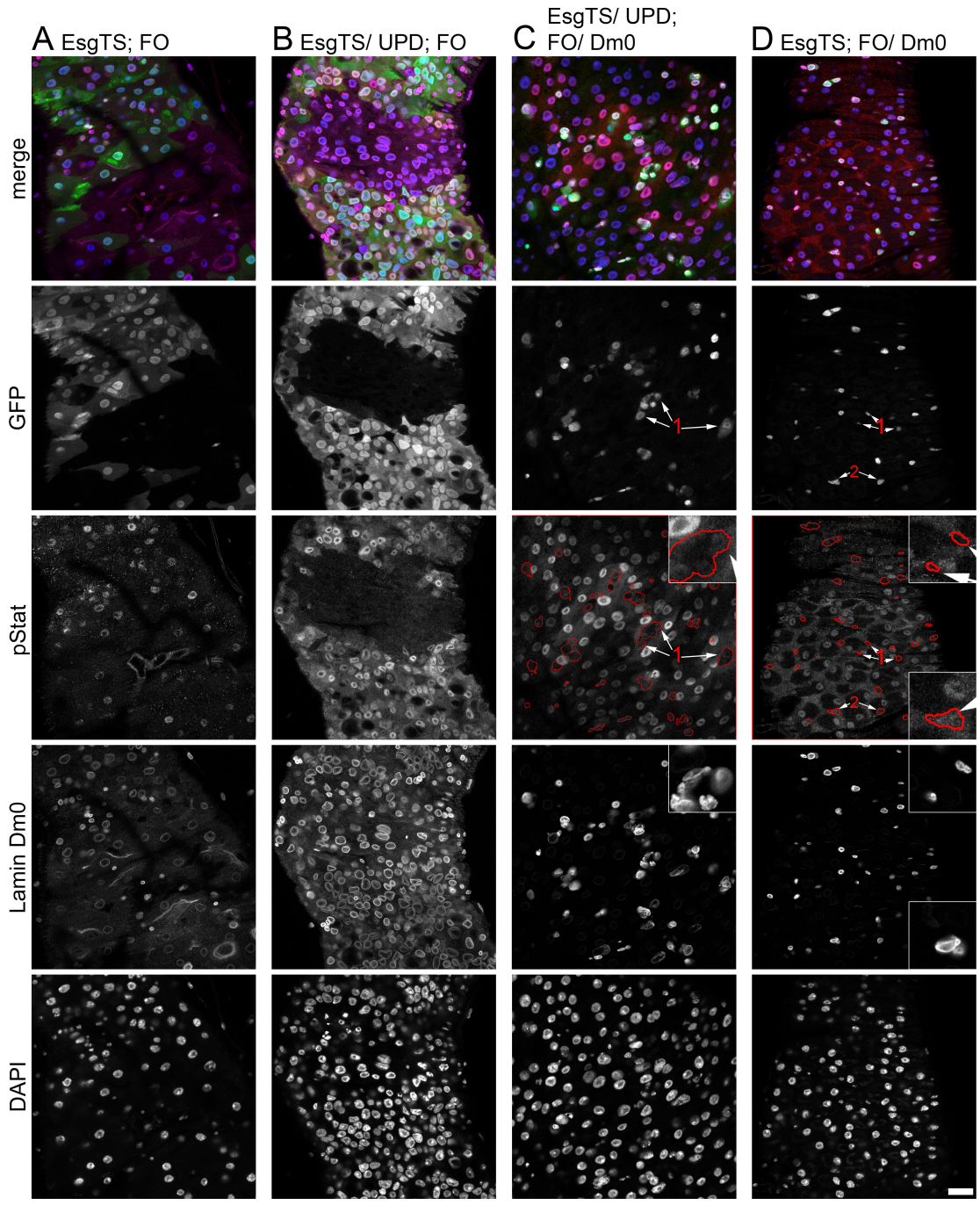

Figure 21: pStat levels are downregulated in Dm0 expressing cells
A: (EsgTS/(Sp/CyO); FO/(Dr/TM3)) Wildtype with variable pStat staining in clonal and non clonal cells. B: (EsgTS/UASt-UPD; FO/(Dr/TM3)) Expression of UPD leads to strong overproliferation. pStat staining is strongly increased in clonal compared to non clonal cells. C: (EsgTS/UASt-UPD; FO/UASt-Lamin Dm0) In coexpression with UPD Dm0 inhibits ISC proliferation similar to levels present in sole Dm0 overexpression. pStat levels are considerably lower in clonal cells but variable in non clonal cells. (D). D: (EsgTS/(Sp/CyO); FO/UASt-Lamin Dm0) Lamin Dm0 overexpression leads to a strong reduction of stem cell proliferation. pStat staining is variable in clonal and non clonal cells. (1) marks clonal cells with reduced pStat staining, (2) marks clonal cells with regular stat staining. 3x enlarged detail of gut-cells in the top right of Dm0 and Stat staining pictures shows clonal cells with low Stat staining, the box on the low right shows clonal cells with strong Stat staining. Clonal induction for 5 days. Scale bar: 25µm

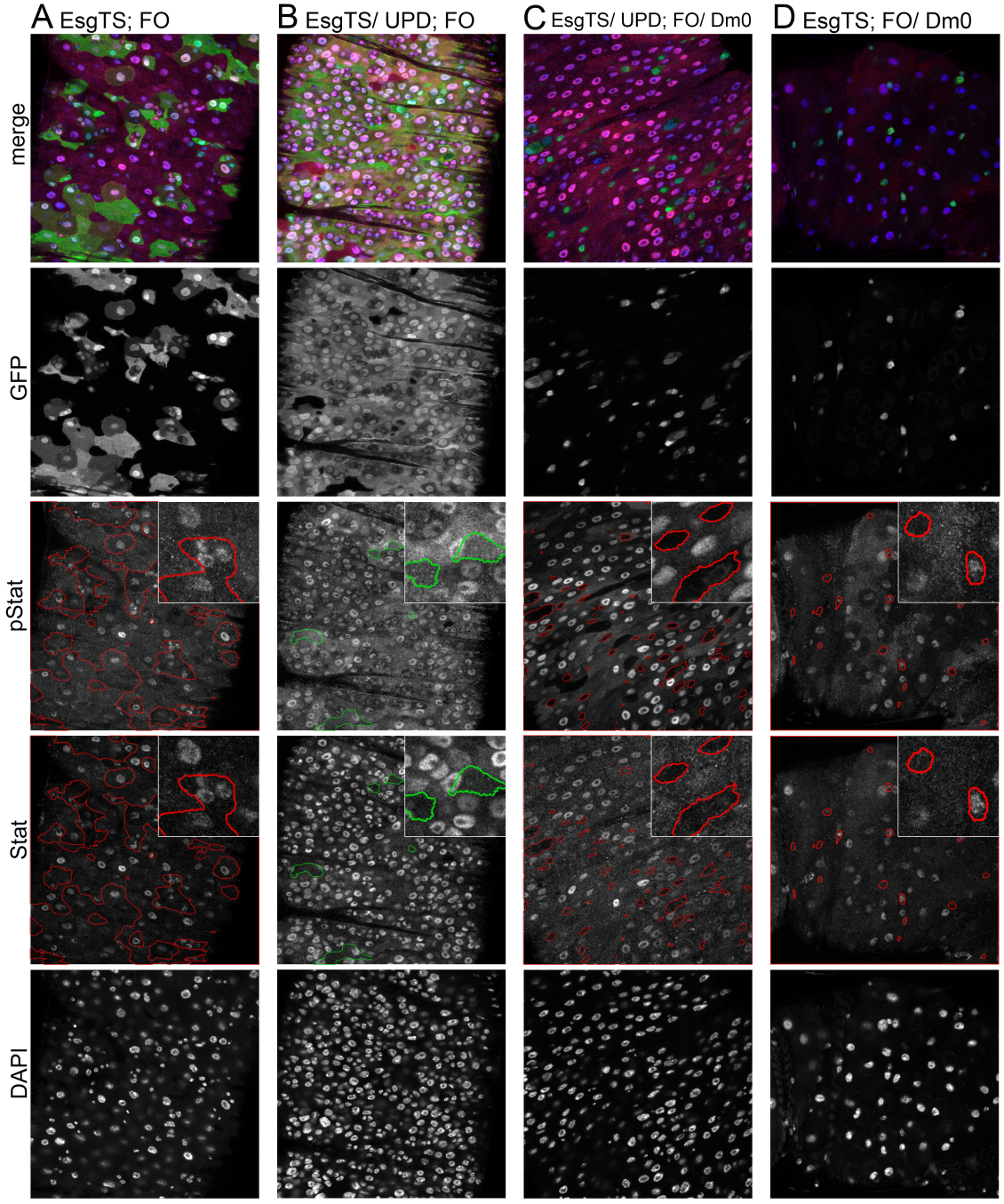

Figure 22: pStat and Stat show equal distribution

A: (EsgTS/(Sp/CyO); FO/(Dr/TM3)) Wildtype shows no difference in clonal vs non clonal cells is visible in pStat or Stat staining. Both forms are closely correlated in all cells. B: (EsgTS/UASt-UPD; FO/(Dr/TM3)) Expression of UPD leads to a dramatic increase in pStat and Stat staining in nearly all clonal cells. pStat and Stat levels are highly correlated. Green outline marks non clonal cells that show less Stat staining in comparison to clonal cells. C: (EsgTS/UASt-UPD; FO/UASt-Lamin Dm0) Dm0 coexpression with UPD leads to a clear decrease of pStat and Stat levels in clonal cells. D: (EsgTS/(Sp/CyO); FO/UASt-Lamin Dm0) Comparison of pStat and Stat antibody staining in Dm0 expressing clones shows no significant difference between both forms. In both cases clonal and non clonal cells show variation in staining. Red outline marks clonal cells, green outline marks non clonal cells. 3x enlarged detail of gut-cells in the top right of Dm0 and Stat staining pictures shows examples clonal cells in A, C and D and non clonal cells in B. Clonal induction for 5 days. Scale bar: 25µm

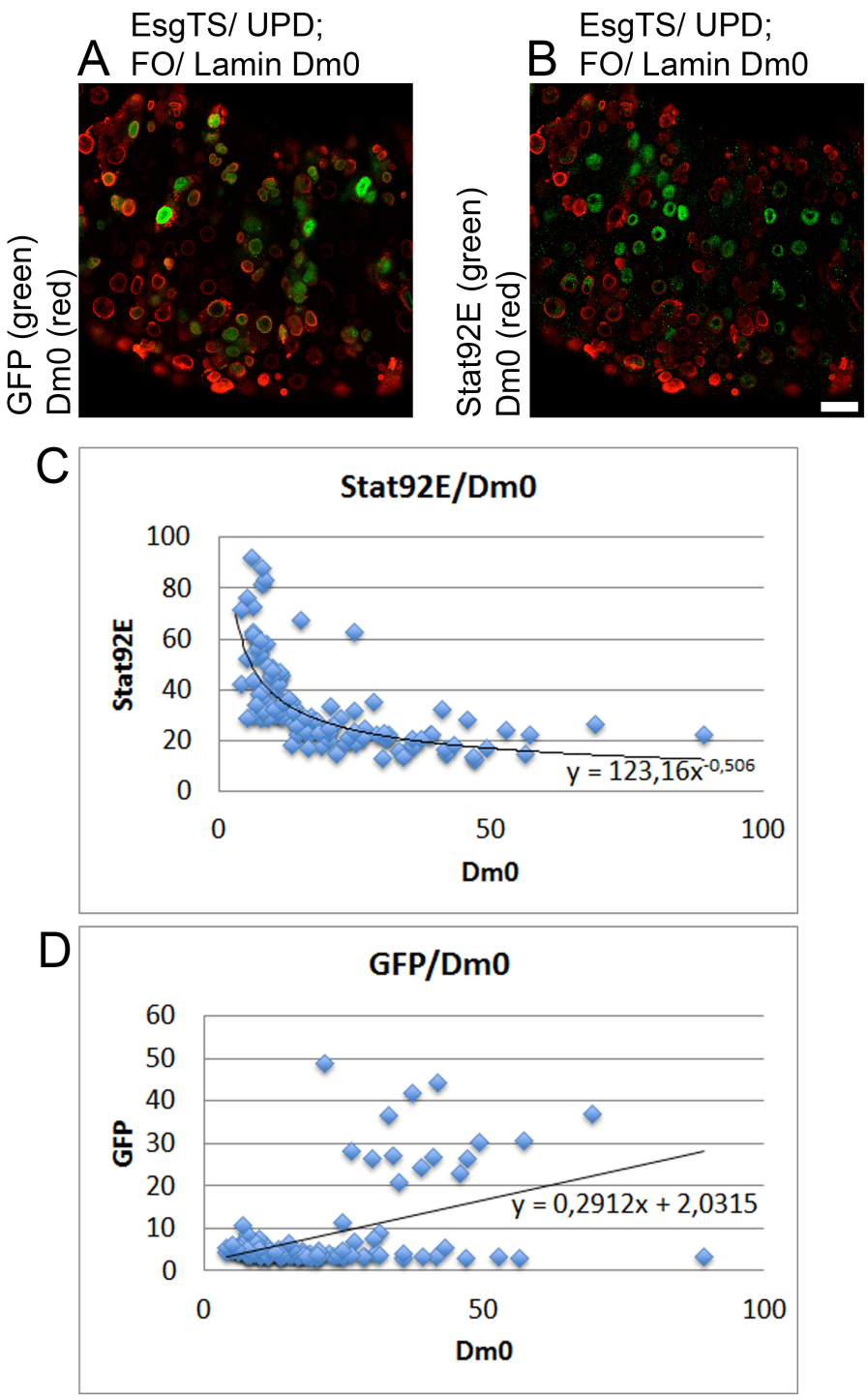

Figure 23: Levels of Dm0 and Stat are anti-correlated
A: (EsgTS/UASt-UPD; FO/UASt-Dm0) Color overlay of GFP and Dm0 staining. B: (EsgTS/UASt-UPD; FO/UASt-Dm0) Color overlay of Stat and Dm0 staining C: Quantification of fluorescence levels of GFP and Dm0 in individual cells indicated anticorrelation. D: Quantification of fluorescence levels of Stat and Dm0 in individual cells indicated positive correlation.

Lamin Dm0 acts downstream of Stat

To determine at which step of the pathway Dm0 inhibits the proliferation signal of the JAK/STAT signaling, Dm0 was co-expressed with a constitutively active form of Stat, StatΔNΔC (Figure 24) [26]. In this instance the JAK/STAT dependent proliferation is induced downstream of Stat, thereby the upstream factors UPD, Domeless and Hopscotch can be taken out out of the equation. Expression of StatΔNΔC only resulted in a mild, insignificant increase in clonal area (Figure 25 B, Figure 26). However the fact that the vast majority of clonal area is devoid of regular Stat staining (Figure 25 B Stat channel) indicates the presence of StatΔNΔC which probably reduced normal Stat levels in clones by a negative feedback loop. Furthermore, cells in the vicinity of clones show increased levels of normal Stat. This could minimize the effect of StatΔNΔC to increase clonal area by ISC proliferation as non clonal areas would compete for gut surface-area due to induced ISC proliferation. Dm0 over-expression together with StatΔNΔC again lead to near complete arrest of ISC proliferation (Figure 25 C, Figure 26). Levels of Stat in clones also remain reduced similar to StatΔNΔC expression alone, indicating the presence of StatΔNΔC displacing Stat. Dm0 expression alone (Figure 25 D) reduces ISC proliferation slightly more than in coexpression with StatΔNΔC (Figure 26) but clonal cells show higher levels of Stat, compared to (Figure 25 C) indicating that Dm0 does not noticeably reduce native levels of Stat.

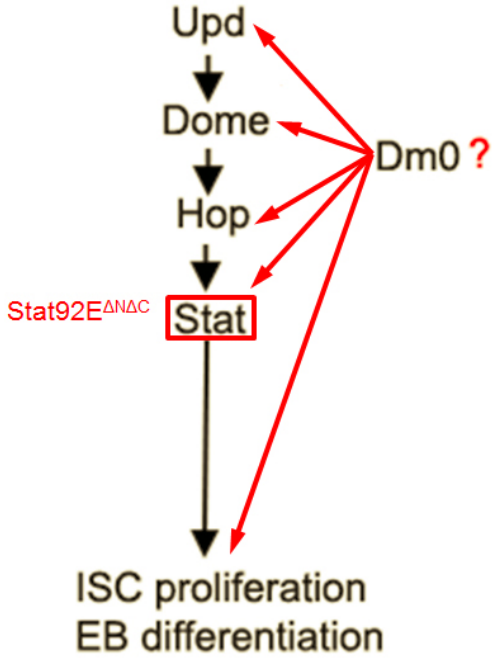

Figure 24: StatΔNΔC
Scheme shows Jak/Stat pathway components. StatΔNΔC activates the JAK/STAT pathway at the level of Stat. Red arrows indicate possible interaction with Dm0

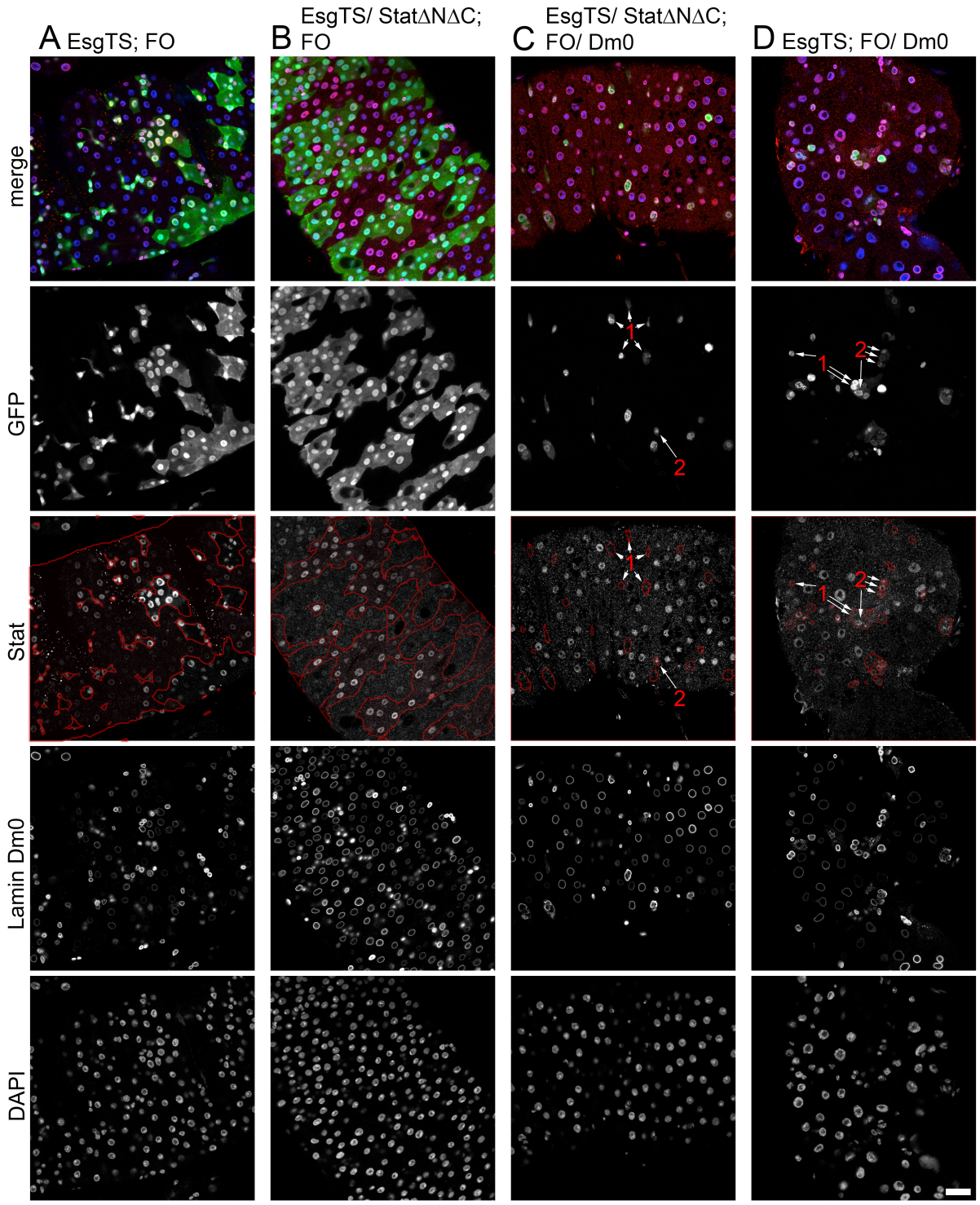

Figure 25: Dm0 supresses proliferation induced by StatΔNΔC
A: (EsgTS/(Sp/CyO); FO/(Dr/TM3)) Control, B: (EsgTS/UAS-StatΔNΔC; FO/(Dr/TM3)) Expression of StatΔNΔC does only induce mild proliferation. Stat staining is increased in non clonal areas and decreased in clonal areas. C: (EsgTS/UAS-StatΔNΔC; FO/UASt-Dm0) Dm0 in coexpression with StatΔNΔC significantly reduced ISC proliferation. Stat staining is increased in non clonal areas and decreased in clonal areas. D: (EsgTS/(Sp/CyO); FO/UASt-Dm0) Dm0 expression significantly reduces ISC proliferation but does not reduce Stat levels in clones. 1: Marks clonal cells without Stat staining. 2: Marks clonal cells with Stat staining. Red lining the Stat channel indicates clonal areas. Clonal induction for 5 days. Scale bar: 25µm

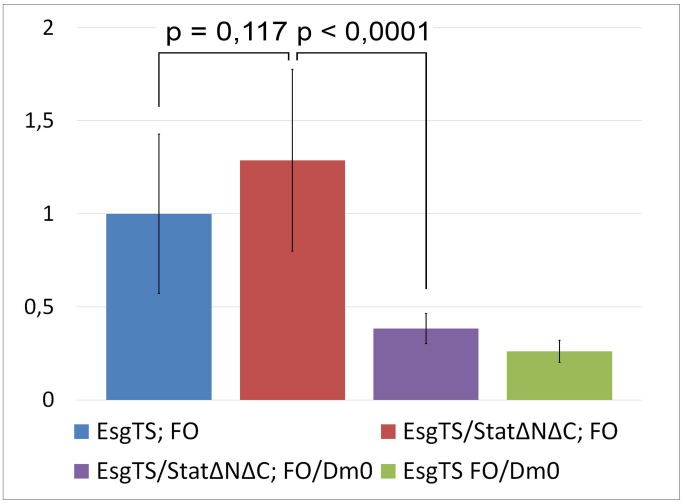

Figure 26: Dm0 supresses proliferation induced by StatΔNΔC
Quantification of stem cell proliferation by mean fluorescence/gut, normalized to control. No significant increase in proliferation was recorded in guts expressing StatΔNΔC, but a significant downregulation upon coexpression of Dm0 and StatΔNΔC.

Lamin Dm0 does not act on dMyc

dMyc, the *Drosophila* homologue of the oncogene Myc, has been reported to act downstream of the JAK/STAT, Hippo and EGFR pathway and mediate their function [74](Figure 27 A). According to previous results, the inhibitory effect of Dm0 overexpression on ISCs can overrule the proliferative signals of both the JAK/STAT and the Hippo pathway. Therefore it is unclear whether Dm0 acts downstream of both pathways on the level of dMyc. To address this question dMyc antibody was used to compare control and Lamin Dm0 overexpression phenotypes (Figure 27 B and C). dMyc staining reveals no change in Dm0 overexpressing clonal cells, indicating no effect of Dm0 on dMyc. However dMyc staining was homogeneous throughout the wildtype gut. This however would have been expected since Stat levels did show significant variation in intestinal cells correlating with potential areas of proliferation (Figure 25 A, Figure 21 A). In the cited paper [74] however only situations of induced proliferation were displayed to have raised dMyc levels. Levels of the dMyc antibody staining occurring in a native, uninduced situation of proliferation were not discussed.

3.1.2 Cell cycle control

To test whether Dm0 expression affects the cell cycle, the fly-FUCCI construct [95] was used to map cell cycle stages of wildtype and Dm0 expressing ISCs/EBs. The FUCCI system uses E2F1 fused GFP and Cyclin B fused RFP to track different cell cycle stages (Figure 28A).

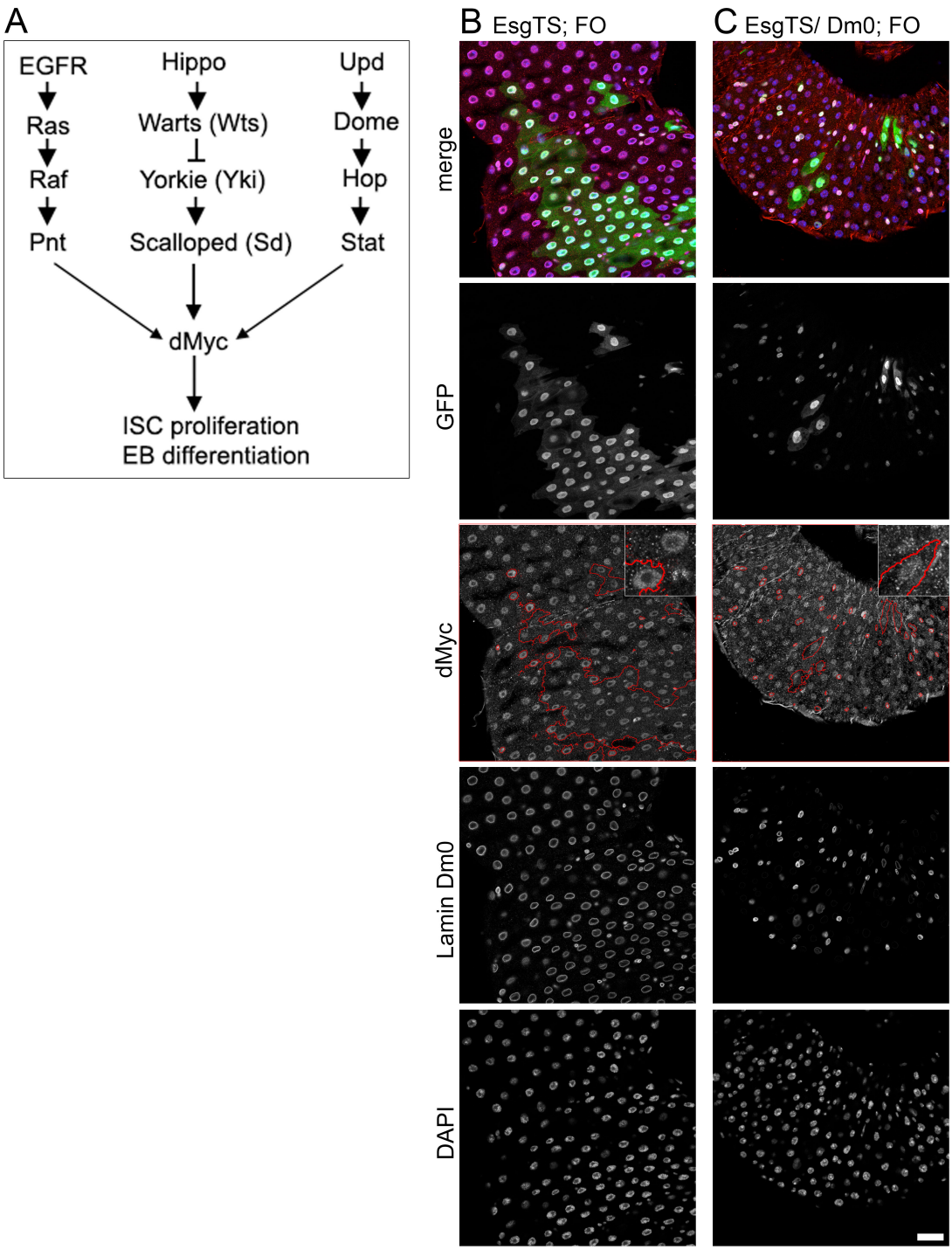

Figure 27: dMyc levels are not altered by Lamin Dm0 overexpression

A:Scheme of the signaling pathways upstream of dMyc shows the JAK/STAT, Hippo and EGFR pathways activating dMyc downstream which in turn mediates the proliferation response. B: (EsgTS/(Sp/CyO); FO/(Dr/TM3)) Control, No changes in dMyc were visible in potential areas of proliferation. Red lining marks GFP positive flipout clones. C: (EsgTS/(Sp/CyO); FO/Dm0) dMyc levels are not altered in Dm0 overexpressing cells. Red lining marks GFP positive, Dm0 overexpressing flipout clones. 3x enlarged detail of gut-cells in the top right of dMyc staining pictures. Scale bar: 25µm

This system was tested in flies expressing the same transgenes as EsgTS but without the UAS-GFP. E2F1-GFP and CyclinB-RFP (UAS-FUCCI) expression is induced by Esg-Gal4/UAS-FUCCI; Gal80TS/(UASt-Dm0 or TM3). So with this system the cell cycle stages of ISCs and EB can be tracked with or without Dm0 expression. Since this is not a clonal system only ISCs and EBs are marked with E2F1-GFP and CyclinB-RFP. We successfully expressed the FUCCI construct in ISCs/EBs and were able to track the cell cycle of those cell types specifically (Figure 28 A/D). Expression of FUCCI without Dm0 resulted in a majority of cells in G2 phase, a small group of cells in G1 and no cells in S phase (Figure 28 B, 29 A and C). Expression of FUCCI with Dm0 also resulted in a majority of cells in G2 phase but no G1 population of cells. Instead a small population of cells showed S phase staining (Figure 28 C, 29 B and C). Therefore Dm0 decreases the number of G1 cells and leads to an increase of cells in S and G2 phase compared to wildtype.

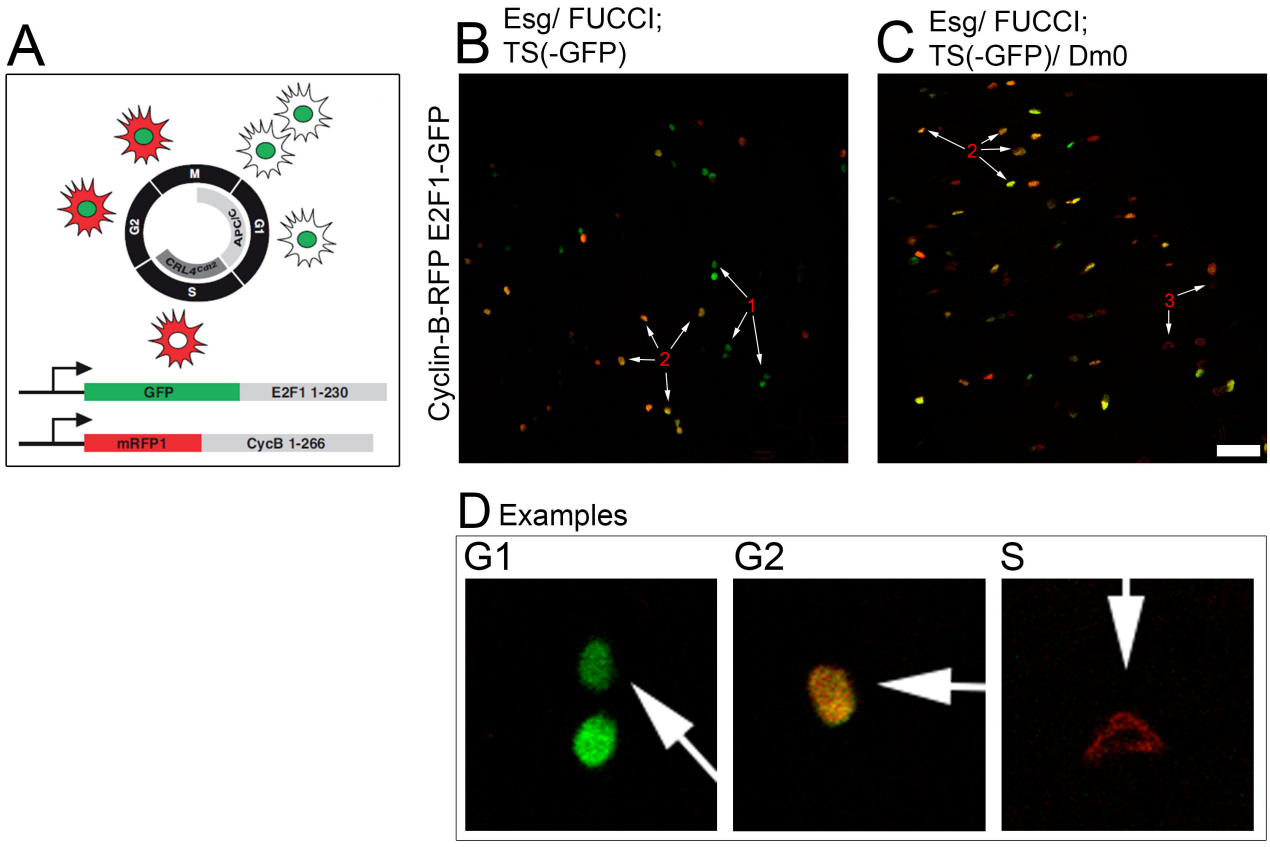

Figure 28: The fly-FUCCI system

A: Schematic of the FUCCI system. GFP alone marks cells in G1 phase, RFP alone marks cells in S phase and both GFP and RFP mark cells in G2 phase. Scheme adopted from[95]. B: Color overlay of E2F1-GFP/Cyclin-B-RFP in ISCs/EBs in wildtype. C: Color overlay of E2F1-GFP/Cyclin-B-RFP in ISCs/EBs with Dm0 expression. 1 marks cells with only E2F1-GFP, 2 marks cells with E2F1-GFP and Cyclin-B-RFP, 3 marks cells with only Cyclin-B-RFP. D: Exemplary cells from B and C for each cell cycle stage, 4x enlarged. Scale bar: 25µm

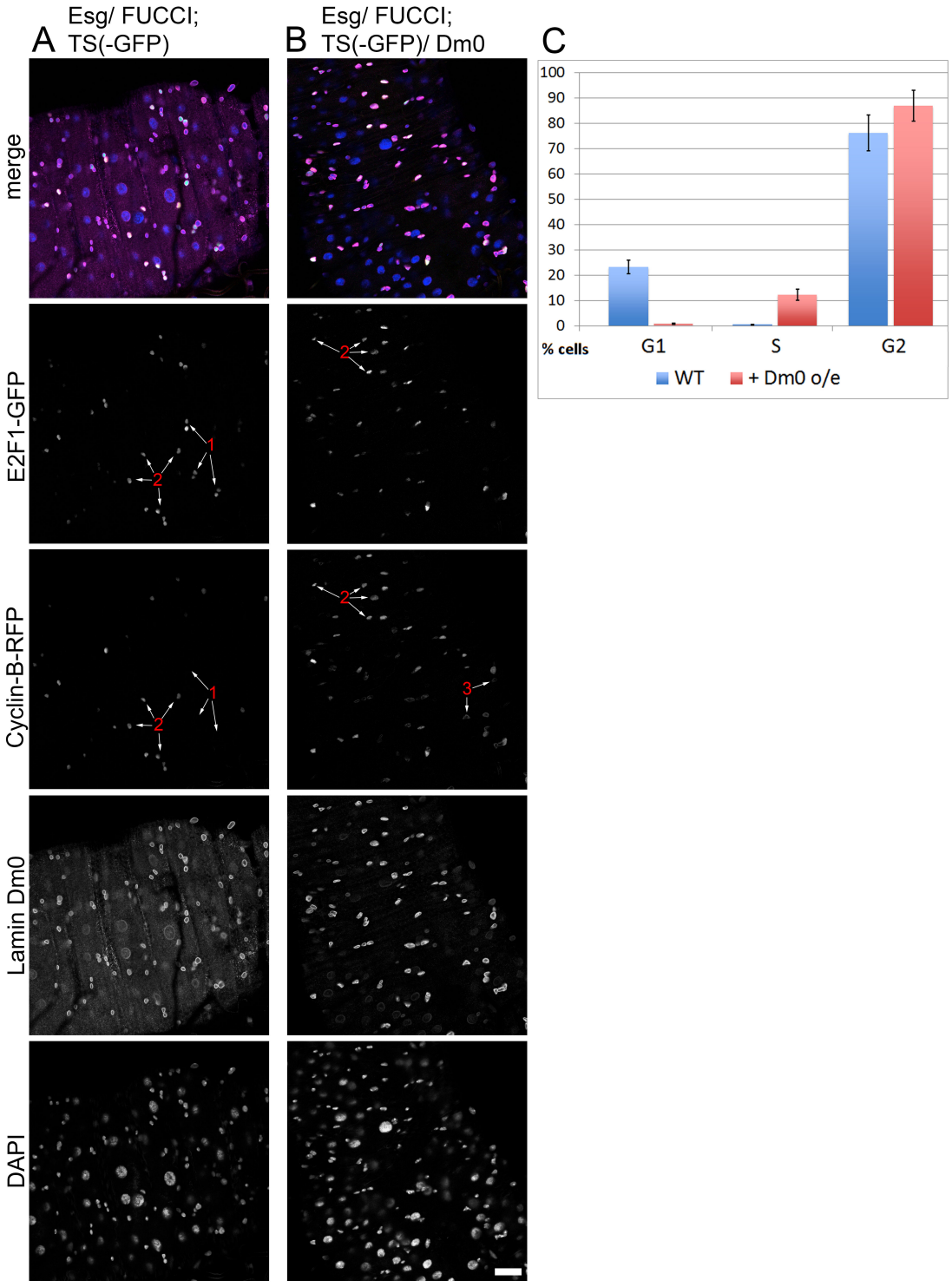

Figure 29: Dm0 alters the cell cycle
A: (Esg/FUCCI; TS(-GFP)/+) Expression of FUCCI in wildtype. B: (Esg/FUCCI; TS(-GFP)/Dm0) Expression of FUCCI and Dm0. 1 marks cells with only E2F1-GFP, 2 marks cells with E2F1-GFP and Cyclin-B-RFP, 3 marks cells with only Cyclin-B-RFP. Scale bar: 25µm C:Quantification of percent of wildtype or Dm0 expressing cells in G1, S and G2 phase. In wildtype cells about 77 % of cells are in G2 and about 23 % in G1 phase. In Dm0 expressing cells about 87 % of cells are in G2, 12 % in S and 1% in G1 phase.

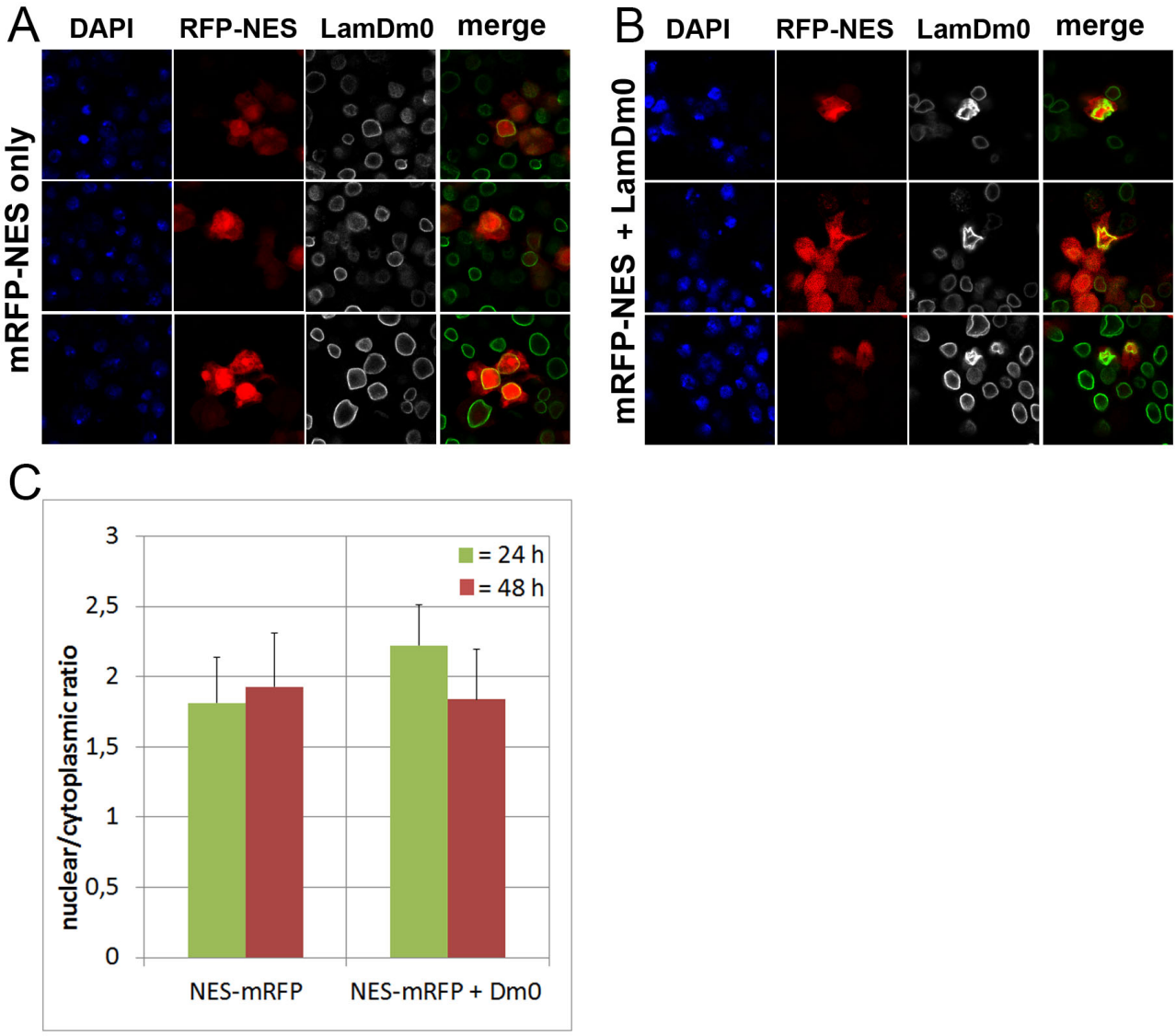

Figure 30: Dm0 has no effect on nuclear transport (Picture provided by Michaela Clever)
A: Kc167 cells 48h after transfection with RFP-NES. B: Kc167 cells 48h after transfection with RFP-NES and Dm0. C: Quantification of measured nuclear/cytoplasmic ratios in Kc167 cell 24h and 48h after transfection with RFP-NES or RFP-NES + Dm0. No significant difference between cells expressing Dm0 and control cells was measured.

3.1.3 Lamin Dm0 overexpresssion has no effect on nuclear transport behavior

One way how Dm0 could affect the proliferative behavior of ISCs is by altering the cell's nuclear/cytoplasmic transport. This has been reported to be the case for Progerin [46], so naturally it was tested whether Dm0 expression would alter transport behavior. Dr. Michaela Clever, a member of the Großhans group, and myself conducted several experiments to test for altered transport behavior upon Dm0 or Kuk expression. Expression of RFP fused with

a nuclear export signal (NES) and a nuclear localization sequence (NLS) in *Drosophila* Kc167 cells would provide the means to detect altered transport behavior as the ratio of nuclear vs cytoplasmic RFP would be altered (Figure 30 A). The cells show RFP staining in the nucleus because NLS and NES sequences establish an import/export balance which lies on the import side. However upon Dm0 expression no change in the nuclear/cytoplasmic ratio was detectable (Figure 30 B). Quantification of the nuclear/cytoplasmic ratio 24 hours and 48 hours after transfection did not show a significant difference between cells with and without Dm0 expression.

3.2 Gene expression of Dm0 overexpressing ISCs/EBs

Previous experiments have indicated an involvement of Dm0 in the JAK/STAT pathway downstream of Stat but the exact mechanism in which Dm0 acts remained elusive. It could be directly affecting the Stat transcription factor by binding to it, or indirectly by acting on the downstream targets of Stat which, via a negative feedback loop, downregulate upstream targets [7]. To answer that question and shed light on how Dm0 might affect other cellular processes a total RNAseq experiment was initiated. Since ISCs are the sources of proliferation in the intestine and Dm0 inhibits proliferation it is conceivable that the focus of transcriptome alterations, in this experiment, is on ISCs. Therefore no flipout cassete was used to mark daughter cells. This way the effects of UPD and Dm0 overexpression on the transcriptome are observed in ISCs/EBs exclusively.

Four phenotypes were compared in this experiment: 1. EsgTS/CyO; Dr/TM3 (control) 2. EsgTS/(Sp/CyO); Dm0/(Dr/TM3) (Dm0 overexpression) 3. EsgTS/UPD; Dr/TM3 (UPD expression, induction of ISC proliferation) 4. EsgTS/UPD; Dm0/(Dr/TM3) (UPD expression together with Dm0). The expression profile of Phenotypes 2, 3, 4 were compared to the control (1) to find candidates of genes which were significantly increased or decreased in expression. To simplify their labeling short terms for each comparison were formed: Control vs UPD for EsgTS/CyO, Dr/TM3 versus EsgTS/UPD; Dr/TM3, Control vs Dm0 for EsgTS/CyO;Dr/TM3 versus EsgTS/(Sp/CyO); Dr/Dm0 and Control vs UPD+Dm0 for EsgTS/CyO; Dr/TM3 versus EsgTS/UPD; Dr/Dm0. So UPD for instance is the shortened term for genes that showed a significant increase in expression in the EsgTS/UPD;Dr/TM3 sample compared to the control sample EsgTS/CyO; Dr/TM3.
In the UPD sample 374 candidates showed decreased expression of less or equal than 50% (log2 < = -1) and 224 candidates showed increased expression of more than 200% (log2 >= 1). The numbers for all significantly up or downregulated candidates are displayed in Table 6. A collection of the 30 highest up and downregulated transcripts, for each group, is displayed in the appendix.

Table 6: Results

Sample	log2 fold change <= -1	log2 fold change >= 1	total
Control vs UPD	374	224	598
Control vs Dm0	1027	673	1700
Control vs UPD + Dm0	778	710	1488

Dm0 expression induces notch expression and affects the JAK/STAT receptor domeless.

Upon analysis of the RNAseq data the transcript collection was screened for candidates involved in ISC proliferation regulating signaling pathways, apoptosis and cell cycle. A selection of affected transcripts is displayed in table 7, transcripts significantly upregulated are marked by 1 (log2 >= 1), transcripts significantly downregulated are marked by -1 (log2 <= -1). The validity of the experiment was confirmed by the expression pattern of UPD1 and Dm0. UPD1 transcripts that were significantly increased in samples UPD and UPD + Dm0 and Dm0 transcripts were significantly increased in samples Dm0 and UPD + Dm0.
Transcripts for JAK/STAT pathway receptor domeless are upregulated in the UPD expressing sample while during coexpression of Dm0 and UPD the transcript levels are normalized. Upd2 transcripts are downregulated upon UPD1 overexpression. *Notch* transcripts are upregulated in all three samples.

Table 7: Examples of affected genes

Transcript	Control vs UPD	Control vs Dm0	Control vs UPD + Dm0
upd1	1	0	1
Lam (Dm0)	0	1	1
dome	1	0	0
upd2	-1	0	0
N (Notch)	1	1	1

Lamin Dm0 can reduce or revert the expression of about half of the genes activated or downregulated by UPD expression

Expression of UPD lead to the upregulation of 224 transcripts and downregulation of 374 transcripts, compared to the control. Since Dm0 has shown to inhibit the JAK/STAT pathway the question whether this inhibition is specific or not has to be addressed. Upon coexpression of UPD and Dm0 about half of the transcripts, differentially expressed upon UPD expression,

did show a normalized or reversed expression (Figure 31). This indicates that Dm0 acts on the JAK/STAT pathway in a specific manor since a random chance of altering these genes is highly unlikely.

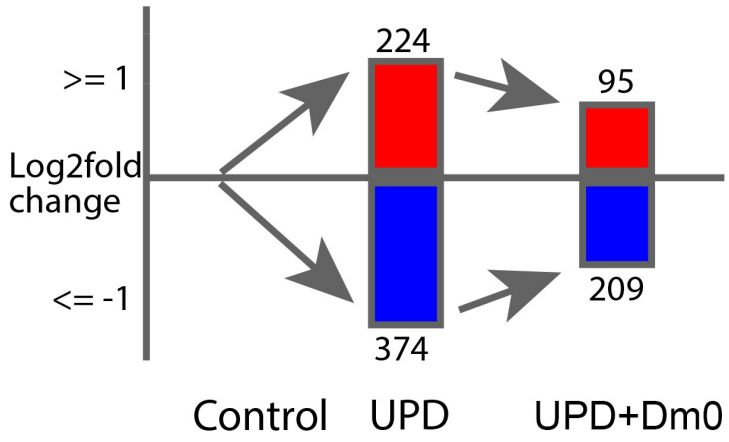

Figure 31: RNAseq Results
Schematic shows the number of transcripts that were significantly up/downregulated upon UPD expression compared to the control (shown by arrows pointing to red/blue bar for up/downregulation). About 50 % of the same transcripts were normalized upon Dm0 coexpression with UPD (right side).

GO annotation

For gene ontology (GO) annotation gene IDs with significant up or downregulation (log2 < -1 or >1) of transcripts were analysed with the Database for Annotation, Visualization and Integrated Discovery (DAVID) v6.8 website. DAVID allows the classification of gene IDs with respect to the biological process, cellular compartment or molecular function they might be involved in. For each of the three options gene IDs are classified into subcategories. For each subcategory the count of gene IDs is given together with other factors that eventually form the false discovery rate FDR. The false discovery rate gives an estimate on how likely the correct classification is. For easier display of small and big values the negative decadic logarithm of the FDR (-log10(FDR)) is used, so a low FDR results in a high (-log10(FDR)), indicating high likelihood of correct categorization. All (-log10(FDR) values above 1 have a FDR lower than 10%, above 2, lower than 1% etc.

It is likely that certain geneIDs are found in several subcategories and that some will not be allotted to a subcategory. Therefore the sum of all geneID counts will not represent the number of geneIDs submitted to the DAVID website. Also if several geneIDs of say downregulated transcripts are found in a certain subcategory, E.g. proteolysis, no definite conclusion about the effect on proteolysis can be made, since it could be all transcripts of either positive or negative-regulating pathway components.

GO-annotations were created for Control vs: Dm0, UPD and UPD+Dm0 (terms explained in the beginning of section 3.2).

A

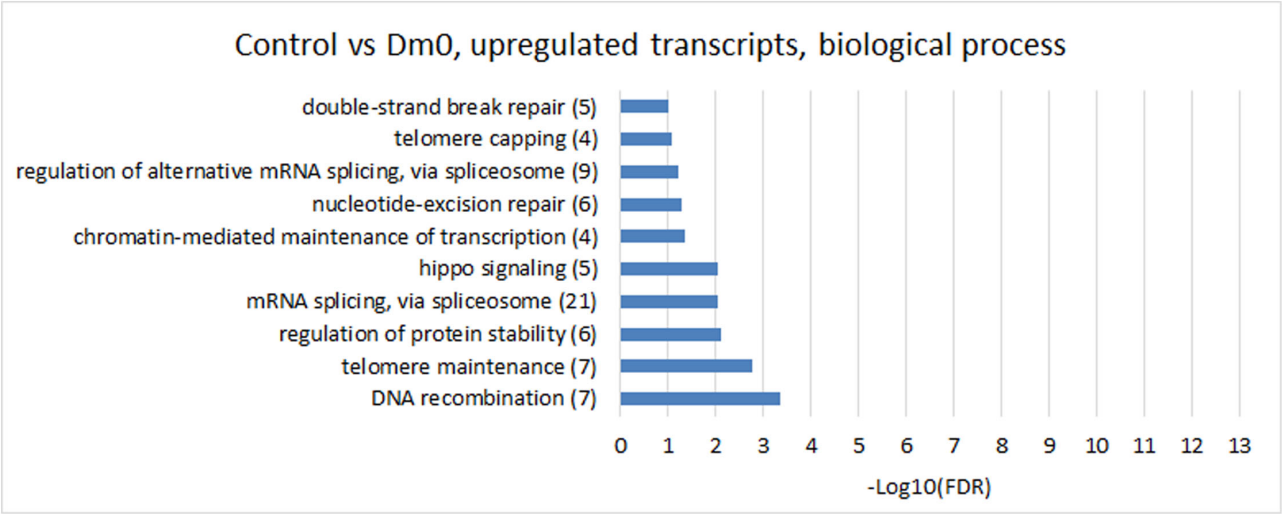

B

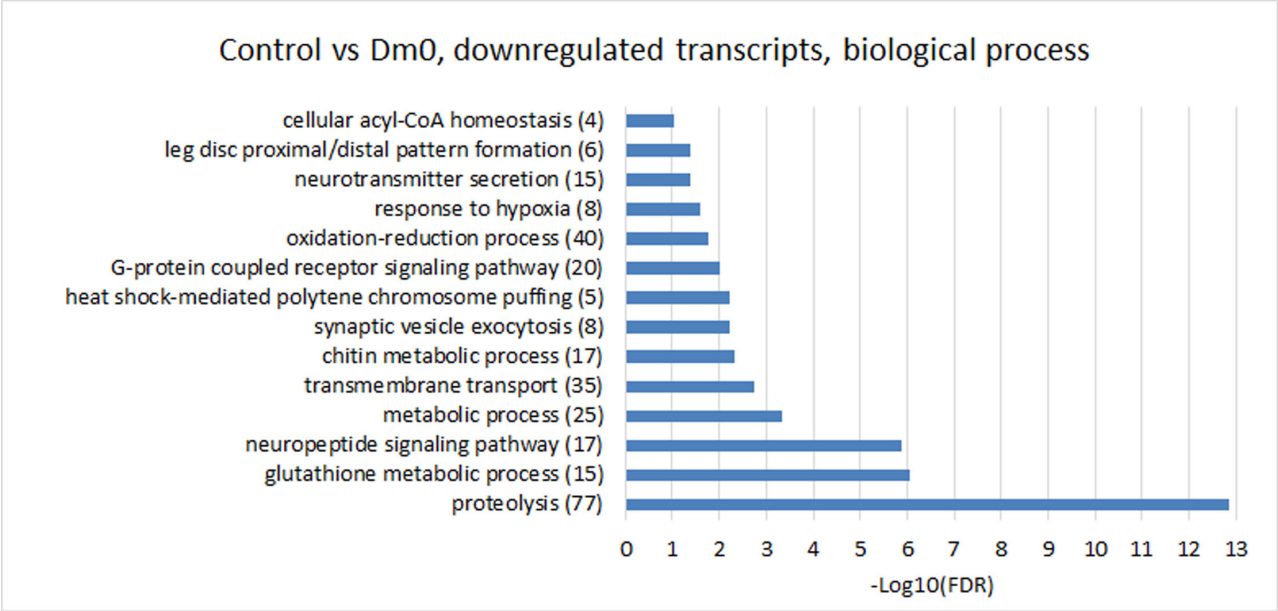

Figure 32: GO annotation of transcripts altered by Dm0 expression
List of GO annotations of transcripts whose levels were significantly altered by Dm0 overexpression, compared to the control. A: GO annotation of upregulated transcripts, upon Dmo overexpression. B:GO annotation of upregulated transcripts, upon Dmo overexpression. -Log10(FDR) is the negative decadic logarithm of the false discovery rate. It gives an estimate about the level of trustwothines of transcripts faling in a certain category. Numbers bigger than 1 have a lower FDR than 10%, higher than 2 equals lower than 1%. Numbers in brackets after the respective term signify the number of gene IDs in that category. A higher number means that more genes in that category are affected by Dm0 overexpression.

Since each comparison (E.g. Control vs Dm0) was divided into upregulated and downregulated transcripts and each group was tested with respect to biological process, cellular compartment or molecular function, 6 different GO annotations were created for each comparison. Resulting in a total of 18. As an example only the biological processes affected by Dm0 are displayed in this chapter (Figure 32), the complete set is listed in the appendix (Table 18 to 35).

Dm0 overexpression resulted in a significant increase of transcripts involved in several aspects of DNA repair and modulation , as well as hippo pathway signaling and protein stability (Figure 32 A, Table 18). Accordingly most counts are located in the categories of nucleus and nucleolus in "cellular compartment" (Table 19) and in DNA/nucleic acid associated processes in "molecular function" (Table 20). On the other hand Dm0 overexpression lead to reduction of transcripts involved in proteolysis, reduction of oxidation and neuronal regulation, among others (Figure 32 B, Table 21). This correlated with mostly membrane associated categories in "cellular compartment" (Table 22) and categories involved with peptidase activity, anti-oxidation (E.g. glutathion metabolic process) and neuropeptide regulation in "molecular function" (Table 23).

Overexpression of UPD did not result in upregulation of transcripts involved in categories of apparent significance (Table 24), however similar to Dm0 overexpression, in a downregulation of transcripts involved in proteolysis and oxidation reduction (Table 27). Accordingly, similar to Dm0 overexpression, categories with membrane associated localization are listed in "cellular compartment" and peptidase as well as glutathion activity in "molecular function" (Table 28/29).

Upon overexpression of Dm0 and UPD together a mixture of subcategories originally found in either sole Dm0 or sole UPD expression and several new subcategories are listed in "biological process" for upregulated transcripts (Table 30). One subcategory from sole UPD overexpression remained , dopamine uptake involved in synaptic transmission. And several subcategories involved with DNA repair/modulation remained from sole Dm0 overexpression. New subcategories involve mostly unrelated processes, proteolysis is the one with the most geneID counts but also with the highest FDR. In a similar fashion "cellular compartment" and "molecular function" display a mix of subcategories from the sole expression of UPD and Dm0 with some new subcategories (Table 31/32). For downregulated transcripts, upon Dm0 and UPD overexpression, in "biological process" also a mixture of subcategories from each sole Dm0 and UPD overexpression and some new subcategories was listed (Table 33). Important subcategories that remained were proteolysis and oxidation reduction from both sole Dm0 and UPD and DNA repair/remodeling from Dm0. New subcategories with a low FDR were flavonoid glucoronidation and flavonoid byosynthetic process. Categories in "cellular compartment" and "molecular function" (Table 34/35) are mixed in a similar fashion and respective to their correlating category in "biological process".

Table 8: Overlap of candidates, induced by Dm0 expression, with LADs

	log2 <= -1	log2 >= 1		all transcripts
Control vs Dm0 + LADs	337	200	+ LADs	1044
Control vs Dm0 - LADs	606	369	- LADs	1893
total	943	569	total	2937
C. vs Dm0 + LADs/total (%)	35.7 %	35.1 %	in LADs/ total (%)	35,6 %

Expression of genes in lamina associated domains is not altered preferentially by Dm0 overexpression

Genome regulation has previousy been associated with lamina associated domains (LADs) [55]. To test whether genes that are located in LADs are affected more by Dm0 expression than genes outside of LADs a list of known LADs was compared to transcripts significantly up or downregulated by Dm0 in comparison to the control. Of transcripts whose coding region lies in LADs 337 transcripts were significantly downregulated and 200 transcripts significantly upregulated (Table 8 Control vs Dm0+LADs). Transcripts whose coding region lies outside of LADs 606 transcripts were significantly downregulated and 369 transcripts significantly upregulated (Table 8 Control vs Dm0-LADs). That results in a ratio of 35.7% of genes that are downregulated upon Dm0 expression and lie in LADS and a ratio of 35.1 % of genes that are upregulated upon Dm0 expression and lie in LADs. However, comparison of all transcripts that were significantly up or downregulated in any of the tested genotypes and were located in LADs (+LADs), with all transcripts that were not located in LADs (-LADs, did result in a ratio of 35.6 % of all transcripts that lie in LADS. This shows that the ratio of transcripts with coding regions in LADs and outside of LADs did not change in transcripts differentially expressed upon Dm0 overexpression. Also no change in the ratio of transcripts whose levels were increased versus transcripts whose levels were reduced,upon Dm0 overexpression, was noted.

Comparison of JAK/STAT targets with other studies

The expression of UPD caused a significant change of expression in 598 candidate genes. To test whether these candidates are typical JAK/STAT target genes they were compared with the results from two other groups. The first study, by the Martin Zeidler lab, used transcript profiling of Drosophila haemocyte-like cells (Kc167) where JAK/STAT signaling was induced with UPD conditioned medium [6]. The second study, by the lab of Erika Bach, did a genome-wide bio-informatics search for genes with Stat92E binding sites [30].

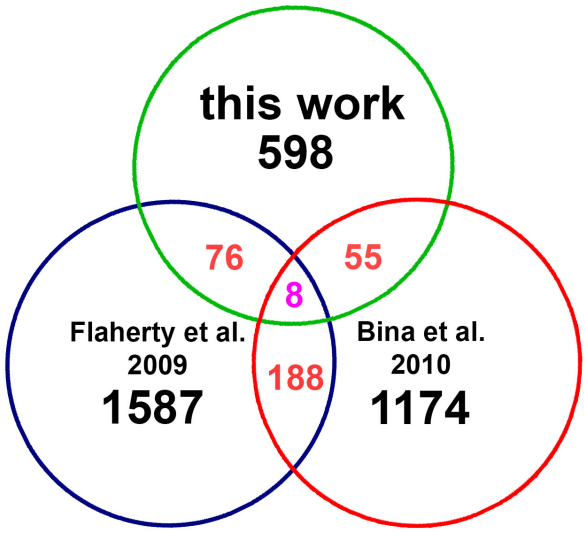

Figure 33: Comparison of JAK/STAT target studies
Schematic of the transcriptional target overlap of three different Studies. This work used ISCs/ EBs and activated JAK/STAT signaling by UPD1 expression. Bina et al. 2010 did a transcript profiling approach of Drosophila haemocyte-like cells and induced Jak Stat signaling by UPD in the medium. Flaherty et al. 2009 did a genome-wide bio-informatics search for genes with Stat92E binding sites. In this work 598 candidate genes were found that showed an overlap of 76 genes with the set of Flaherty et al. and 55 genes with Bina et al. In comparison the sets of Bina et al. and Flaherty et al. show an overlap of 188 candidates. Only 8 candidate genes did show an overlap with all tree studies.

Table 9: Comparison with other studies

	this work/Bina et al. 2010	this work/Flaherty et al. 2009	Bina et al./Flaherty et al.
overlap candidates	55	76	188
overlap in %	3,2	3,6	7,3
number of candidates by random overlap	40,9	55,3	109,6
random overlap in %	2.4	2,6	4,1
overlap in % / random overlap in %	1,35	1,38	1,72

While Bina et al. 2010 did show an overlap of 55 candidates with this work and Flaherty et al. did show an overlap of 76 candidates, both studies did show an overlap of 188 candidate genes. Since both studies have more candidates they also have a higher statistical chance of overlap. Only 8 genes were found in all three studies (Figure 33). So the overlap of candidates is relatively small, only 3,6 % in this work and Flaherty et al. 2009, 3,2 % in this work and Bina et al. 2010 and 7,3 % in Flaherty et al. and Bina et al. This indicates that the JAK/STAT downstream target genes are quite divers and differ greatly in different tissues (Table 9 "overlap

in %"). However, the percentage of overlap is higher than a purely random chance of overlap by the same numbers of genes, in all three cases (Table 9 "random overlap in %"). This amounts to a 35% higher overlap than by random chance comparing this work and Bina et al., 38% higher overlap comparing this work and Flaherty et al. and 72% higher overlap comparing Flaherty et al. and Bina et al. (Table 9 "overlap in % / random overlap in %").

3.3 Lamin function

The role of Dm0 in *Drosophila* intestinal cells is not well understood. To understand the function of Dm0 for ISC proliferation and its effect on other nuclear and cell cycle components the Dm0 null mutant LamD395 was used in combination with the MARCM clonal system (Figure 35). MARCM uses the Gal4/ Gal80 system in combination with the Flp/FRT system. In the Gal4/Gal80 system, Gal4 is repressed by Gal80 and prevents Gal4 binding to UAS (upstream activating sequence) enhancer sites. When Gal80 is removed Gal4 can bind to UAS enhancer sites and induce the expression of a transgene, in this case GFP. In the Flp/FRT system a flippase mediates the recombination of cromatids at specific FRT recombination sites (FRT: flippase recognition target). Combined the MARCM system shows the presence of a homozygous mutant chromatid in a cell by the absence of the, Gal80 expressing, wildtype chromatid and henceforth expression of GFP. Therefore cells that are homozygous mutant will be marked by GFP. As control a wildtype chromatid with the FRT recombination site is used, creating wildtype clones with GFP expression.

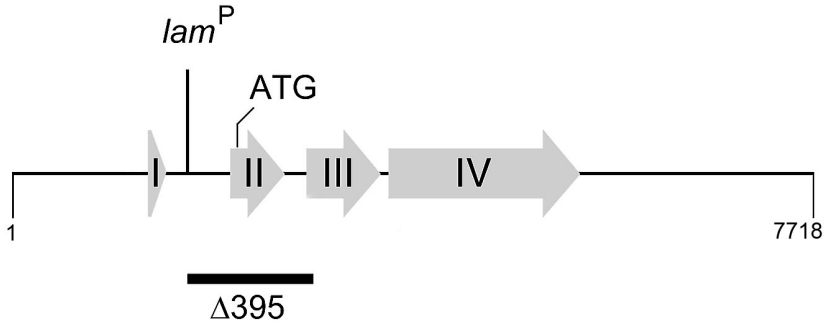

Figure 34: Molecular characterization of null allele lamD395 (picture from [62])
Schematic of the *LMNA* locus. Exons are presented as large grey arrows. LamP marks the P-element insertion site.Δ395 bar indicates the range of the lamD395 P-element excision.

The Lamin D395 null mutant was generated by a P-element mediated deletion of the second exon, containing the translation start codon (Figure 34 A). This lead to a complete loss of the Dm0 protein [62]. A survival screen demonstrated a 41% mortality during larval stage, 58% during pupal stage and 1% escapers [62]. This indicates a significant yet not absolutely essential role during larval and pupal development. Using the same mutant another group found a role

for Dm0 in the testis of the adult fly [18]. Another work using a different null allele reported no change in proliferation behavior in larval development, no change in nuclear shape and chromosomal structure [67]. No such characterization of Dm0 had been implemented in the adult midgut therefore several aspects such as potential changes in heterochromatin, cell cycle, proliferation or in Lamin C levels are addressed in this work.

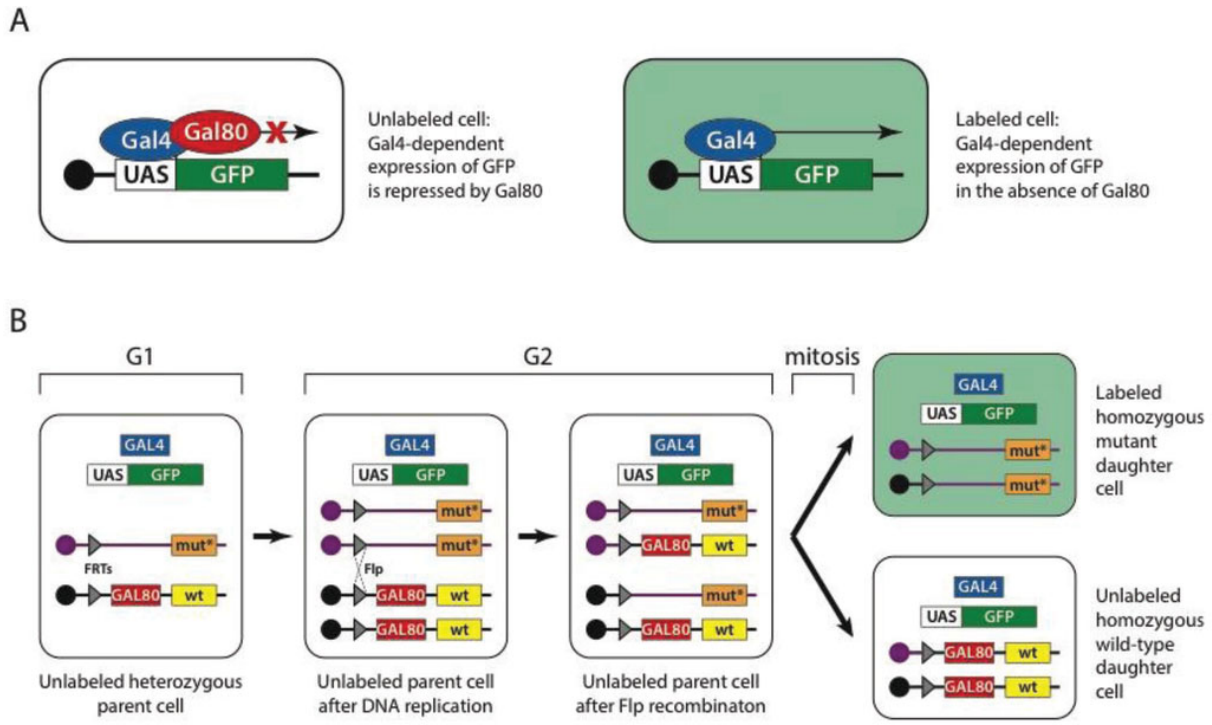

Figure 35: MARCM system (Scheme adopted from [25])
(A) Gal4-Gal80 system. In absence of Gal80 Gal4 binds to UAS (upstream activating sequence) and induces expression of GFP
(B) Scheme describing the MARCM recombination from mother to daughter cell. After DNA duplication in G2, recombination between FRT sites (grey triangle) can occur when Flippase is expressed. FRT sites are located on the same chromatids as either Gal80 with a wildtype allele or the mutant allele of interest. Upon recombination sister cromatids are formed that carry the wild-type allele and GAL80 and the mutant allele. After mitosis only daughter cells that received both mutant alleles will be marked with GFP, other daughter cells, still carrying Gal80 alleles will continue to repress GFP.

Knockdown of Lamin Dm0 does not reduce native stem cell proliferation

Comparison of control clones (just the FRT2L recombination site on a wildtype chromatid) (Figure 36 A, B) with Dm0 null clones (FRT2L recombination site and Dm0 null allele on the same chromatid) (Figure 36 C, D), that were induced one month prior dissection, confirmed successful knockout of Dm0. However comparison of clonal areas did not show a significant reduction or increase in Dm0 null clones vs control clones. This indicates that either small hardly detectable traces of Dm0 remain that still maintain their function or that absence of Dm0 has no effect on ISC proliferation.

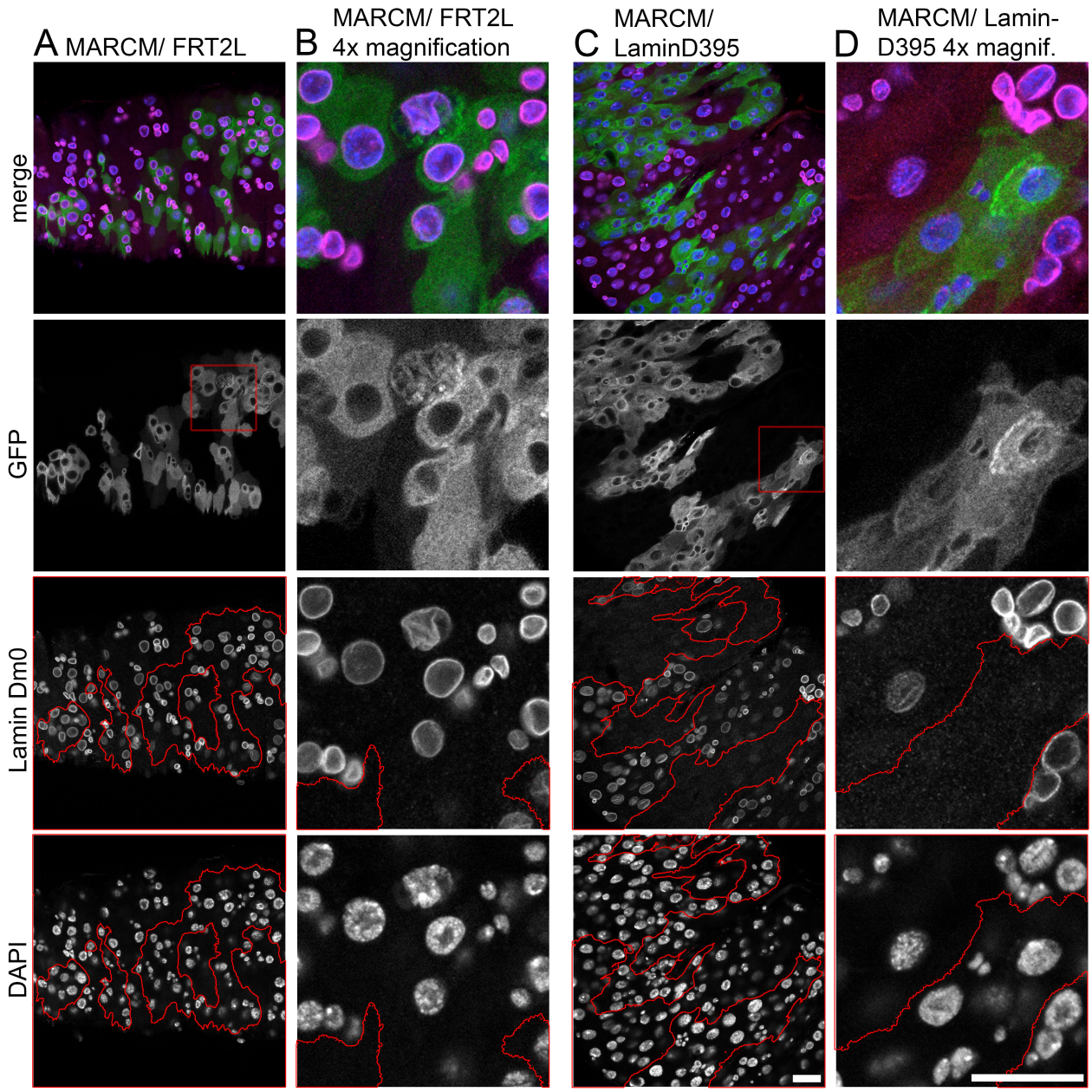

Figure 36: Lamin Dm0 null-clones show no change in uninduced stem cell proliferation
A: (UAS-CD8-GFP/+; tub-Gal80, FRT2L/ FRT2L; tub-gal4/+) Control showing no difference in Dm0 staining comparing clonal and non clonal areas. Red border marks magnified sector B: 4 fold magnification of selected area of (A) C: (UAS-CD8-GFP/+; tub-Gal80, FRT2L/LamD395, FRT2L; tub-gal4/+) Lamin null clone showing no detectable Dm0 staining in clones and normal Dm0 staining in non clonal areas. D: 4 fold magnification of selected area of (C) Flies were sacrificed 1 month after clonal induction. Scale bar: 25µm

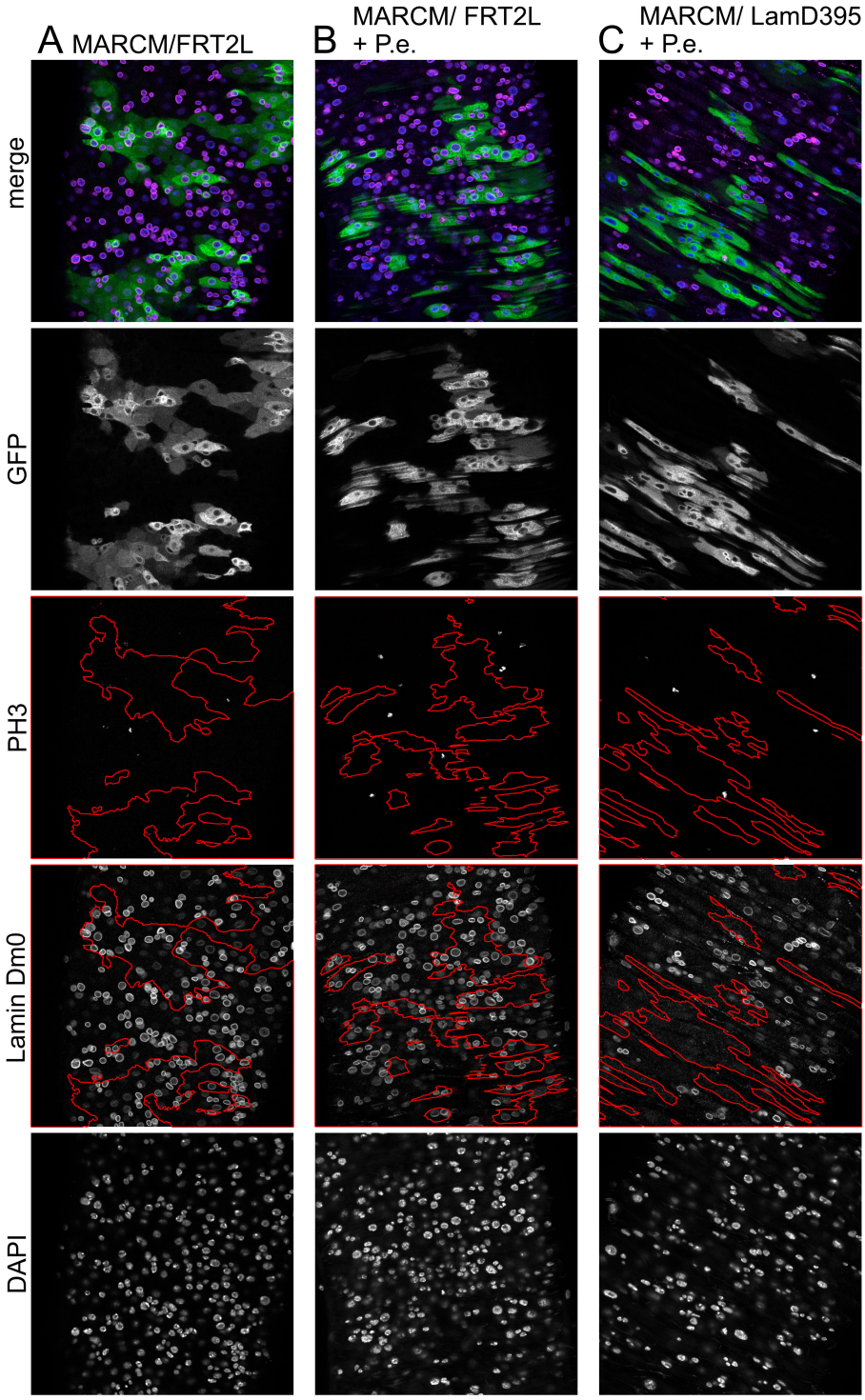

Figure 37: Induced stem cell proliferation in Lamin Dm0 null clones
A: (UAS-CD8-GFP/+; tub-Gal80, FRT2L/ FRT2L; tub-gal4/+) Control without P.e. B: Control with P.e. shows no obvious increase in clonal vs non clonal size. C: (UAS-CD8-GFP/+; tub-Gal80, FRT2L/LamD395, FRT2L; tub-gal4/+) Dm0 null colones do not show an obvious decrease compared to non clonal tissue. Red outline marks GFP + clones. Scale bar: 25µm

Dm0 null clones during induced stem cell proliferation

Since native ISC proliferation was not reduced by Dm0 knockdown, ISCs were challenged additionally by feeding the flies *Pseudomonas entomophila* (P.e.). This bacterium is a part of the *Drosophila* gut microbiome and induces high amounts of proliferation by activation of the JAK/STAT pathway [43]. The effect of P.e. infection was quantified by measurement of clonal area and by counting of phosphorylated Histone 3 (PH3) positive cells per gut inside and outside of clones (Figure 37). PH3 marks the G2/M transition and stains condensed chromatin just before chromosomal segregation and is therefore a short term marker of cell proliferation. Quantification of clonal area of P.e. infected flies did show an increase of clonal area in control-infected vs. control non-infected flies (Figure 38 A). Infected guts with Dm0 null clones show a reduction of clonal area with a nearly significant p-value of 0.063. Quantification of PH3 cells of infected control flies vs. non-infected control flies shows a significantly increased amount of PH3 cells within and outside clones (Figure 38 B, 1 and 2). However no significant decrease in PH3 cells inside clones was noted in infected guts with Dm0 null clones compared to infected control guts (Figure 38 B, 2 and 3). A ratio of clonal versus non clonal PH3 cells was formed to compensate for fluctuations of PH3 cells per gut, however no significant increase in PH3 positive cells was noted comparing infected control with Dm0-null clones (p value = 0.111).

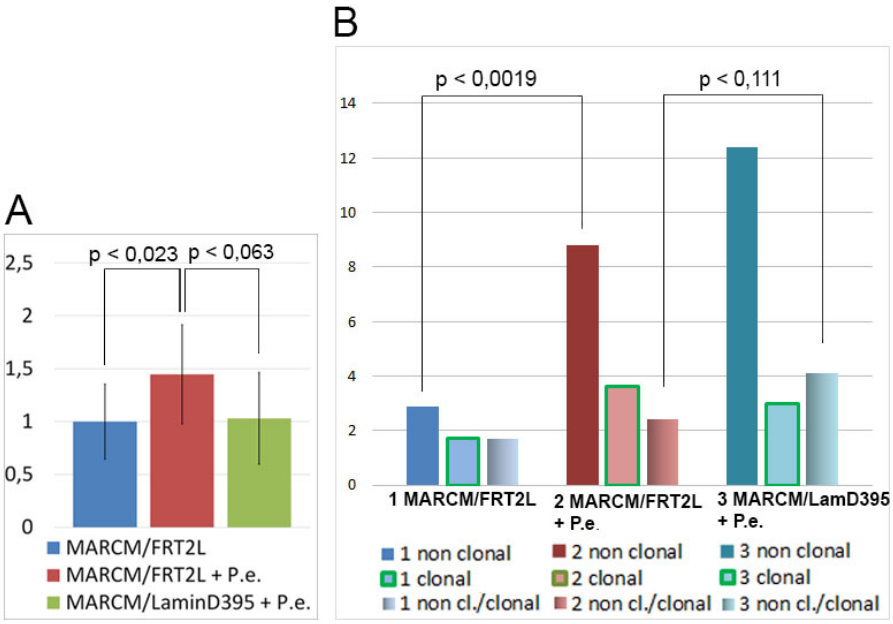

Figure 38: Quantification of Induced stem cell proliferation in Lamin Dm0 null clones
A:Quantification of clonal area of P.e. infected flies. Infected control flies do show an increase on clonal area compared to uninfected control flies. Infected flies with Dm0 null clones show a, hardly significant, decrease in clonal area compared to infected control flies. B: Quantification of PH3 cells in and outside of clones. Last row for each sample shows the ratio of non clonal/clonal PH3 cells. Infected control cells show a significant increase of PH3 cells in and outside of clones, compared to uninfected control flies. Dm0 null clonal flies do not show a significant enough increase of non clonal/clonal PH3 ratio compared to infected control flies.

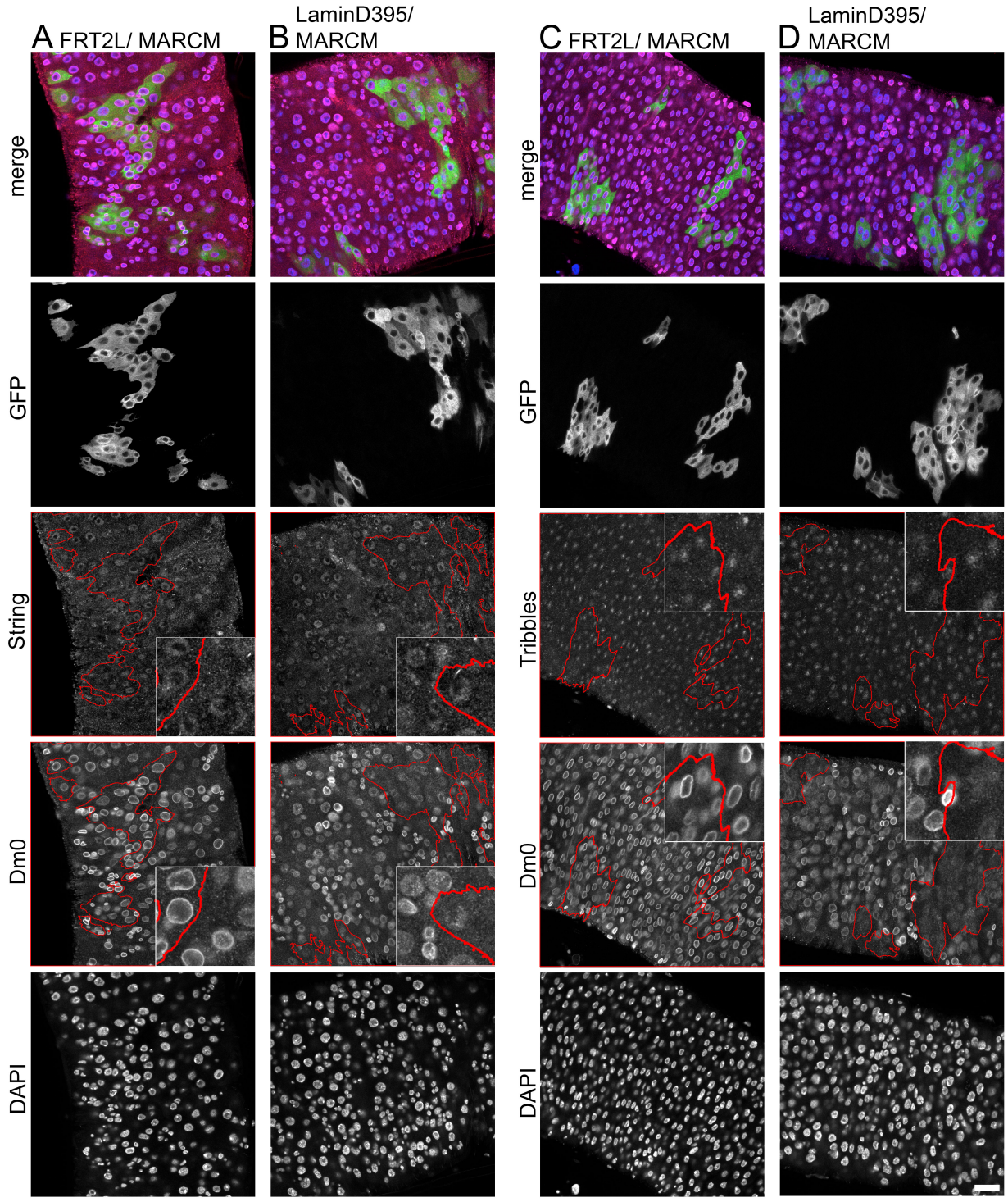

Figure 39: String and Tribbles levels are normal in Dm0 null clones

A and C: (UAS-CD8-GFP/+; tub-Gal80, FRT2L/ FRT2L; tub-gal4/+) Control showing no difference in String/Tribbles staining in and outside clonal areas. B and D: (UAS-CD8-GFP/+; tub-Gal80, FRT2L/LamD395, FRT2L; tub-gal4/+) Lamin Dm0 null clones did not show altered levels of String/Tribbles. Some clonal cells did show remaining Dm0 staining others did show nucleoplasmic Dm0. Scale bar: 25µm

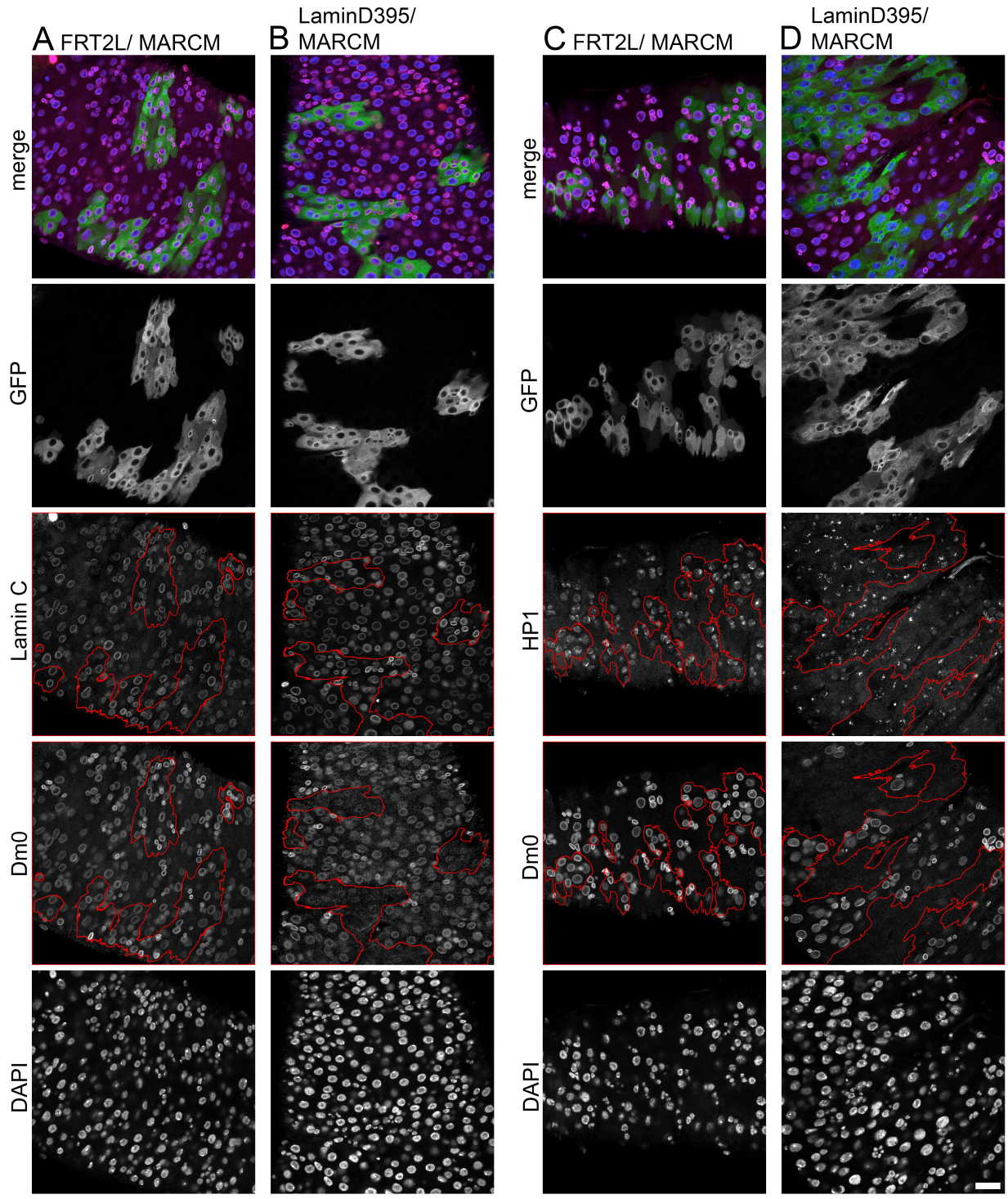

Figure 40: Lamin C and HP1 levels are normal in Dm0 null clones

A and C: (UAS-CD8-GFP/+; tub-Gal80, FRT2L/ FRT2L; tub-gal4/+) Control showing no difference in Lamin C/HP1 staining in and outside clonal areas. B/D: (UAS-CD8-GFP/+; tub-Gal80, FRT2L/LamD395, FRT2L; tub-gal4/+) Lamin Dm0 null clones did not show altered levels of Lamin C/HP1. Red outline marks GFP + clones. Scale bar: 25µm

LaminD395 clones show no aberrant levels of cell cycle markers Tribbles and String

Antibody staining for cell cycle markers String and Tribbles was used to test whether knockout of Dm0 affects the cell cycle. Though Dm0 was successfully knocked out in clonal cells, no change in String and Tribbles staining, in Dm0 null vs control clones, was recorded (Figure 39 A versus B and C versus D). Some cells in Dm0 null clones did show remaining nucleoplasmic Dm0 staining (Figure 39 B, D). This could be due to cross reactivity with the String/Tribbles antibody or, in some cases a non clonal cell overlayed by the GFP signal of clonal cells. In all, the results indicate no change in cell cycle regulation in clonal vs non clonal-cells.

LaminD395 clones show no change in Lamin C and HP1 levels

Dm0 null clones were stained with Lamin C to test for altered levels possibly compensating for Dm0 loss due to redundant functions. No considerable changes in Lamin C levels were noted in clones vs non-clonal area or control clones (Figure 40 A, B). HP1 staining was used to test whether the nuclear architecture or general levels of heterochromatin were changed. Also in this case no changes in HP1 levels or its positioning in the nucleus were noticeable in clones vs non-clones or control clones (Figure 40 C, D).

3.4 Electron microscopy (EM) analysis of Lamina proteins

Expression of Dm0 in ISCs/EBs is associated with nuclear morphological changes that were beforehand only recorded by immunostaining (Figure 41 A, B). Other types of nuclear changes were recorded for Kugelkern (Figure 43 A, B) and Lamin C CaaX (Figure 42 A, B), the Lamin C mutant allele that contains a farnesylation motif (CaaX). To gain a deeper insight into the nature of the morphological changes associated with these proteins, a collaboration with Prof. Georg Krohne was initiated for the use of high resolution EM imaging. Dm0, Kuk and Lamin C CaaX were expressed in ISCs/EBs by Esg; TS and in ECs by Myo; TS.

3.4.1 Overexpression of Lamin Dm0, Kugelkern and Lamin C CaaX lead to diverse nuclear alterations

Expression of Dm0 induced abnormal nuclear lobulations and increased immunofluorescence in GFP-positive ISCs/EBs and ECs (Figure 41 A, B). However, also non GFP-positive ECs show nuclear deformations. Possibly GFP-mRNA transport, GFP expression or GFP degradation, in ECs, is affected by Dm0 expression.

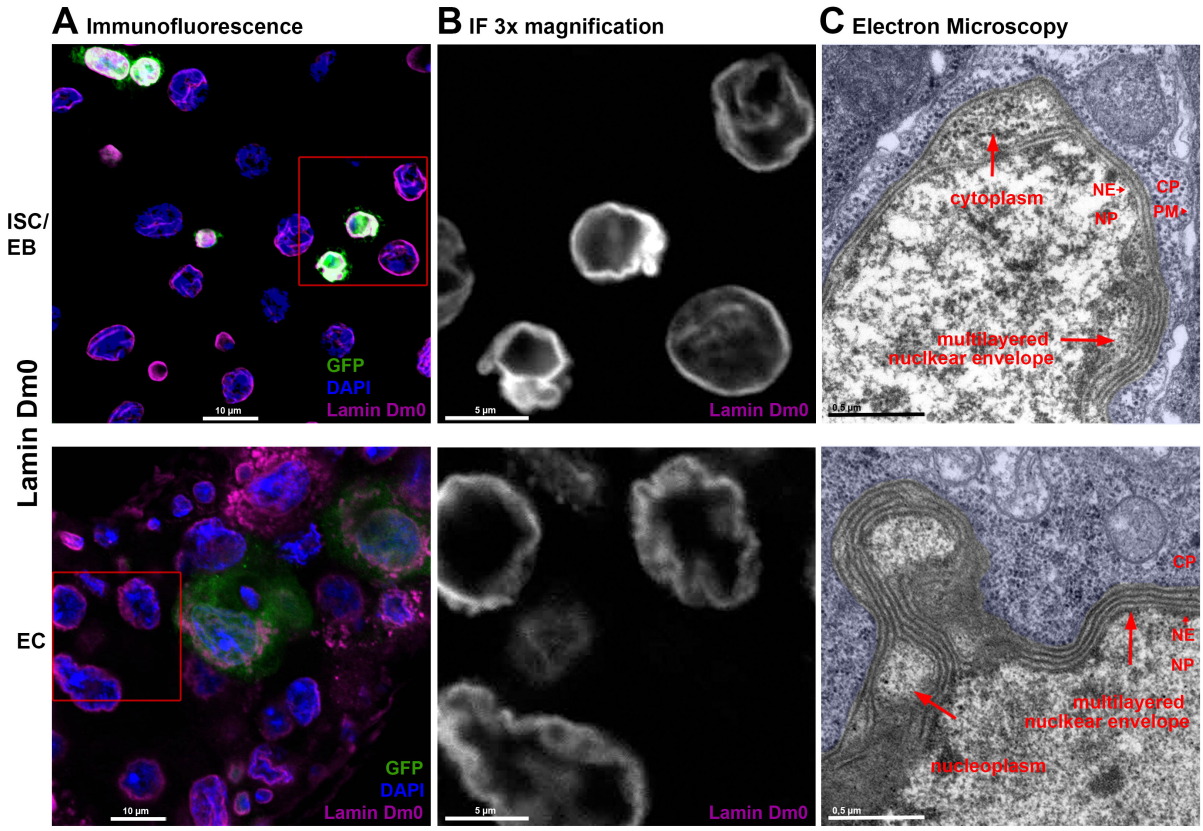

Figure 41: Effect of Lamin Dm0 on nuclear morphology
A: Overlay of GFP, DAPI and Dm0 immunostaining in ISCs/EBs and ECs. All GFP positive cells show nuclear abnormalities, in the EC expressed Dm0 sample also non GFP cells show nuclear abnormalities. Red box marks magnified area. B Magnification of Dm0 staining from (A). Both ISCs/EBs and ECs show nuclear lobulations C: EM recording of ISCs/EBs and ECs. All cell types show a multilayered nuclear envelope with lobulations and infoldings which contain either nucleoplasm or cytoplasm. NP: nucleoplasm, NE: nuclear envelope, CP: cytoplasm, PM: plasma membrane. Blue overlay marks non nuclear regions. ISC/EB: (Esg/+; TS/UASt-Lamin Dm0), EC: (Myo/+; TS/UASt-Lamin Dm0). 5 days of induction.

In EM recordings, ISCs/EBs as well as ECs show a multilayered nuclear envelope with lobulations and pockets of ribosome-containing cytoplasm or nucleoplasm (Figure 41 C). Considering that a multilayered envelope naturally contains more Dm0-specific antibody binding sites, the increased Dm0 immunostaining of GFP positive ISCs/EBs (Figure 41 A, B, ISC/EB) is likely due to this cause.

Expression of Lamin C CaaX lead to increased immunostaining in GFP-positive ISCs/EBs and ECs. Additionally, cytoplasmic aggregations were visible in all GFP-positive cells, in particular ECs (Figure 42 A, B). EM imaging shows a thickened nuclear lamina in all Lamin C expressing cells; cytoplasmic aggregations however are not visible in EM images (Figure 42 C). Possibly Lamin C CaaX forms very thin aggregates or co-localizes with other cellular compartments and thereby remains undetectable in EM imaging.

Expression of Kuk lead to a strong immunostaining throughout the nucleus in all GFP positive cells (Figure 43 A, B). EM recordings show vesicular structures or invaginations of

two types inside the nucleus: vesicles with a double membrane, filled with ribosome-containing cytoplasm, and vesicles with a single membrane filled with mostly clear fluid (Figure 43 C). The here mentioned results are of particular interest because the show unique cellular effects dependent on the type of lamina protein that is overexpressed. This indicates a different set of functions for different lamina proteins, rather than mere redundancy.

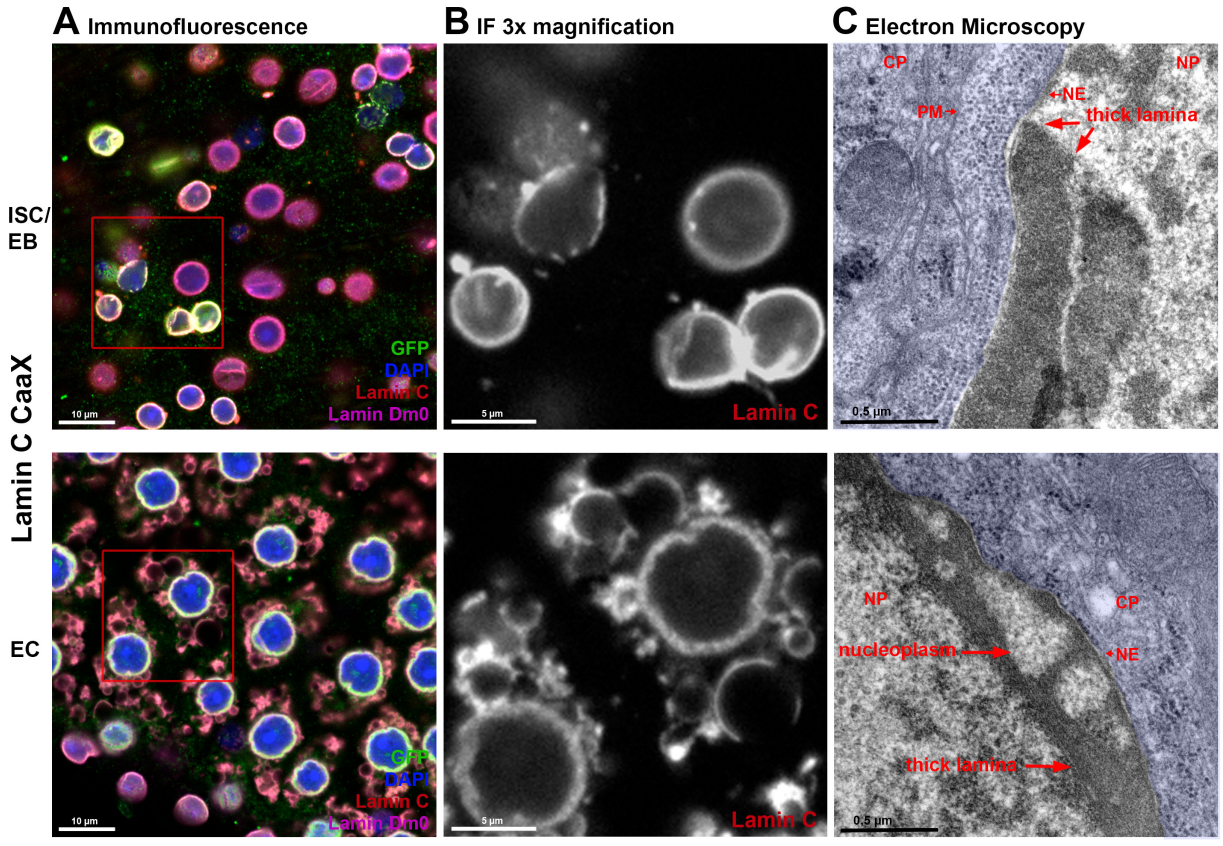

Figure 42: Effect of Lamin C CaaX on nuclear morphology
A: Overlay of GFP, DAPI and Dm0 immunostaining in ISCs/EBs and ECs. Red box marks magnified area. B Magnification of Lamin C staining from (A). ISCs/EBs show strond nuclear staining and nuclear deformations compared to GFP negative cells. ECs show strong nuclear staining and spheric cytoplasmic aggregates. C: EM recording of ISCs/EBs and ECs. All cell types show a thickened nuclear lamina. Cytoplasmic aggregates in ECs were not visible. NP: nucleoplasm, NE: nuclear envelope, CP: cytoplasm, PM: plasma membrane. Blue overlay marks non nuclear regions. ISC/EB: (Esg/UASt-Lamin C CaaX; TS/+), EC: (Myo/UASt-Lamin C CaaX; TS/+). 5 days of induction.

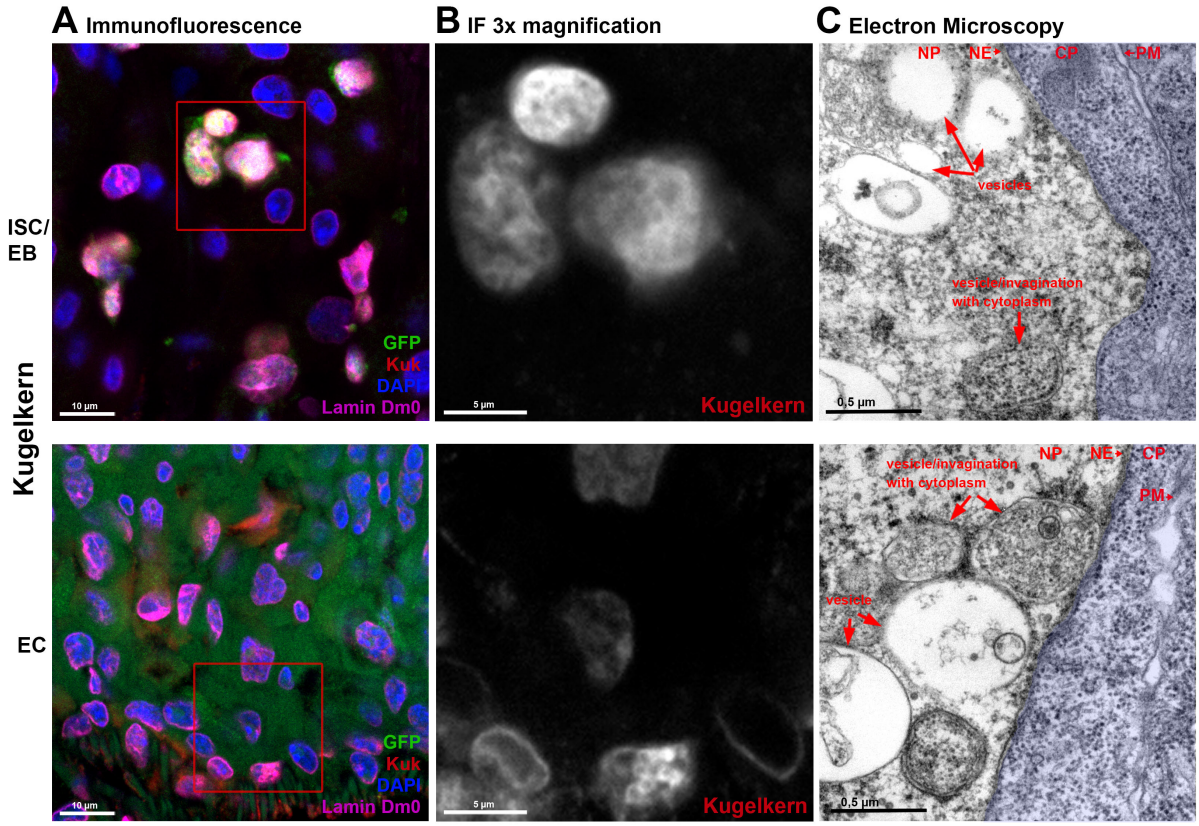

Figure 43: Effect of Kugelkern on nuclear morphology
A: Overlay of GFP, DAPI and Dm0 immunostaining in ISCs/EBs and ECs. Red box marks magnified area. B Magnification of Kugelkern staining from (A). ISCs/EBs and ECs show increased Kuk staining throughout the nucleus. C: EM recording of ISCs/EBs and ECs. All cell types show vesicular structures/infoldings either with a double membrane and cytoplasmic contents or a singular membrane with clear fluid. NP: nucleoplasm, NE: nuclear envelope, CP: cytoplasm, PM: plasma membrane. Blue overlay marks non nuclear regions. ISC/EB: (Esg/UASt-Kuk; TS/+), EC: (Myo/UASt-Kuk; TS/+). 5 days of induction.

3.4.2 *Lipin* RNAi does not ameliorate the effects of Lamin Dm0 overexpression

Lipin is known to play a key role in the synthesis of phospholipids, which are an essential part of the nuclear membrane. Also, in *C. elegans,* Lipin knockdown causes nuclear envelope defects [36]. So it was assumed that knockdown of Lipin could lead to an amelioration of the multi-nuclear envelope effect known from EM recordings of Dm0 overexpressing cells. Therefore, a Lipin-specific antibody was generated and tested in *Lipin* RNAi clones (Figure 44 B). Lipin was successfully downregulated in *Lipin* RNAi clones, compared to non-clonal cells, or wildtype cells (Figure 44 A). In these clones no particular effect on Dm0 levels or distribution was conceivable. Induction of *Lipin* RNAi in Dm0 expressing cells neither ameliorated the inhibitory effect of Dm0 on proliferation, nor lead to changes in nuclear morphology. EM pictures were also acquired from *Lipin* RNAi expressing ECs but no changes were notable (data not shown).

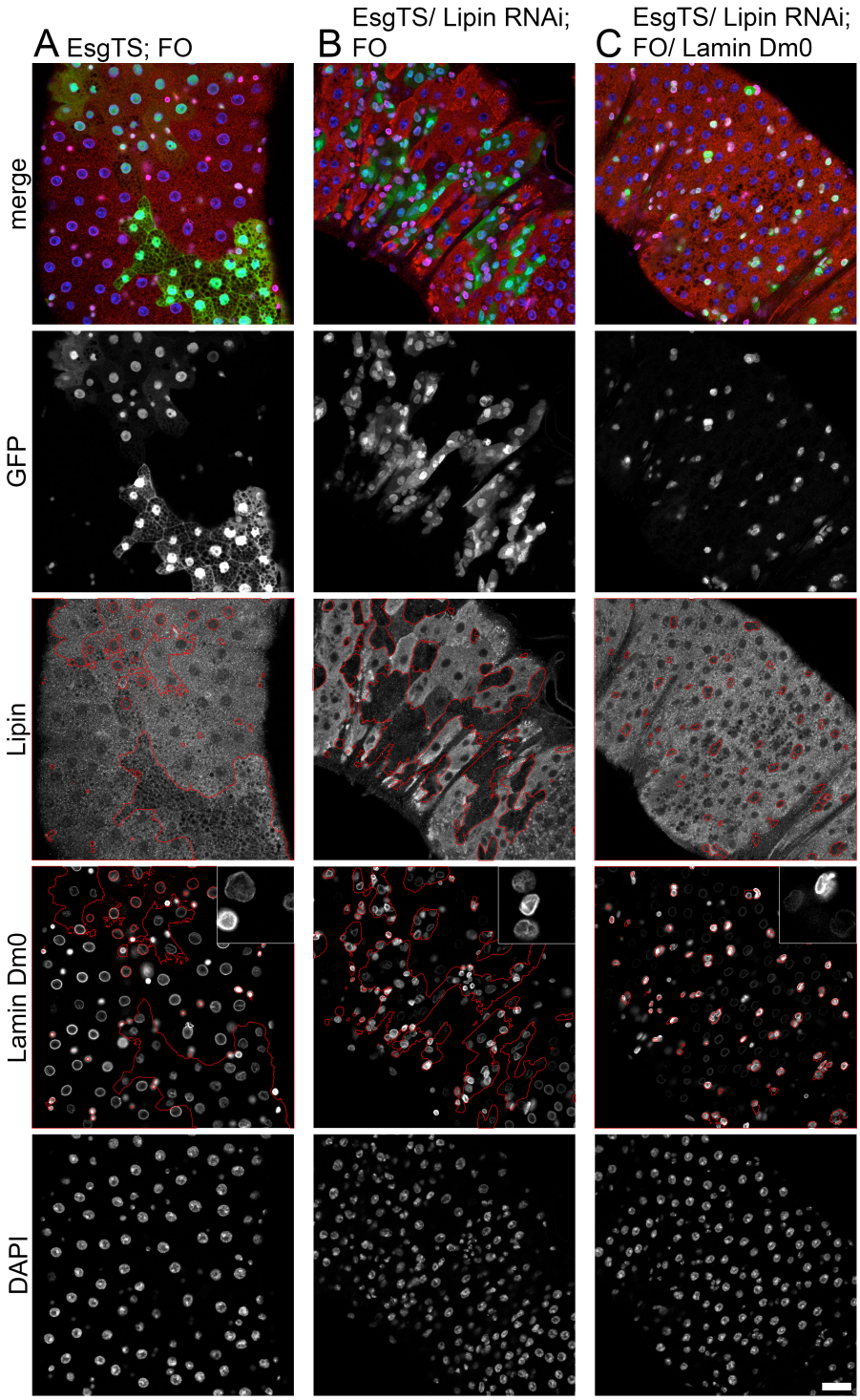

Figure 44: Knockdown of Lipin does not alter Dm0 induced reduction of proliferation
A: (EsgTS/(Sp/CyO); FO/(Dr/TM3)) Control showing uniform lipin staining in the cytoplasm. B: (EsgTS/UAS-*Lipin*-RNAi; FO/+) Expression of *Lipin* RNAi successfully downregulated Lipin in clones but did not cause visible changes to Dm0 staining. C: (EsgTS/UAS-*Lipin*-RNAi; FO/UASt-Dm0) Coexpression of *Lipin* RNAi with Dm0 did not alter the inhibiting effect of Dm0 on ISC proliferation. No changes in nuclear morphology are visible. Red lining marks clones. 3x enlarged detail of gut-cells in the top right of Dm0 channel pictures. Scale bar: 25µm

3.5 Kugelkern

Since Dm0 expression caused a strong inhibitory effect on ISCs in flipout clones, other proteins were also tested in this system. Among them were Kugelkern (Kuk), Lamin C CaaX and Progerin, the altered form of the human Lamin A, causing HGPS. Apart from Kuk no other protein did caused an inhibitory effect on ISC proliferation similar to Dm0. Therefore, Kuk was also tested for inhibition of native and JAK/STAT-induced proliferation, apoptosis and altered nuclear transport.

Overexpression of Kugelkern inhibits native stem cell proliferation

Similar to overexpression of Dm0 in unchallenged ISCs/EBs, overexpression of Kuk in flipout clones lead to a strong reduction in clonal area (Figure 45 B) compared to control flies (Figure 45 A). Indicating either a strong inhibitory effect on the proliferation of intestinal stem cells or induced apoptosis. Quantification of mean fluorescence intensity of guts, overexpressing Kuk in flipout clones, shows a highly significant reduction of clonal area in guts overexpressing Kuk (Figure 45 C). The quantification further shows that the reduction of clonal area, upon Kuk overexpression, has very little variability compared to control flies. This effect is also reminiscent of Dm0 overexpression in flipout clones. The overexpression of Kuk was confirmed by the localization of Kuk throughout the nucleus, previously known from overexpression of Kuk in Esg; TS and Myo; TS lines (Figure 43 A, B).

Kugelkern overexpression does not induce apoptosis

Compared to wildtype (Figure 46 A) Caspase staining neither changed in intensity nor localization, in Kuk expressing clones (Figure 46 B). In both cases clonal cells with (Figure 46 2) and without (Figure 46 1) Caspase staining were recorded. The positive control in wing discs (Figure 14 C, D) indicates that those Caspase positive cells show low level background staining of the Caspase antibody and not Caspase levels equal to actual activation of apoptosis.
Additionally it was attempted to ameliorate the effects of Kuk by coexpressing Kuk and the "*Drosophila* inhibitor of apoptosis" (DIAP) protein (Figure 47). Coexpression of DIAP however did not change the proliferative behavior of Kuk overexpressing ISCs. In all, the results indicate that Kuk overexpression in ISCs does not induce apoptosis and that the reduction of clonal area, in Kuk overexpressing flipout clones, is likely due to inhibition of ISC proliferation.

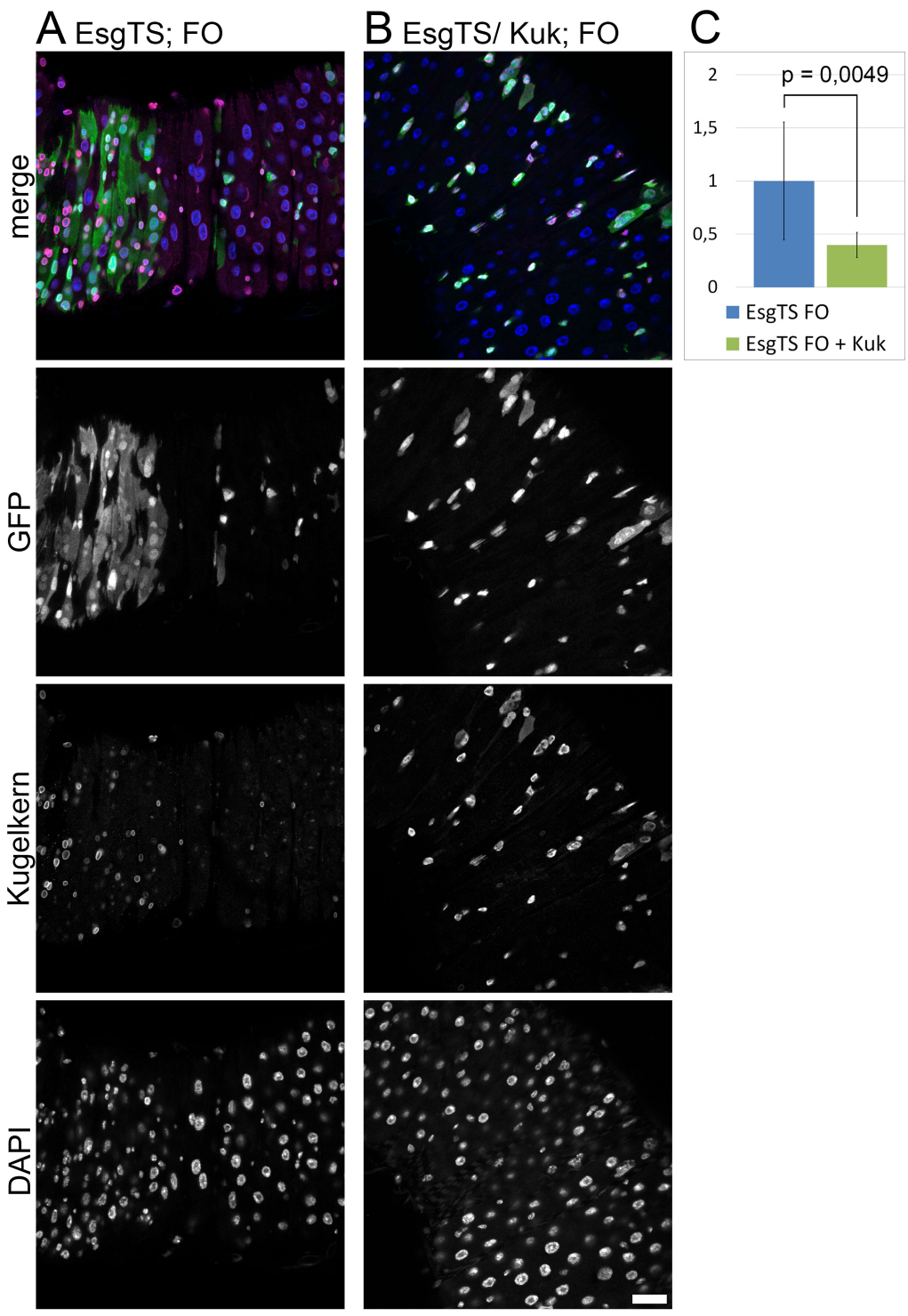

Figure 45: Kugelkern overexpression inhibits native stem cell proliferation
A: (EsgTS/(Sp/CyO); FO/(Dr/TM3)) Control. B: (EsgTS/UASt-Kuk; FO/+) Kuk overexpression leads to a strong reduction of stem cell proliferation. C: Quantification of stem cell proliferation by mean fluorescence/gut, normalized to control. Clonal induction for 5 days. Scale bar: 25 µm

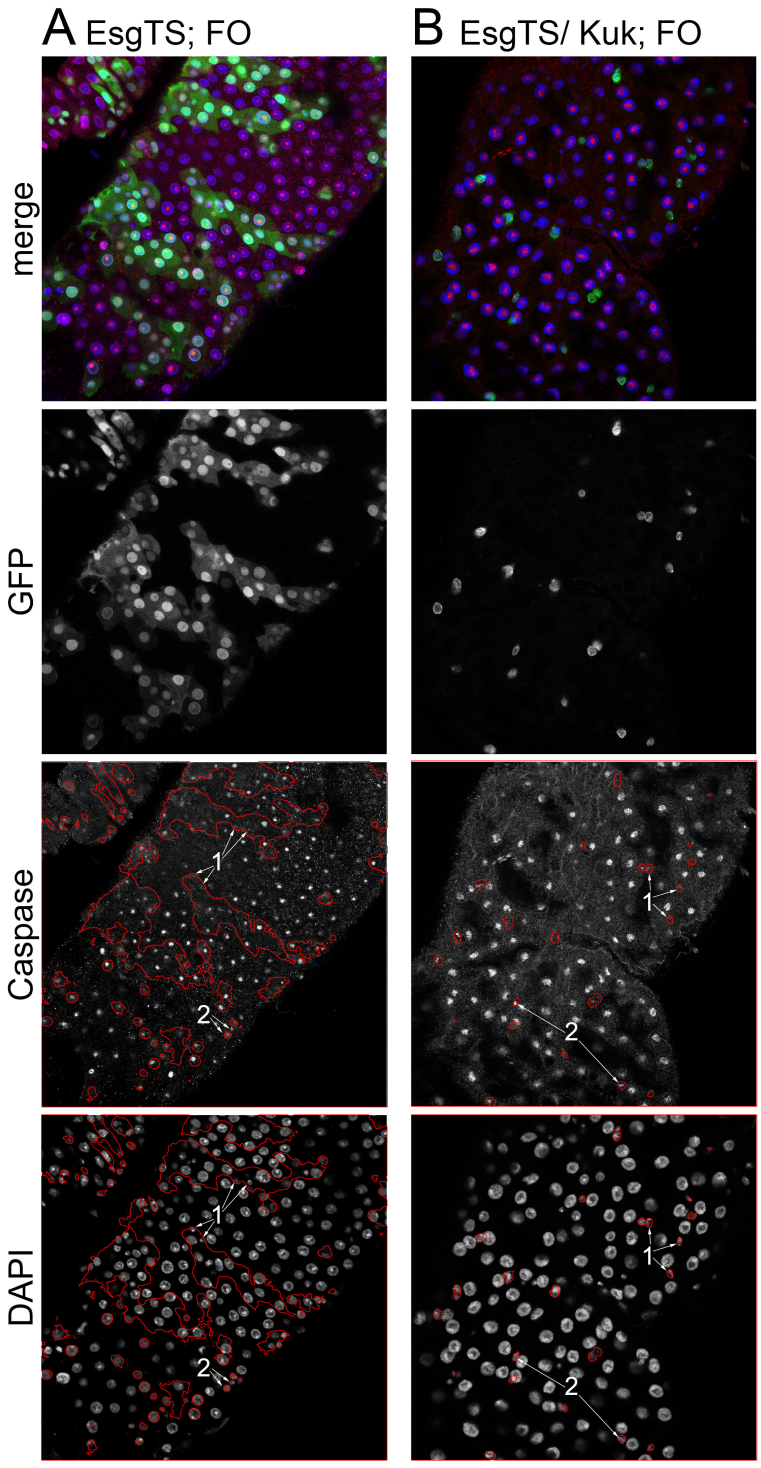

Figure 46: Kugelkern overexpression does not affect Caspase levels
A: (EsgTS/(Sp/CyO); FO/(Dr/TM3)) Control showing relatively uniform Caspase staining of cells in the optical plane. B: (EsgTS/UASt-Kuk; FO/+) Expression does not change levels of Caspase staining. (1) Clonal cells without Caspase staining. (2) Clonal cells with Caspase staining. Clonal induction for 5 days. Red outline marks GFP + clones. Scale bar: 25µm

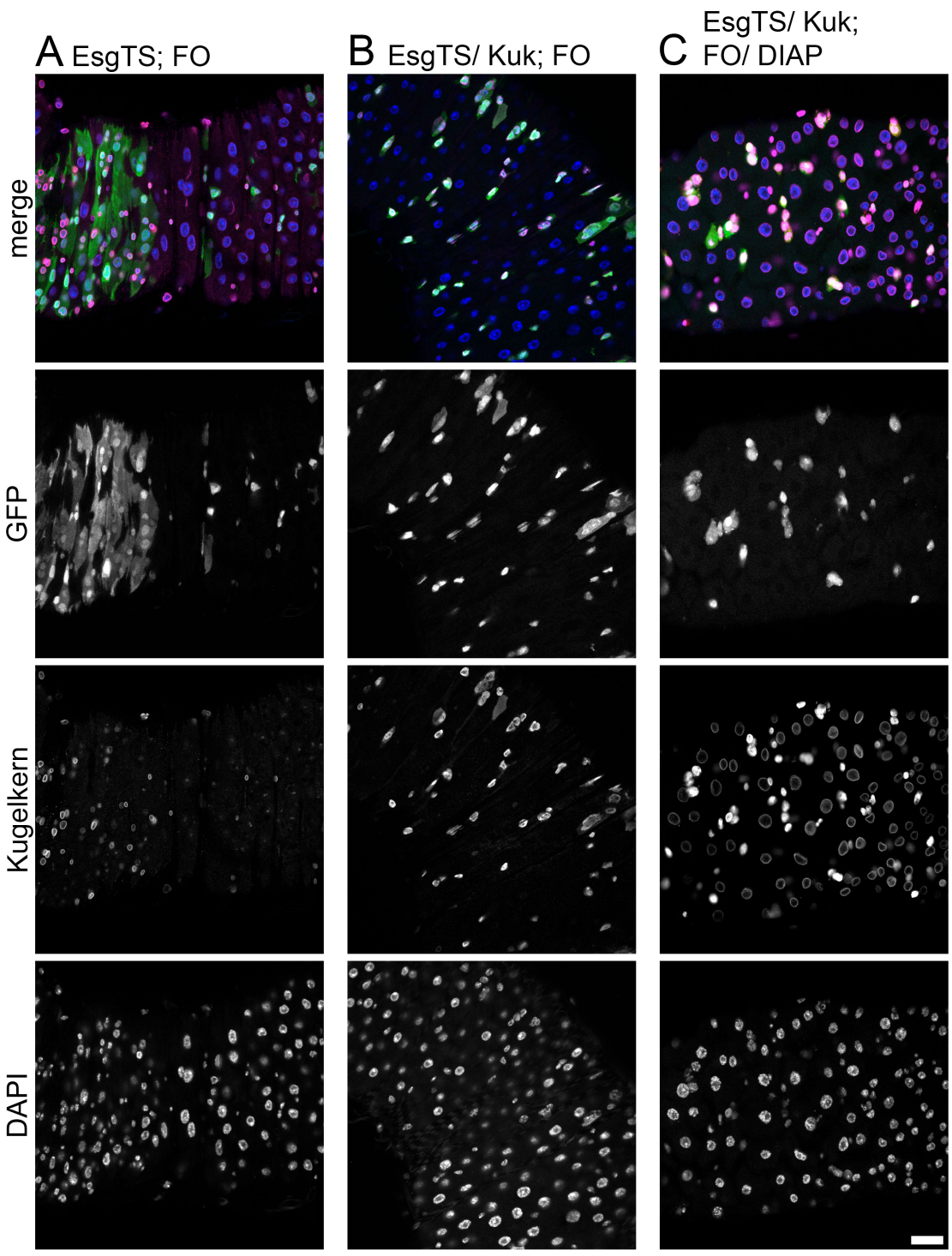

Figure 47: Expression of DIAP does not reduce Kugelkern induced reduction of stem cell proliferation

A: (EsgTS/(Sp/CyO); FO/(Dr/TM3)) Control. B: (EsgTS/UASt-Kuk; FO/+) Kuk expression reduces ISC proliferation compared to control. C: (EsgTS/UASt-Kuk; FO/UAS-DIAP) Coexpression of DIAP does not change proliferation behavior of Kuk expressing ISCs. Clonal induction for 5 days. Scale bar: 25µm

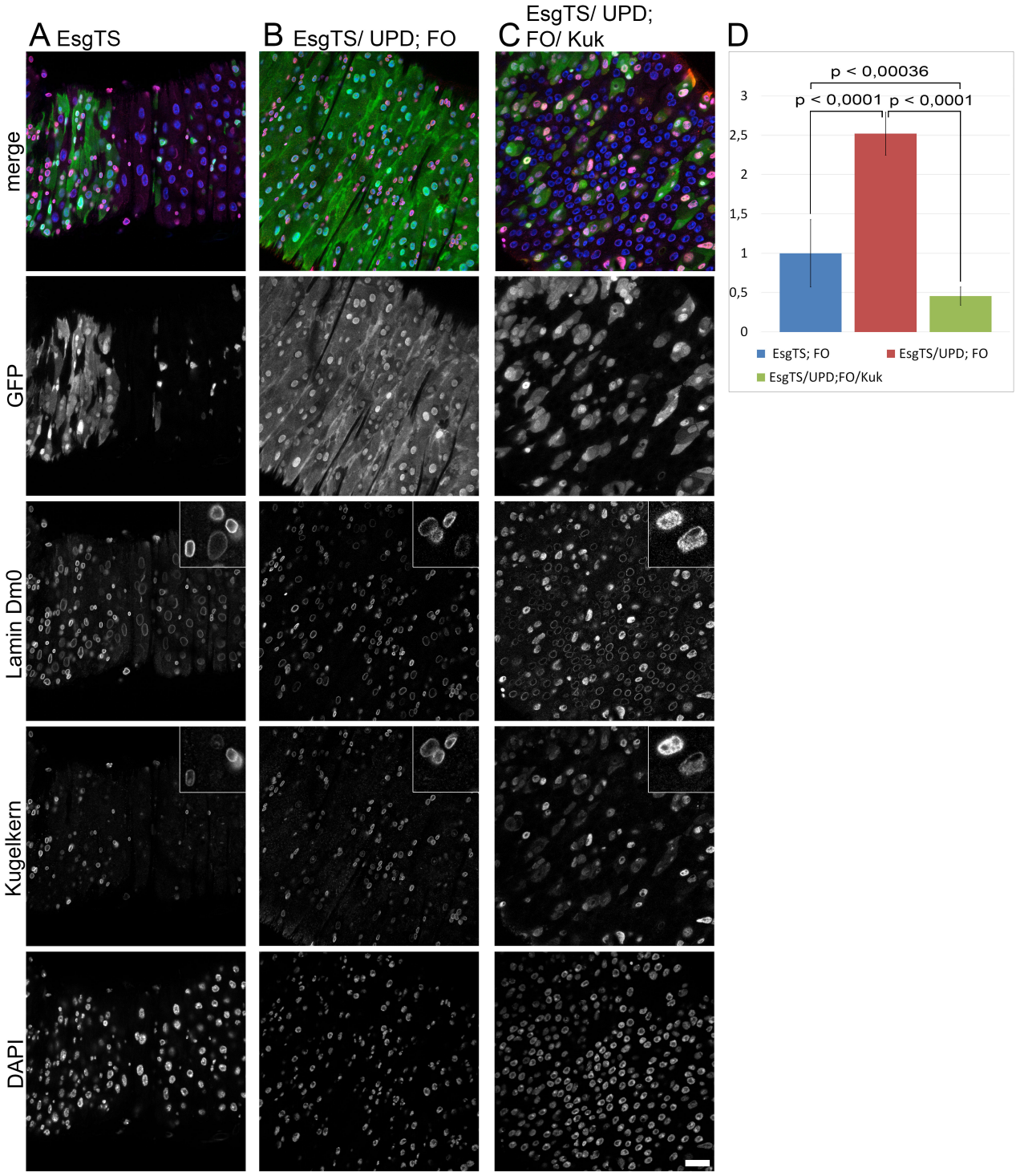

Figure 48: Kugelkern overexpression inhibits UPD induced stem cell proliferation
A: (EsgTS/(Sp/CyO); FO/(Dr/TM3)) Control. B: (EsgTS/UAS-UPD; FO/+) Expression of UPD induces strong ISC proliferation with clones covering most of the intestinal surface. C: (EsgTS/UAS-UPD; FO/UASt-Kuk) Coexpression of Kuk with UPD significantly reduces proliferation even below wildtype levels. D: Quantification of mean fluorescence of phenotypes A, B, C. Clonal induction for 5 days. White box in Dm0 and Kuk staining marks 3 x enlarged exemplary cells. Scale bar: 25µm

Kugelkern inhibits UPD induced stem cell proliferation

To test whether Kuk expression could inhibit JAK/STAT-induced ISC proliferation similar to Dm0, Kuk was coexpressed with UPD in flipout-clones and compared to wildtype and cells expressing only UPD (Figure 48 A, B, C). Immunostaining in UPD expressing guts revealed a higher occurrence of small cell types with higher Kuk and Dm0 staining (Figure 48 B), indicating increased prolifaration of ISCs. Also a significant increase in clonal area was recorded in these guts (Figure 48 D). In cells with UPD and Kuk overexpression Dm0 and Kuk staining was distributed throughout the nucleus in a similar manner (Figure 48 C, small box). Dm0 shows costaining with Kuk throughout the nucleus. This was recorded before and is typical for Kuk overexpression. Kuk overexpression significantly reduced JAK/STAT-induced proliferation to levels even significantly lower than wildtype (Figure 48 D).

3.5.1 Effect of Kugelkern on nuclear transport

To test whether the inhibitory effect of Kuk is due to impairment of nuclear transport, a set of different sized GFP constructs was used to probe for altered transport behavior of Kc167 cells. The fusion-constructs are 1x, 2x, 5x, and 10x repetitions of GFP plus a DAM methylase and a nuclear localization sequence (NLS). After transfection, the cells showed different limitations of the constructs to enter the nucleus (Figure 49). All cells transfected with the 1x GFP and 2x GFP constructs showed a binary logarithm (log2) of the nucleoplasmic/cytoplasmic (np/cp) ratio bigger/equal to 1, indicating no hindrance of the constructs to enter the nucleus. However, cells transfected with the 5x GFP and 10x GFP construct showed increasing numbers of cells with smaller NP/CP ratios (Figure 50 A), indicating increased numbers of cells where the fusion constructs were unable to enter the nucleus. For instance about 27% of cells transfected with the 5x GFP construct showed a log2 NP/CP smaller/equal 1 (and bigger/equal to 0) and about 14% with a log2 (NP/CP) bigger/equal to -1 (and smaller/equal to 0). This trend intensifies in 10x GFP transfected cells where the majority of cells has a stronger cytoplasmic than nucleoplasmic staining, indicating that in most cells the majority of 10x fusion constructs were unable to enter the nucleus. Upon coexpression of Kuk, the general distribution of cells with nucleoplasmic ratios typical to their constructs does not change significantly (Figure 50 B). According to this result, Kuk overexpression does not influence the nuclear transport.

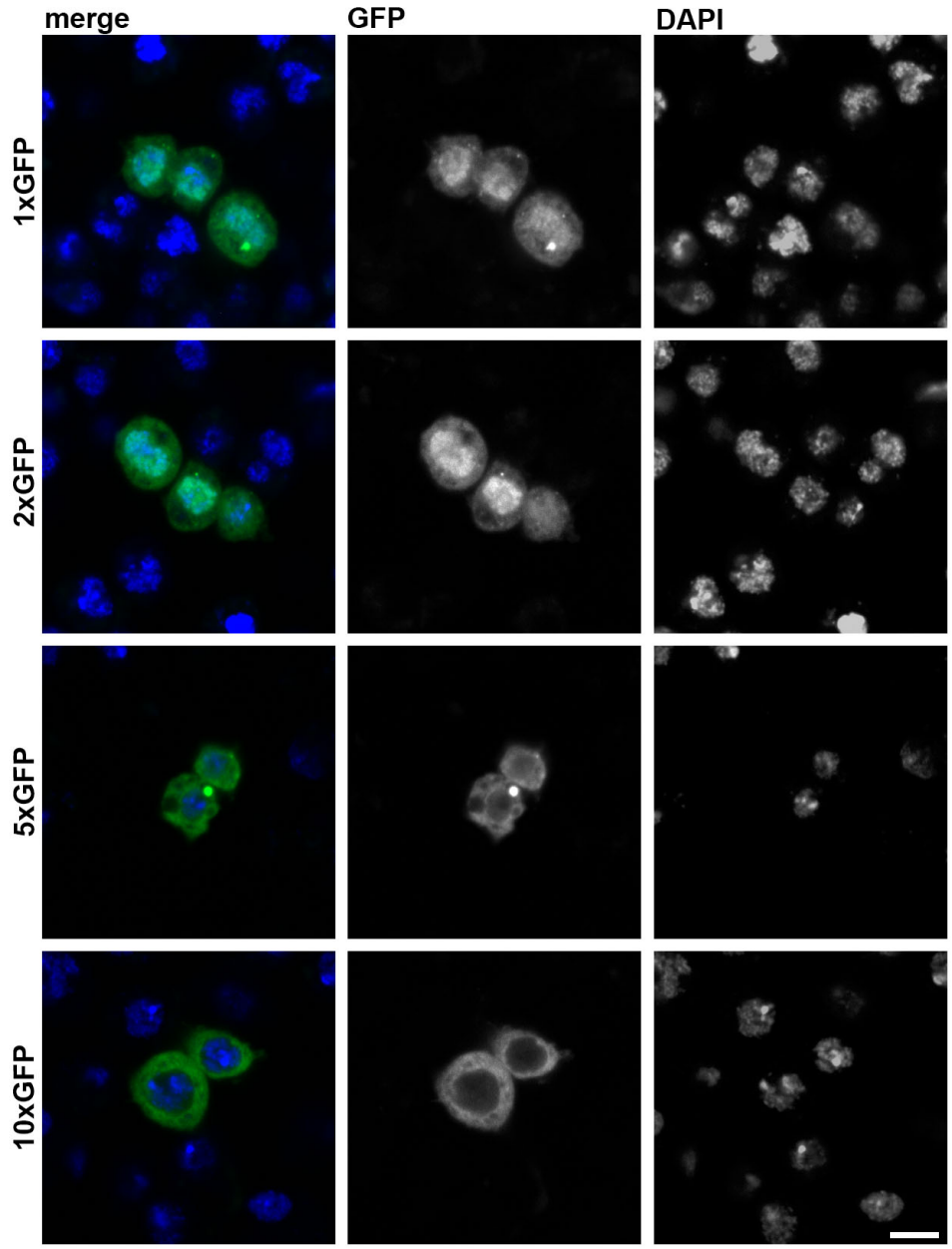

Figure 49: 1x, 2x, 5x, 10x GFP constructs.

Exemplary selection of cells transfected with 1x, 2x, 5x, 10x-GFP constructs shows typical nucleoplasmic/cytoplasmic distribution for each transfected construct. Nuclei are identified by DAPI and increased (1xGFP, 2x-GFP) or decreased (5xGFP, 10x-GFP) GFP signal. GFP constructs are able to enter the nucleus at sizes 1xGFP to 2xGFP but are increasingly excluded from the nucleus at sizes 5xGFP to 10xGFP. Scale bar 5 µm.

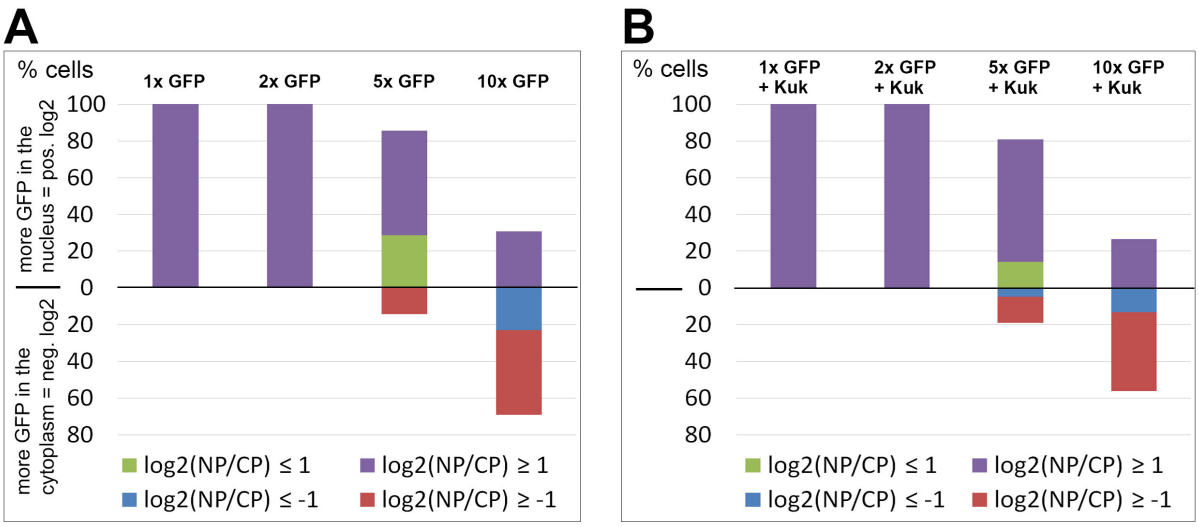

Figure 50: Overexpression of Kugelkern does not alter nuclear transport. Quantification Bar diagram of % of cells transfected with 1x, 2x, 5x, 10x GFP constructs, without Kuk (A) and with Kuk (B), with binary logarithms of measured nucleoplasmic/cytoplasmic ratios ranging from bigger/equal 1 (more GFP measured in the nucleus) to smaller/equal -1 (more GFP measured in the cytoplasm). Both A and B show an increase of cells that have more GFP in the cytoplasm when higher number GFP constructs (5x, 10x) are expressed.

3.5.2 Treatment with the farnesyl transferase inhibitor ABT100

To reproduce previous results that were generated by Dr. Annely Brandt and were indicating that treatment of cells with the farnesyl transferase inhibitor ABT100 could reduce nuclear shape changes induced by Kuk expression (unpublished data-Dr Annely Brandt). Kc167 cells were treated with different concentrations of ABT100. The cells however did not respond to previously reported doses (6 µm of ABT100) so several higher doses were tested (12,4 µM, 60 µM, 120 µM, Figure 51 B, C, D). However, even at double the dose of ABT100, cells did not show nucleoplasmic Kuk or Dm0 staining (Figure 51 A, 1, B, 1). Some cells did show increased nucleoplasmic staining of Kuk and Dm0 in comparison to their peers but this effect was also visible in the control cells (Figure 51 2), which was probably due to cells lying in a different optical plane. Only at a 10 times higher dose of ABT did cells show increased levels of nucleoplasmic Kuk but not Dm0 (Figure 51 C, 3). Only at a 20 times higher dose of ABT100 did cells show also an increase of nucleoplasmic Dm0 (Figure 51 C, 4).

Since Kc167 cells showed an effect of ABT100, though at much higher doses than reported, similar doses were tested in flies. However neither in gut nor in muscle tissue did these doses had any effect. In a last attempt, a 161 times higher dose was administered to GFP-Kuk expressing cells (Figure 52 B, D) but did not result in significant changes of Kuk or GFP-Kuk in muscle or intestinal cells. It can be argued that the strongest effect should be visible in GFP-Kuk levels since GFP-Kuk is freshly synthesized together with ABT100 treatment, due to transfection, but Kuk and GFP-Kuk distribution at the nuclear envelope and the nucleoplasm was similar.

It can be concluded that though ABT100 did show an effect on Kc167 cells, it was at much higher doses and therefore ABT probably lost most of its activity. Since this ABT100 sample was a one time gift of Abbot to the Großhans lab and production of ABT100 never initiated, no new ABT100 could be acquired. It is unclear however why high doses of ABT100, that were significantly inhibiting farnesylation in Kc167 cells, were not able to inhibit farnesylation in gut and muscle tissues. Presumably only a small portion of ingested ABT100 can be taken up by the intestine. Considering the potential reduction of ABT100 activity, the portion of active ABT100 taken up by the intestine route would be negligible for any cellular effect in muscles. Also gut cells were stained for Dm0 and Kuk upon ingestion of high ABT100 doses (data not shown) and no significant effect was observable.

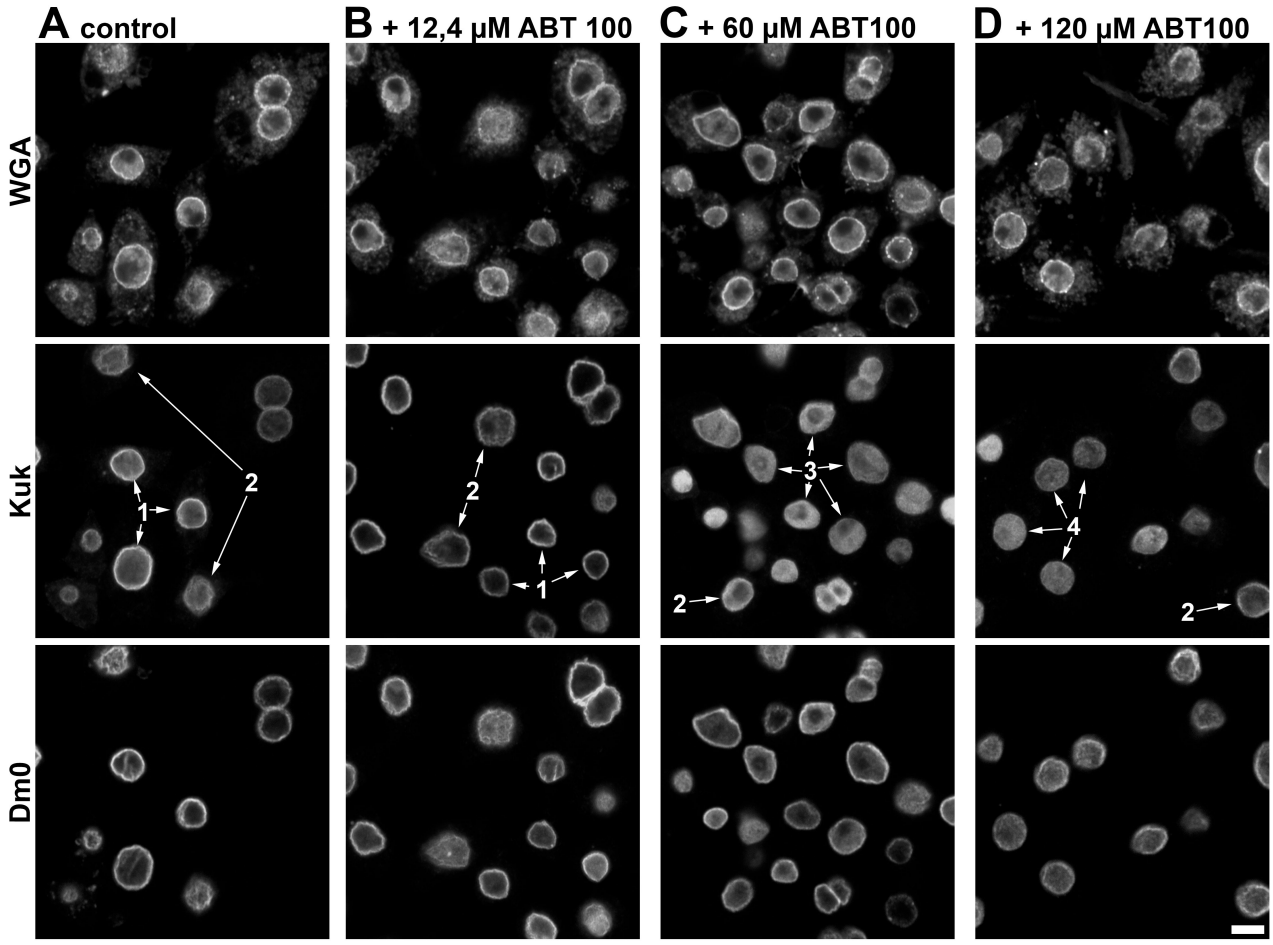

Figure 51: ABT100 treatment in Kc167 cells

Treatment of Kc167 cells with ABT100 for 3 days. A: control, B: ABT concentration in supernatant 12,4 µM C: 60 µM, D: 120 µM. (1) Cells which show no change in nucleoplasmic Kuk or Dm0 levels. (2) Cells which appear to be having increased levels of nucleoplasmic Kuk/Dm0 but are also found in control and are probably in a different optical plane. (3) Cells which show increased levels of nucleoplasmic Kuk but not Dm0. (4) cells which show increased nucleoplasmic Kuk and Dm0. WGA: Wheat germ aglutinin, Scale bar: 5µm

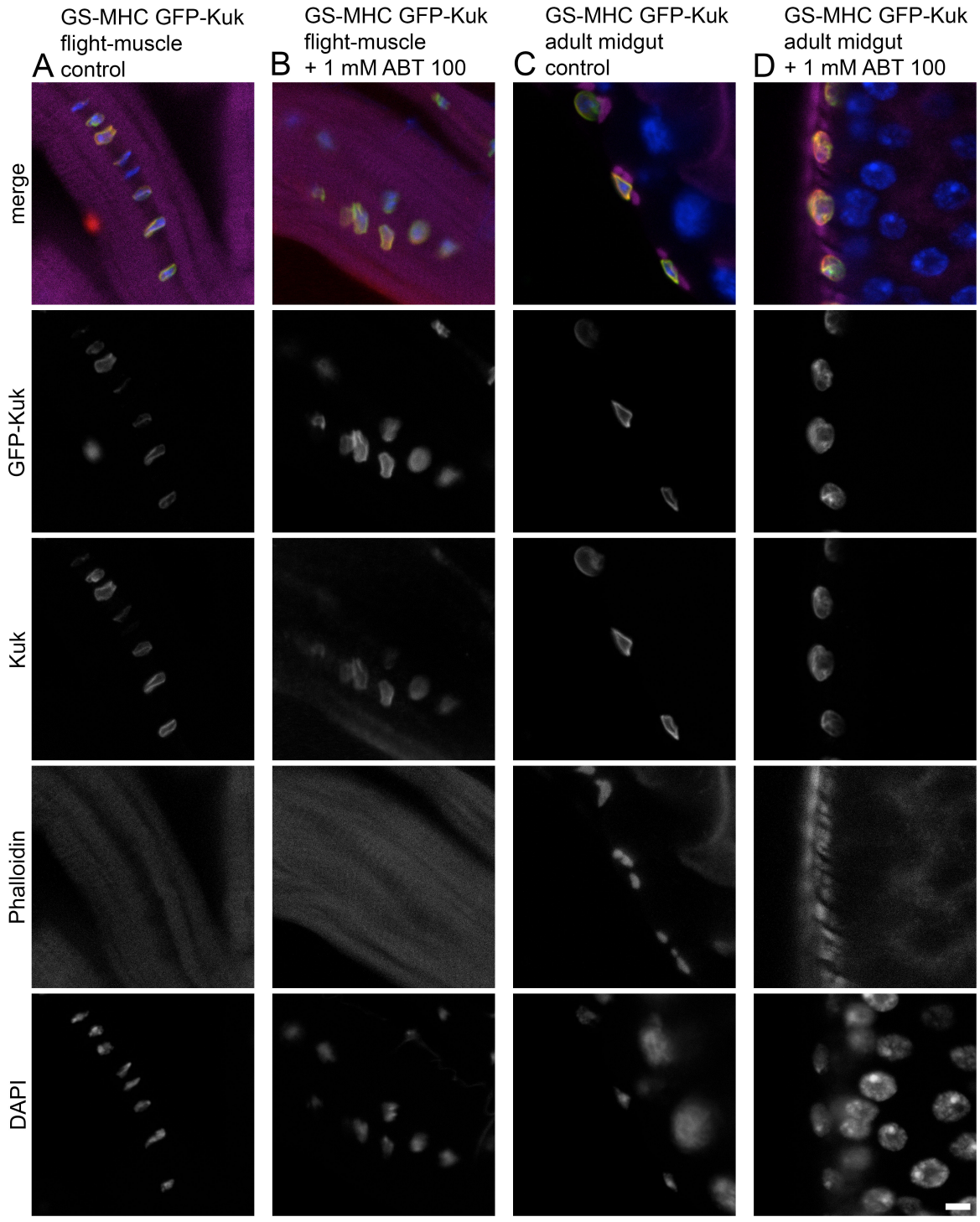

Figure 52: ABT100 treatment in muscle and midgut

A: Control. Muscle cells expressing Kuk without ABT100. B: Muscle cells expressing Kuk with 1 mM ABT100 concentration in food. C: Control. Intestinal cells expressing Kuk without ABT100. Sideview of gut epithelium with lumen on the right. D: Intestinal cells expressing Kuk with 1 mM ABT100 concentration in food. Sideview of gut epithelium with lumen on the right. Treatment of flies with ABT100 for 3 days in all displayed cases. Scale bar: 5µm

4 Discussion

4.1 Lamin Dm0

4.1.1 Overexpression of Dm0 inhibits ISC proliferation by inhibition of the JAK/STAT pathway

Initial experiments have shown that Dm0 overexpression induces a significant reduction in ISC proliferation in native conditions (Figure 12). This could possibly result from ablation of either ISCs or EBs. However, no significant decline of GFP-positive ISCs/EBs was noted that could explain such a strong effect. Also, midguts of flies with Dm0 overexpression were stained with Caspase-3 antibody that was successfully tested in fly wing discs (Figure 14 C and D) and by the supplier (Figure 14 E). Though the antibody stained both the active form of Caspase-3 and the inactive procaspase form, it showed a much higher specificity to the active form. Considering this and the fact that Caspase-3 staining of wildtype cells was similar to Caspase-3 staining in Dm0 overexpressing cells (Figure 14 A and B), it can be concluded that levels of active Caspase 3 were not increased in Dm0 overexpressing cells. Additionally, the effect of Dm0 overexpression could be overruled by the coexpression of *Notch* RNAi in ISCs (Figure 15 C1 and C2). This lead to the formation of Notch-tumors which were smaller than Notch-tumors induced in wildtype flies but similar in occurrence throughout the midgut. This shows that Dm0 overexpressing ISCs did not lose their ability to proliferate.

Since Dm0 overexpression did not harm or alter basic ISC identity, it was reasonable to test whether it affects the signaling pathways responsible for ISC proliferation. However only activation of JAK/STAT and Hippo signaling pathways resulted in a clear increase in ISCs proliferation (Figure 17, Figure 19 A and B, Figure 18 A and B). Coexpression of Dm0 with UPD or *Warts* RNAi resulted in a drastic reduction of ISC proliferation in both cases (Figure 19 C, Figure 18 C) but since Hippo-induced Stem cell proliferation requires a basic level of JAK/STAT signaling, both phenotypes could result from an inhibition of the JAK/STAT pathway.

The comparative analysis of Dm0 and Stat levels in UPD and Dm0 overexpressing midguts revealed that Dm0 and Stat levels are anticorrelated (Figure 23). This further strengthens the hypothesis that Dm0 affects the JAK/STAT pathway. However, no general decrease in Stat levels was recorded in ISCs/EBs during Dm0 expression alone. Instead, some GFP-positive

cells have higher Stat levels while others don't show Stat staining (Figure 22 D, 1 and 2). It is possible that Stat levels are different in ISCs, EBs and EEs. Since all three cell types are marked by GFP in the flipout system, no distinction is possible. Additional experiments might help to answer that question.

Expression of StatΔNΔC was used to initiate the JAK/STAT pathway activation at the level of Stat to test whether Dm0 would act upstream or downstream of Stat. No significant increase in proliferation was noted upon StatΔNΔC expression however Stat staining was drastically reduced in clonal cells in contrast to increased Stat staining in non clonal cells. This indicates that StatΔNΔC was expressed effectively and that Stat levels would decrease due to SOCS36E-mediated feedback. StatΔNΔC is possibly also inducing upregulation if JAK/STAT signaling in neighboring non clonal cells. This would likely increase their proliferation and thereby put them in direct competition to clonal cells, which would explain why clonal area did not increase upon StatΔNΔC expression. If this scenario is true, Dm0 overexpression did successfully downregulate StatΔNΔC-induced proliferation, thereby indicating a point of effect downstream of Stat.

dMyc was reported to function downstream of JAK/STAT, Hippo and EGFR signaling and regulate their effects on ISC proliferation (Figure 27 A) [74]. Therefore it was conceivable to test whether Dm0 overexpression would alter dMyc levels. However no significant changes were noted. It is possible that dMyc requires a higher level of upstream pathway activation first, to increase levels significantly enough to be affected by Dm0. It could also mean that Dm0 overexpression in a situation of low JAK/STAT, Hippo and EGFR pathway activity inhibits proliferation differently than in a situation of cellular stress with high pathway activity. Both hypotheses fit with the observation that small GFP-positive cell types show a mixed Stat staining with Dm0 overexpresson alone whereas in a situation with Dm0 and UPD coexpression levels of Stat in clonal cells are lower throughout. At this stage, at any rate, no conclusive estimation about the role of dMyc in Dm0 mediated inhibition of proliferation can be given.

RNAseq analysis has revealed a possible modus operandi for Dm0 mediated inhibition of ISCs. Transcripts for the UPD receptor domeless (dome) are significantly increased in samples with JAK/STAT pathway activation (Table 7 dome). However upon coexpression of Dm0 and UPD domeless transcripts are reduced to normal levels. This indicates that Dm0 affects JAK/STAT signaling on a transcriptional level, by downregulating the UPD receptor domeless. Secreted UPD from enterocytes can not effectively activate the JAK/STAT pathway and thereby initiate the proliferative response of ISCs.

Interestingly domeless transcript levels are not downregulated upon Dm0 expression alone. This indicates that in a regular situation with low JAK/STAT activity Dm0 likely represses ISC proliferation in a different manner.

It can be concluded that Dm0 likely suppresses the activated JAK/STAT pathway on a transcriptional level by downregulating the UPD receptor domeless.

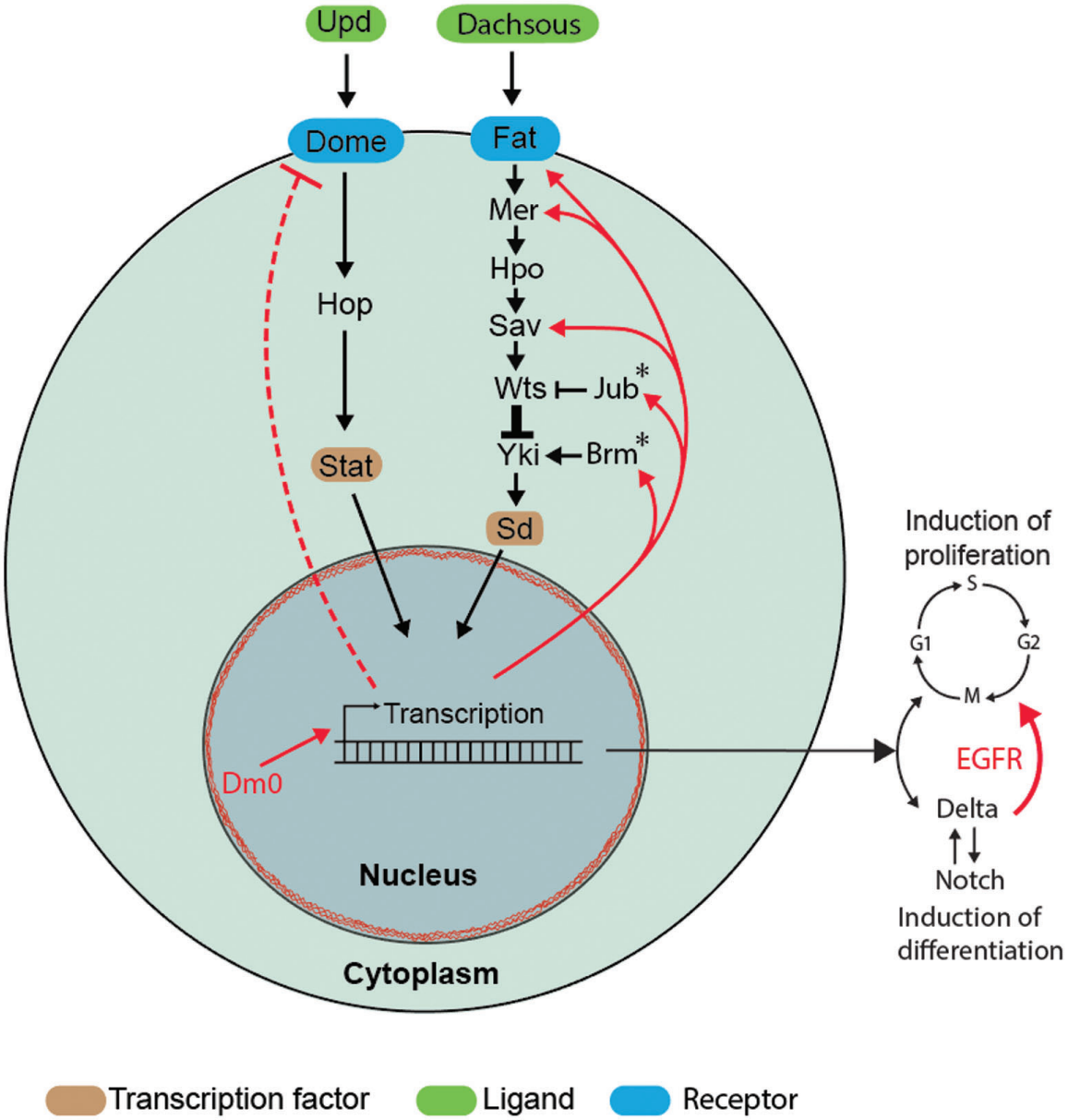

Figure 53: Model for Dm0 mediated inhibition of ISC proliferation
Upon overexpression, Dm0 downregulates domeless transcripts which leads to the inhibition of the JAK/STAT pathway and thereby, decrease in ISC proliferation. Hippo pathway induced proliferation is dependent on a basal level of JAK/STAT activity, the pathway is possibly inhibited indirectly by downregulation of Jak/Stat or more directly, by Dm0 affecting transcription and upregulating pathway components (Red arrows). (*) markes Hippo pathway components (Jub, Brm) that induce proliferation. Fat, Mer, Sav were upregulated and reduce proliferation. Dm0 induced inhibition of ISC proliferation can be overruled by Delta/Notch signaling which activates the EGFR pathway in ISCs, thereby inducing proliferation.
Jack/Stat pathway components: Unpaired (UPD), Domeless (Dome), Hopscotch (Hop), Stat. Hippo pathway components: Dachsous, Fat, Merlin (Mer), Hippo (Hpo), Yorkie (Yki), Salvador (Sav), Warts (Wts), Ajuba (Jub), Brahma (Brm), Scalloped (Sd).

The Hippo pathway is possibly repressed by Dm0 indirectly since it requires a certain level

of JAK/STAT activity to induce proliferation (Picture 53). However Dm0 is likely also affecting the Hippo pathway directly. 5 genes that are part of Hippo signal transduction were identified by GO analysis that were upregulated upon Dm0 overexpression. Two of them would result in increased proliferation, Ajuba a negative regulator of Warts [73] and Brahma(Brm) which binds Yorkie (Yki) and is required for Yki activation [94]. The three other genes are tumor suppressors that play key roles upstream of Warts. Salvador (Sav) which forms a repressive complex with Hpo and Warts [69, 88], Merlin (Mer) which recruits Wts for consecutive phosphorylation and activation [91] and fat which is is a cell-surface receptor that binds to Dachsous and thereby promotes Hippo signaling[57]. Though the five upregulated genes represent a mixed situation for increase ore decrease of ISC proliferation, the balance is on the side of inhibition. 3 of the five genes decrease proliferation and the strongest increase in transcript numbers is noted with the receptor fat (Table 36). Also in its function as receptor the strongest regulatory function can be considered here. Therefore it can be concluded that Dm0 overexpression leads to a reduction of proliferation by affecting the Jak/Stat and Hippo pathway. Whether the effects on Hippo are due to the downregulation of Jak/Stat or more directly remains unclear. Delta/Notch signaling however can partially overrule the inhibitory effect of Dm0, possibly by activation of EGFR signaling [71].

4.1.2 Cell cycle control

The authors that introduced the flyFUCCI system tested it in ISCs, under the control of the Delta promoter, and in EEs, under the control of the prospero promoter, in wildtype flies [95]. They reported that about 40% of ISCs were in G2, about 57% in G1 and about 3% in S-phase. EEs were about 90% in G2, 7% in G1 and 3% in S-phase. EBs were not tested. Upon stress induction by feeding of *Pseudomonas entomophila*, the number of ISCs in G2 increased from about 57% to 70% and the number of ISCs in S phase from 3% to 8%.

The fact that most of the ISCs/EBs that were tested in this work were found in G2-phase (Figure 29) indicates that EBs are likely, similar to EEs, mostly in G2 phase and that the cells in G1 are mostly ISCs. Overexpression of Dm0 in ISCs/EBs lead to an increase in the number of cells in G2 and S-phase. Considering that ISCs reportedly shifted into G2 and S-phase upon stress induction, this might indicate a type of stress response in ISCs upon Dm0 overexpression. However the increase in S phase reported in the paper[95] is possibly a byproduct of increased division.

To summarize, Dm0 affects the cell cycle in ISCs/EBs though it is not clear which of the two cell types are affected in which way. Thereby it is uncertain how to interpret the finding at this point. If ISCs are the cells that shift from G1 to G2 and S-phase, this indicates a similar response to Dm0 overexpression as to P.e. ingestion. However since Dm0 has an inhibitory effect on proliferation the increase in S-phase is unlikely a result of proliferation. However cells

could be arrested or slowed in S-phase.

4.1.3 Gene expression of Dm0 overexpressing ISCs/EBs

Since overexpression of Dm0 together with UPD lead to the normalization of about 50% of the UPD-induced transcripts, the effect of Dm0 on UPD is likely specific (Figure 31). The normalization of domeless transcripts in UPD and Dm0 coexpressing samples gives also a locus for this interaction. Therefore many target genes of JAK/STAT signaling might simply be affected downstream. On the other hand, GO analysis of Dm0 and UPD overexpressing samples revealed that also Dm0 specific transcripts were affected by UPD expression (Figure 32 C). These transcripts mostly lie in the transport category, a category that was also present in samples with UPD expression alone. It seems that Dm0 and UPD affect each other in this particular field leading to the complete absence of transport specific transcripts with significant up or downregulation. No effect on transport behavior was found in cell culture experiments with transfected Dm0 (Figure 30 C) so at least nuclear/cytoplasmic transport appears to be unaffected. What other types of transport might be altered by Dm0 and possibly normalized by UPD or vice versa, is uncertain. Additionally UPD and Dm0 overexpressing samples show the appearance of transcripts categorized into the group "G-protein coupled receptor signaling pathway " ,a new category that was not present before in either only UPD or Dm0 overexpressing samples. As G-protein signaling is involved in many different processes no particular interpretation can be made at this point [41].
Several pathway candidates were specifically searched for in the pool of significantly up or downregulated transcripts. The tested categories involved apoptosis, cell cycle and the ISC proliferation regulating signaling pathways EGFR, JAK/STAT, Hippo, Wg/Wn and BMP/Dpp. UPD2 is downregulated upon UPD1 overexpression likely due to the effect of the SOCS36E-mediated negative feedback loop that is however overruled by constant UPD1 transcript expression. Interestingly *Notch* transcripts are upregulated in all three samples however possibly due to different reasons. In case of UPD the increased overproliferation of ISCs probably leads to an increased number of EBs which have higher levels of Notch expression. On the other hand the fact that *Notch* transcripts are upregulated upon Dm0 overexpression might indicate a similar effect on stem cells as was reported by Scaffidi and Misteli 2008 [78]. The authors reported an upregulation of Notch target genes in HGPS-patient mesenchymal stem cells.
Comparison of LADs with significantly up or downregulated transcripts showed no correlation with either induction or repression of genes in samples with Dm0 overexpression. It is possible that Dm0 plays no role in the organization of LADs as this result falls into line with a recently published paper, stating that lamins play no role in organization of LADs in mouse [4].

4.1.4 Lamin function

Quantification of clonal area of P.e. infected flies did show an increase of clonal area in control-infected vs. control non-infected flies (Figure 38 A). Infected guts with Dm0 null clones show a reduction of clonal area with a p-value of 0.063 which is close to the generally accepted statistical significance level of 0.05. This alone could indicate a repressive effect on the ability of clonal cells to proliferate. However the increase of clonal area in infected control cells vs. non-infected control cells rather indicates a general variability of the system as there is no reason why clonal cells in the infected control sample should proliferate more than non-clonal cells. This reasoning clearly reduces the chance of a significant effect of Dm0 knockdown on the ability of ISCs to proliferate. Quantification of PH3 cells of infected control flies vs. non-infected control flies shows a significantly increased amount of PH3 cells within and outside clones (Figure 38 B). This indicates that the P.e. infection was successfully inducing ISC proliferation. Infected flies with Dm0 knockdown clones showed an even stronger increase of PH3-positive cells in non-clonal areas but a decreased amount of PH3-positive cells in Dm0 null clones, compared to infected control cells. The effect however, was not significant enough to justify the proposal of an inhibitory effect. It could be argued that since P.e. infectiousness varies from fly to fly the best indicator for an inhibitory effect of Dm0 knockdown would be the ratio of clonal vs non-clonal cells, indicating how much proliferation would be inhibited in clones vs non-clonal cells. An increase in this ratio would indicate a stronger discrepancy in clonal vs non-clonal proliferation. Flies with clonal Dm0 knockdown indeed show the highest non-clonal/clonal ratio in PH3-positive cells. However the effect was still not significant due to strong variation of PH3 cells per gut in all infected flies. Therefore a preliminary conclusion is that an inhibitory effect of Dm0 knockdown on stem cells is possible; however more data has to be generated to increase the significance of the effect. Furthermore, it is unclear whether a complete knockdown was achieved since an ISC, with the recombination event, starts with a normal amount of Dm0 that is consecutively thinned out with each division. A remaining rest however might still hold essential functionality.

4.2 EM analysis of Lamina proteins

EM recordings of Dm0 overexpressing ISCs and ECs both show a multi layered nuclear phenotype with enclosures of ribosome containing cytoplasm (Figure 41 C). It is conceivable that the proliferating nuclear envelope wraps itself several times around the nucleus thereby trapping cytoplasmic content. This scenario could explain why Dm0 overexpressing ISCs often show a distinct GFP staining at the nuclear cortex. It is also intriguing that despite such a severe phenotype ISCs are still able to proliferate upon *Notch* RNAi expression. It can be hypothesized that either the multi-layered nuclear envelope is not limiting for cell division or it is thinned out

enough by consecutive division to not reach limiting levels. It is also surprising that, considering the likely obstruction of a multi-layered nuclear envelope, no change in transport behavior was observed in Kc167 cells (Figure 30). Dm0 overexpressing Kc167 cells show changed nuclear morphology and increased Dm0 staining at the nuclear cortex but it is unclear if this results from the same structural origin as in Dm0 overexpressing intestinal cells.
Immuno pictures of ISCs and ECs overexpressing Lamin C CaaX did show several cytoplasmic aggregations in particular in ECs (Figure 42 A and B) these aggregations, that even can form ring structures, were not visible in EM pictures (Figure 42 C). Instead they show a thickened lamina which is also represented by increased immunostaining . It is possible however that the sphere shaped cytoplasmic aggregates indicate a general tendency of farnesylated Lamins to assemble into round shapes. This is plausible since one of the functions of the lamina is to provide stability to the nucleus.
EM recordings of Kuk overexpressing ISCs and ECs both show invaginations or vesicles with either cytoplasmic content or a clear fluid (Figure 43 C). It is conceivable that the first type is caused by invagination of the nuclear envelope from the cytoplasm, therefore containing ribosomes, and the second type by invagination of the inner nuclear membrane, therefore only containing fluid present in the perinuclear space and ER. The density of vesicles also explains why immuno-staining of cells that overexpress Kuk led to a staining throughout the nucleus instead of only the nuclear cortex. Kuk is likely coating the vesicles/invaginations thereby directing antibodies to the vesicles/invaginations. It can be hypothesized whether Kuk plays a role in the formation of the nucleoplasmic reticulum since also the nucleoplasmic reticulum has two known forms. One with cytoplasmic content enveloped with a double membrane and one with inter membrane space enveloped with a single membrane. [38, 56]. Farnesylated Prelamin A plays a role in the formation of the nucleoplasmic reticulum in mice [38] but since Drosophila does not have a Lamin A allele it is possible that Kuk has taken over this role, possibly in concert with condensins [11].

4.3 Kugelkern

Kuk and Dm0 have shown several functional similarities. Overexpression of both induces ageing-like phenotypes in Drosophila, like decrease in fitness and lifespan. They also both show cellular effects attributed to HGPS, like misshaped nuclei, decrease in heterochromatin and increase in DNA damage [13]. However the nuclear distribution of Kuk and Dm0 is different for the overexpression of each protein. While Dm0 overexpression induces a thick layer of Dm0 staining at the nuclear envelope, Kuk overexpression induces immunostaining of Kuk and Dm0 throughout the nucleus. Both effects can be explained by the recorded EM pictures. While Dm0 staining is increased due to a multilayered nuclear envelope, upon Dm0 overexpression, Kuk staining is found throughout the nucleus due to invaginations or vesicles that entered

the nuclear space (Figure 41 C, Figure 43 C). The fact that Dm0 co-localizes with Kuk in these cases, indicates that in both situations the two lamina proteins, and likely others, were transported along with invaginations/vesicles or multilayered nuclear envelope. In this work it is shown that Kuk also inhibits native ISC proliferation (Figure 45) and UPD1 induced proliferation, though to a slightly lower degree. It is remarkable that, despite these similarities, Dm0 and Kuk show very different cellular phenotypes upon overexpression . Also despite the apparent severity of the nuclear phenotype, Kuk overexpression did not not change Caspase levels compared to control (Figure 46 A and B) and expression of DIAP did not change the inhibiting effect on ISC proliferation (Figure 47). Both findings indicate that overexpression of Kuk does not induce apoptosis. Considering the severety of the structural changes visible in EM pictures of Kuk overexpressing ISCs/EBs and ECs it is surprizing that Kuk overexpressing Kc167 cells did not show any significant changes in nuclear transport behavior (Figure 50 A and B). It is possible that Kuk acts differently on Kc167 cells than intestinal cells.

List of Figures

List of Tables

Bibliography

[1] Robert P Aaronson and Gunter Blobel. Isolation of nuclear pore complexes in association with a lamina. *Proceedings of the National Academy of Sciences*, 72(3):1007–1011, 1975. 1.1

[2] Ueli Aebi, Julie Cohn, Loren Buhle, and Larry Gerace. The nuclear lamina is a meshwork of intermediate-type filaments. 1986. 1.1

[3] Kamna Aggarwal and Neal Silverman. Positive and negative regulation of the drosophila immune response. *BMB reports*, 41(4):267–277, 2008. 1.2

[4] Mario Amendola and Bas van Steensel. Nuclear lamins are not required for lamina-associated domain organization in mouse embryonic stem cells. *EMBO reports*, page e201439789, 2015. 4.1.3

[5] Allison J Bardin, Carolina N Perdigoto, Tony D Southall, Andrea H Brand, and François Schweisguth. Transcriptional control of stem cell maintenance in the drosophila intestine. *Development*, 137(5):705–714, 2010. 1.3

[6] Samira Bina, Victoria M Wright, Katherine H Fisher, Marta Milo, and Martin P Zeidler. Transcriptional targets of drosophila jak/stat pathway signalling as effectors of haematopoietic tumour formation. *EMBO reports*, 11(3):201–207, 2010. 3.2

[7] Samira Bina and Martin Zeidler. Jak/stat pathway signalling in drosophila melanogaster. 2000. 3.2

[8] B. Biteau, C.E. Hochmuth, and H. Jasper. JNK activity in somatic stem cells causes loss of tissue homeostasis in the aging Drosophila gut. *Cell Stem Cell*, 3(4):442–455, 2008. 1.3

[9] Benoît Biteau and Heinrich Jasper. Egf signaling regulates the proliferation of intestinal stem cells in drosophila. *Development*, 138(6):1045–1055, 2011. 1.3

[10] Gisèle Bonne, Marina Raffaele Di Barletta, Shaida Varnous, Henri-Marc Bécane, El-Hadi Hammouda, Luciano Merlini, Francesco Muntoni, Cheryl R Greenberg, Françoise Gary, Jon-Andoni Urtizberea, et al. Mutations in the gene encoding lamin a/c cause autosomal dominant emery-dreifuss muscular dystrophy. *Nature genetics*, 21(3):285–288, 1999. 1.2

[11] Julianna Bozler, Huy Q Nguyen, Gregory C Rogers, and Giovanni Bosco. Condensins exert force on chromatin-nuclear envelope tethers to mediate nucleoplasmic reticulum formation in drosophila melanogaster. *G3: Genes| Genomes| Genetics*, 5(3):341–352, 2015. 4.2

[12] Annely Brandt, Georg Krohne, and Jörg Großhans. The farnesylated nuclear proteins kugelkern and lamin b promote aging-like phenotypes in drosophila flies. *Aging cell*, 7(4):541–551, 2008. 1.2

[13] Annely Brandt, Fani Papagiannouli, Nicole Wagner, Michaela Wilsch-Bräuninger, Martina Braun, Eileen E Furlong, Silke Loserth, Christian Wenzl, Fanny Pilot, Nina Vogt, et al. Developmental control of nuclear size and shape by kugelkern and kurzkern. *Current biology*, 16(6):543–552, 2006. 1.2, 4.3

[14] Joanna M Bridger and Ian R Kill. Aging of hutchinson–gilford progeria syndrome fibroblasts is characterised by hyperproliferation and increased apoptosis. *Experimental gerontology*, 39(5):717–724, 2004. 1.2

[15] JLV Broers, FCS Ramaekers, G Bonne, R Ben Yaou, and CJ Hutchison. Nuclear lamins: laminopathies and their role in premature ageing. *Physiological reviews*, 86(3):967–1008, 2006. 2

[16] Nicolas Buchon, Nichole A Broderick, Takayuki Kuraishi, and Bruno Lemaitre. Drosophila egfr pathway coordinates stem cell proliferation and gut remodeling following infection. *BMC biology*, 8(1):152, 2010. 1.3

[17] Nicolas Buchon, Nichole A Broderick, Mickael Poidevin, Sylvain Pradervand, and Bruno Lemaitre. Drosophila intestinal response to bacterial infection: activation of host defense and stem cell proliferation. *Cell host & microbe*, 5(2):200–211, 2009. 1.2

[18] Haiyang Chen, Xin Chen, and Yixian Zheng. The nuclear lamina regulates germline stem cell niche organization via modulation of egfr signaling. *Cell Stem Cell*, 13(1):73–86, 2013. 1.2, 3.3

[19] Haiyang Chen, Xiaobin Zheng, and Yixian Zheng. Age-associated loss of lamin-b leads to systemic inflammation and gut hyperplasia. *Cell*, 159(4):829–843, 2014. 1.2

[20] Na Hyun Choi, Elena Lucchetta, and Benjamin Ohlstein. Nonautonomous regulation of drosophila midgut stem cell proliferation by the insulin-signaling pathway. *Proceedings of the National Academy of Sciences*, 108(46):18702–18707, 2011. 1.3

[21] Alexandre Chojnowski, Peh Fern Ong, Esther SM Wong, John SY Lim, Rafidah A Mutalif, Raju Navasankari, Bamaprasad Dutta, Henry Yang, Yi Y Liow, Siu K Sze, et al. Progerin reduces lap2α-telomere association in hutchinson-gilford progeria. *eLife*, page e07759, 2015. 1.2

[22] H.D.M. Coutinho, V.S. Falcão-Silva, G.F. Gonçalves, and R.B. da Nóbrega. Molecular ageing in progeroid syndromes: Hutchinson-Gilford progeria syndrome as a model. *Immunity & Ageing*, 6(1):4, 2009. 1.2

[23] Annachiara De Sandre-Giovannoli, Rafaelle Bernard, Pierre Cau, Claire Navarro, Jeanne Amiel, Irene Boccaccio, Stanislas Lyonnet, Colin L Stewart, Arnold Munnich, Martine Le Merrer, et al. Lamin a truncation in hutchinson-gilford progeria. *Science*, 300(5628):2055–2055, 2003. 1.2

[24] Michelle L Decker, Elizabeth Chavez, Irma Vulto, and Peter M Lansdorp. Telomere length in hutchinson-gilford progeria syndrome. *Mechanisms of ageing and development*, 130(6):377–383, 2009. 1.2

[25] Radoslaw K Ejsmont and Bassem A Hassan. The little fly that could: wizardry and artistry of drosophila genomics. *Genes*, 5(2):385–414, 2014. 35

[26] Laura A Ekas, Timothy J Cardozo, Maria Sol Flaherty, Elizabeth A McMillan, Foster C Gonsalves, and Erika A Bach. Characterization of a dominant-active stat that promotes tumorigenesis in drosophila. *Developmental biology*, 344(2):621–636, 2010. 3.1.1

[27] Maria Eriksson, W Ted Brown, Leslie B Gordon, Michael W Glynn, Joel Singer, Laura Scott, Michael R Erdos, Christiane M Robbins, Tracy Y Moses, Peter Berglund, et al. Recurrent de novo point mutations in lamin a cause hutchinson–gilford progeria syndrome. *Nature*, 423(6937):293–298, 2003. 1.2

[28] Jesús Espada, Ignacio Varela, Ignacio Flores, Alejandro P Ugalde, Juan Cadiñanos, Alberto M Pendás, Colin L Stewart, Karl Tryggvason, María A Blasco, José MP Freije, et al. Nuclear envelope defects cause stem cell dysfunction in premature-aging mice. *The Journal of cell biology*, 181(1):27–35, 2008. 1.2, 3.1.1

[29] Don W Fawcett. On the occurrence of a fibrous lamina on the inner aspect of the nuclear envelope in certain cells of vertebrates. *American Journal of Anatomy*, 119(1):129–145, 1966. 1.1

[30] Maria Sol Flaherty, Jiri Zavadil, Laura A Ekas, and Erika A Bach. Genome-wide expression profiling in the drosophila eye reveals unexpected repression of notch signaling by the jak/stat pathway. *Developmental Dynamics*, 238(9):2235–2253, 2009. 3.2

[31] Roland Foisner and Larry Gerace. Integral membrane proteins of the nuclear envelope interact with lamins and chromosomes, and binding is modulated by mitotic phosphorylation. *Cell*, 73(7):1267–1279, 1993. 1.1

[32] Spyros D Georgatos, Christos Stournaras, and GUNTER Blobel. Heterotypic and homotypic associations between the nuclear lamins: site-specificity and control by phosphorylation. *Proceedings of the National Academy of Sciences*, 85(12):4325–4329, 1988. 1.1

[33] Larry Gerace and Brian Burke. Functional organization of the nuclear envelope. *Annual review of cell biology*, 4(1):335–374, 1988. 1.1

[34] AD Gerstein, TJ Phillips, GS Rogers, and BA Gilchrest. Wound healing and aging. *Dermatologic clinics*, 11(4):749–757, 1993. 1.2

[35] Martin Goldberg. Import and export at the nuclear envelope. *The Nuclear Envelope*, pages 115–134, 2004. 1.1

[36] Andy Golden, Jun Liu, and Orna Cohen-Fix. Inactivation of the c. elegans lipin homolog leads to er disorganization and to defects in the breakdown and reassembly of the nuclear envelope. *Journal of cell science*, 122(12):1970–1978, 2009. 3.4.2

[37] Robert D Goldman, Yosef Gruenbaum, Robert D Moir, Dale K Shumaker, and Timothy P Spann. Nuclear lamins: building blocks of nuclear architecture. *Genes & development*, 16(5):533–547, 2002. 1.2

[38] Chris N Goulbourne, Ashraf N Malhas, and David J Vaux. The induction of a nucleoplasmic reticulum by prelamin a accumulation requires ctp: phosphocholine cytidylyltransferase-α. *Journal of cell science*, 124(24):4253–4266, 2011. 4.2

[39] Michael R Green and Joseph Sambrook. *Molecular cloning: a laboratory manual*, volume 1. Cold Spring Harbor Laboratory Press New York, 2012. 2.2.1, 2.2.5

[40] Zheng Guo, Ian Driver, and Benjamin Ohlstein. Injury-induced bmp signaling negatively regulates drosophila midgut homeostasis. *The Journal of cell biology*, 201(6):945–961, 2013. 1.3

[41] Heidi E Hamm. The many faces of g protein signaling. *Journal of Biological Chemistry*, 273(2):669–672, 1998. 4.1.3

[42] Raoul Hennekam. Hutchinson–gilford progeria syndrome: review of the phenotype. *American journal of medical genetics Part A*, 140(23):2603–2624, 2006. 1.2

[43] Huaqi Jiang, Parthive H Patel, Alexander Kohlmaier, Marc O Grenley, Donald G McEwen, and Bruce A Edgar. Cytokine/jak/stat signaling mediates regeneration and homeostasis in the drosophila midgut. *Cell*, 137(7):1343–1355, 2009. 1.3, 3.1.1, 3.1.1, 3.3

[44] Arnold Kahn and Mario F Fraga. Epigenetics and aging: status, challenges, and needs for the future. *The Journals of Gerontology Series A: Biological Sciences and Medical Sciences*, 64(2):195–198, 2009. 1.3

[45] Phillip Karpowicz, Jessica Perez, and Norbert Perrimon. The hippo tumor suppressor pathway regulates intestinal stem cell regeneration. *Development*, 137(24):4135–4145, 2010. 1.3

[46] Joshua B Kelley, Sutirtha Datta, Chelsi J Snow, Mandovi Chatterjee, Li Ni, Adam Spencer, Chun-Song Yang, Caelin Cubeñas-Potts, Michael J Matunis, and Bryce M Paschal. The defective nuclear lamina in hutchinson-gilford progeria syndrome disrupts the nucleocytoplasmic ran gradient and inhibits nuclear localization of ubc9. *Molecular and cellular biology*, 31(16):3378–3395, 2011. 3.1.3

[47] Isabelle Krimm, Cecilia Östlund, Bernard Gilquin, Joël Couprie, Paul Hossenlopp, Jean-Paul Mornon, Gisèle Bonne, Jean-Claude Courvalin, Howard J Worman, and Sophie Zinn-Justin. The ig-like structure of the c-terminal domain of lamin a/c, mutated in muscular dystrophies, cardiomyopathy, and partial lipodystrophy. *Structure*, 10(6):811–823, 2002. 1.1

[48] Zhouhua Li, Yan Zhang, Lili Han, Lai Shi, and Xinhua Lin. Trachea-derived dpp controls adult midgut homeostasis in drosophila. *Developmental cell*, 24(2):133–143, 2013. 3.1.1

[49] Lili Liang, Huiwen Zhang, and Xuefan Gu. Homozygous lmna mutation r527c in atypical hutchinson–gilford progeria syndrome: evidence for autosomal recessive inheritance. *Acta Paediatrica*, 98(8):1365–1368, 2009. 1.2

[50] Guonan Lin and Rongwen Xi. Intestinal stem cell, muscular niche and wingless signaling. *Fly*, 2(6):310–312, 2008. 1.3

[51] Guonan Lin, Na Xu, and Rongwen Xi. Paracrine wingless signalling controls self-renewal of drosophila intestinal stem cells. *Nature*, 455(7216):1119–1123, 2008. 1.3, 1.3

[52] Guonan Lin, Na Xu, and Rongwen Xi. Paracrine unpaired signaling through the jak/stat pathway controls self-renewal and lineage differentiation of drosophila intestinal stem cells. *Journal of molecular cell biology*, 2(1):37–49, 2010. 1.3

[53] Baohua Liu, Jianming Wang, Kui Ming Chan, Wai Mui Tjia, Wen Deng, Xinyuan Guan, Jian-dong Huang, Kai Man Li, Pui Yin Chau, David J Chen, et al. Genomic instability in laminopathy-based premature aging. *Nature medicine*, 11(7):780–785, 2005. 1.2

[54] Yiyong Liu, Antonio Rusinol, Michael Sinensky, Youjie Wang, and Yue Zou. Dna damage responses in progeroid syndromes arise from defective maturation of prelamin a. *Journal of cell science*, 119(22):4644–4649, 2006. 1.2

[55] Teresa R Luperchio, Xianrong Wong, and Karen L Reddy. Genome regulation at the peripheral zone: lamina associated domains in development and disease. *Current opinion in genetics & development*, 25:50–61, 2014. 3.2

[56] Ashraf Malhas, Chris Goulbourne, and David J Vaux. The nucleoplasmic reticulum: form and function. *Trends in cell biology*, 21(6):362–373, 2011. 4.2

[57] Hitoshi Matakatsu and Seth S Blair. Interactions between fat and dachsous and the regulation of planar cell polarity in the drosophila wing. *Development*, 131(15):3785–3794, 2004. 4.1.1

[58] Melissa A Merideth, Leslie B Gordon, Sarah Clauss, Vandana Sachdev, Ann CM Smith, Monique B Perry, Carmen C Brewer, Christopher Zalewski, H Jeffrey Kim, Beth Solomon, et al. Phenotype and course of hutchinson–gilford progeria syndrome. *New England Journal of Medicine*, 358(6):592–604, 2008. 1.2

[59] C.A. Micchelli and N. Perrimon. Evidence that stem cells reside in the adult Drosophila midgut epithelium. *Nature*, 439(7075):475–479, 2006. 1.3, 1.3

[60] John MK Mislow, James M Holaska, Marian S Kim, Kenneth K Lee, Miriam Segura-Totten, Katherine L Wilson, and Elizabeth M McNally. Nesprin-1α self-associates and binds directly to emerin and lamin a in vitro. *FEBS letters*, 525(1):135–140, 2002. 1.1

[61] Sean J Morrison, Antoni M Wandycz, Koichi Akashi, Amiela Globerson, and Irving L Weissman. The aging of hematopoietic stem cells. *Nature medicine*, 2(9):1011–1016, 1996. 1.3

[62] Andrés Muñoz-Alarcón, Maja Pavlovic, Jasmine Wismar, Bertram Schmitt, Maria Eriksson, Per Kylsten, and Mitchell S Dushay. Characterization of lamin mutation phenotypes in drosophila and comparison to human laminopathies. *PloS one*, 2(6):e532, 2007. 1.2, 34, 3.3

[63] Laura A Nilson and Trudi Schüpbach. Egf receptor signaling in drosophila oogenesis. *Current topics in developmental biology*, 44:203–244, 1999. 1.2

[64] Emi K Nishimura, Scott R Granter, and David E Fisher. Mechanisms of hair graying: incomplete melanocyte stem cell maintenance in the niche. *Science*, 307(5710):720–724, 2005. 1.3

[65] B. Ohlstein and A. Spradling. The adult Drosophila posterior midgut is maintained by pluripotent stem cells. *Nature*, 439(7075):470–474, 2005. 1.3, 1.3, 3.1.1

[66] B. Ohlstein and A. Spradling. Multipotent Drosophila intestinal stem cells specify daughter cell fates by differential notch signaling. *Science*, 315(5814):988, 2007. 1.3, 1.3, 3.1.1

[67] Shinichi Osouda, Yoshihiro Nakamura, Brigitte de Saint Phalle, Maeve McConnell, Tsuneyoshi Horigome, Shin Sugiyama, Paul A Fisher, and Kazuhiro Furukawa. Null mutants of drosophila b-type lamin dm 0 show aberrant tissue differentiation rather than

obvious nuclear shape distortion or specific defects during cell proliferation. *Developmental biology*, 284(1):219–232, 2005. 1.2, 3.3

[68] Laurin Marie Pacheco, Lourdes Adriana Gomez, Janice Dias, Noel M Ziebarth, Guy A Howard, and Paul C Schiller. Progerin expression disrupts critical adult stem cell functions involved in tissue repair. *Aging (Albany NY)*, 6(12):1049, 2014. 1.2

[69] Sophie Pantalacci, Nicolas Tapon, and Pierre Léopold. The salvador partner hippo promotes apoptosis and cell-cycle exit in drosophila. *Nature cell biology*, 5(10):921–927, 2003. 4.1.1

[70] D. A. Parry, J. F. Conway, and P. M. Steinert. Structural studies on lamin. Similarities and differences between lamin and intermediate-filament proteins. *Biochem. J.*, 238(1):305–308, Aug 1986. 1.1, 1.2

[71] Parthive H Patel, Devanjali Dutta, and Bruce A Edgar. Niche appropriation by drosophila intestinal stem cell tumours. *Nature cell biology*, 2015. 3.1.1, 4.1.1

[72] G Patrizi and M Poger. The ultrastructure of the nuclear periphery: The zonula nucleum limitans. *Journal of ultrastructure research*, 17(1):127–136, 1967. 1.1

[73] Cordelia Rauskolb, Shuguo Sun, Gongping Sun, Yuanwang Pan, and Kenneth D Irvine. Cytoskeletal tension inhibits hippo signaling through an ajuba-warts complex. *Cell*, 158(1):143–156, 2014. 4.1.1

[74] Fangfang Ren, Qing Shi, Yongbin Chen, Alice Jiang, Y Tony Ip, Huaqi Jiang, and Jin Jiang. Drosophila myc integrates multiple signaling pathways to regulate intestinal stem cell proliferation during midgut regeneration. *Cell research*, 23(9):1133–1146, 2013. 3.1.1, 4.1.1

[75] Derrick J Rossi, David Bryder, and Irving L Weissman. Hematopoietic stem cell aging: mechanism and consequence. *Experimental gerontology*, 42(5):385–390, 2007. 1.3

[76] A.E. Rusiñol and M.S. Sinensky. Farnesylated lamins, progeroid syndromes and farnesyl transferase inhibitors. *Journal of cell science*, 119(Pt 16):3265, 2006. 1.1

[77] PK Sarkar and RA Shinton. Hutchinson-guilford progeria syndrome. *Postgraduate medical journal*, 77(907):312–317, 2001. 1.2

[78] P. Scaffidi and T. Misteli. Lamin A-dependent misregulation of adult stem cells associated with accelerated ageing. *Nature cell biology*, 10(4):452–459, 2008. 1.2, 3.1.1, 4.1.3

[79] N.E. Sharpless and R.A. DePinho. How stem cells age and why this makes us grow old. *Nature Reviews Molecular Cell Biology*, 8(9):703–713, 2007. 1.3

[80] Norman E Sharpless and Gerald Schatten. Stem cell aging. *The Journals of Gerontology Series A: Biological Sciences and Medical Sciences*, page gln070, 2009. 1.3

[81] Rachael L Shaw, Alexander Kohlmaier, Cédric Polesello, Cornelia Veelken, Bruce A Edgar, and Nicolas Tapon. The hippo pathway regulates intestinal stem cell proliferation during drosophila adult midgut regeneration. *Development*, 137(24):4147–4158, 2010. 1.3, 3.1.1

[82] Allan Spradling, Daniela Drummond-Barbosa, and Toshie Kai. Stem cells find their niche. *Nature*, 414(6859):98–104, 2001. 1.3

[83] Colin L Stewart, Kyle J Roux, and Brian Burke. Blurring the boundary: the nuclear envelope extends its reach. *Science*, 318(5855):1408–1412, 2007. 1

[84] Nico Stuurman, Susanne Heins, and Ueli Aebi. Nuclear lamins: their structure, assembly, and interactions. *Journal of structural biology*, 122(1):42–66, 1998. 1.1

[85] M Azim Surani. Reprogramming of genome function through epigenetic inheritance. *Nature*, 414(6859):122–128, 2001. 1.3

[86] Valerie LRM Verstraeten, Julie Y Ji, Kiersten S Cummings, Richard T Lee, and Jan Lammerding. Increased mechanosensitivity and nuclear stiffness in hutchinson–gilford progeria cells: effects of farnesyltransferase inhibitors. *Aging cell*, 7(3):383–393, 2008. 1.2

[87] Vera Wenzel, Daniela Roedl, Diana Gabriel, Leslie B Gordon, Meenhard Herlyn, Reinhard Schneider, Johannes Ring, and Karima Djabali. Naive adult stem cells from patients with hutchinson-gilford progeria syndrome express low levels of progerin in vivo. *Biology open*, 1(6):516–526, 2012. 1.2

[88] Shian Wu, Jianbin Huang, Jixin Dong, and Duojia Pan. hippo encodes a ste-20 family protein kinase that restricts cell proliferation and promotes apoptosis in conjunction with salvador and warts. *Cell*, 114(4):445–456, 2003. 4.1.1

[89] Na Xu, Si Qi Wang, Dan Tan, Yawei Gao, Guonan Lin, and Rongwen Xi. Egfr, wingless and jak/stat signaling cooperatively maintain drosophila intestinal stem cells. *Developmental biology*, 354(1):31–43, 2011. 1.3, 3.1.1

[90] Qian Ye and Howard J Worman. Protein-protein interactions between human nuclear lamins expressed in yeast. *Experimental cell research*, 219(1):292–298, 1995. 1.1

[91] Feng Yin, Jianzhong Yu, Yonggang Zheng, Qian Chen, Nailing Zhang, and Duojia Pan. Spatial organization of hippo signaling at the plasma membrane mediated by the tumor suppressor merlin/nf2. *Cell*, 154(6):1342–1355, 2013. 4.1.1

[92] Stephen G Young, Loren G Fong, Susan Michaelis, et al. Prelamin a, zmpste24, misshapen cell nuclei, and progeria -new evidence suggesting that protein farnesylation could be important for disease pathogenesis. *J Lipid Res*, 46(12):2531–58, 2005. 1.2

[93] Qiuping Zhang, Cassandra D Ragnauth, Jeremy N Skepper, Nathalie F Worth, Derek T Warren, Roland G Roberts, Peter L Weissberg, Juliet A Ellis, and Catherine M Shanahan. Nesprin-2 is a multi-isomeric protein that binds lamin and emerin at the nuclear envelope and forms a subcellular network in skeletal muscle. *Journal of cell science*, 118(4):673–687, 2005. 1.1

[94] Ye Zhu, Dong Li, Yadong Wang, Chunli Pei, Song Liu, Lei Zhang, Zengqiang Yuan, and Peng Zhang. Brahma regulates the hippo pathway activity through forming complex with yki–sd and regulating the transcription of crumbs. *Cellular signalling*, 27(3):606–613, 2015. 4.1.1

[95] Norman Zielke, Jerome Korzelius, Monique van Straaten, Katharina Bender, Gregor FP Schuhknecht, Devanjali Dutta, Jinyi Xiang, and Bruce A Edgar. Fly-fucci: a versatile tool for studying cell proliferation in complex tissues. *Cell reports*, 7(2):588–598, 2014. 3.1.2, 28, 4.1.2

Appendix

Table 10: Control vs Dm0 overexpression: 30 candidates with strongest increase in transcript levels compared to control

Nr	Flybase gene id	external gene name	log2 fold change
1	FBgn0035638	Tektin-C	7.03
2	FBgn0039551	Or98a	5.29
3	FBgn0085386	CG34357	5.29
4	FBgn0034415	CG15116	4.50
5	FBgn0261804	CG42750	4.47
6	FBgn0263219	Dscam4	4.40
7	FBgn0051708	CG31708	4.18
8	FBgn0034506	CG13870	4.11
9	FBgn0035776	CG8564	3.74
10	FBgn0036654	CG9692	3.62
11	FBgn0250910	Octbeta3R	3.62
12	FBgn0034692	CG13502	3.60
13	FBgn0002525	Lamin Dm0	3.59
14	FBgn0052207	CG32207	3.52
15	FBgn0034505	CG16739	3.50
16	FBgn0263332		3.46
17	FBgn0031747	CG9021	3.45
18	FBgn0035187	Trh	3.45
19	FBgn0052364	CG32364	3.35
20	FBgn0263328		3.29
21	FBgn0262169	magu	3.18
22	FBgn0263250	CG43393	3.16
23	FBgn0052625	CG32625	3.13
24	FBgn0034408	sano	3.03
25	FBgn0264721		3.03
26	FBgn0034910	CG4763	2.92
27	FBgn0033469	CG12133	2.90
28	FBgn0259683	Ir40a	2.90
29	FBgn0085452	CG34423	2.89
30	FBgn0036997	CG5955	2.87

Table 11: Control vs Dm0 overexpression: 30 candidates with strongest decrease in transcript levels compared to control

Nr	Flybase gene id	external gene name	log2 fold change
1	FBgn0040104	lectin-24A	-4.02
2	FBgn0032336	Ast-C	-4.01
3	FBgn0015591	Ast	-3.56
4	FBgn0042110	CG18765	-3.53
5	FBgn0039470	CG6296	-3.46
6	FBgn0004430	LysS	-3.26
7	FBgn0082950	snoRNA:Me18S-G1952	-3.25
8	FBgn0004428	LysE	-3.21
9	FBgn0031248	CG11912	-3.13
10	FBgn0259722	CG42376	-3.11
11	FBgn0036101	NijA	-3.10
12	FBgn0039316	CG11893	-3.07
13	FBgn0039114	Lsd-1	-3.04
14	FBgn0053867	His-:CR33867	-3.02
15	FBgn0082926	snoRNA:Me28S-U1848	-3.01
16	FBgn0086057	snoRNA:Me28S-G2017	-2.99
17	FBgn0038147	CCHa2	-2.95
18	FBgn0037291	CG14662	-2.90
19	FBgn0053346	CG33346	-2.88
20	FBgn0004872	piwi	-2.87
21	FBgn0036953	CG17145	-2.85
22	FBgn0264002	DmsR-2	-2.84
23	FBgn0000071	Ama	-2.77
24	FBgn0013276	Hsp70Ab	-2.77
25	FBgn0053337	CG33337	-2.76
26	FBgn0036713	Mip	-2.74
27	FBgn0085415	CG34386	-2.68
28	FBgn0036440	CG17177	-2.62
29	FBgn0086677	jeb	-2.59
30	FBgn0013678	mt:Cyt-b	-2.59

Table 12: Control vs UPD overexpression: 30 candidates with strongest increase in transcript levels compared to control

Nr	Flybase gene id	external gene name	log2 fold change
1	FBgn0004956	UPD1	4.84
2	FBgn0053508	ppk13	4.46
3	FBgn0053543	CG33543	4.40
4	FBgn0031935	CG13793	3.72
5	FBgn0033574	Spn47C	3.62
6	FBgn0027578	CG14526	3.42
7	FBgn0031936	CG13794	3.38
8	FBgn0050104	NT5E-2	3.31
9	FBgn0034462	CG15905	3.12
10	FBgn0032713	CG17323	3.00
11	FBgn0034374	CG15086	2.94
12	FBgn0053509	CG33509	2.87
13	FBgn0034195	Spn53F	2.67
14	FBgn0032683	kon	2.60
15	FBgn0034196	CG15605	2.57
16	FBgn0015400	kek2	2.54
17	FBgn0031850	Tsp	2.53
18	FBgn0085753	pseudogene:CR40596	2.41
19	FBgn0034463	CG15125	2.38
20	FBgn0000527	e	2.38
21	FBgn0036951	CG7017	2.36
22	FBgn0020414	Idgf3	2.30
23	FBgn0044812	TotC	2.25
24	FBgn0033921	tej	2.23
25	FBgn0028945	CG7631	2.21
26	FBgn0051148	CG31148	2.17
27	FBgn0052198	CG32198	2.16
28	FBgn0039670	CG7567	2.15
29	FBgn0052302	CG32302	2.08
30	FBgn0052817	CG32817	2.05

Table 13: Control vs UPD overexpression: 30 candidates with strongest decrease in transcript levels compared to control

Nr	Flybase gene id	external gene name	log2 fold change
1	FBgn0033774	CG12374	-6.27
2	FBgn0004428	LysE	-6.10
3	FBgn0004430	LysS	-6.04
4	FBgn0027109	npf	-4.77
5	FBgn0036953	CG17145	-4.41
6	FBgn0039470	CG6296	-4.40
7	FBgn0004426	LysC	-3.99
8	FBgn0011556	zetaTry	-3.98
9	FBgn0039471	CG6295	-3.63
10	FBgn0003357	Jon99Ciii	-3.58
11	FBgn0000337	cn	-3.57
12	FBgn0004427	LysD	-3.43
13	FBgn0003358	Jon99Ci	-3.39
14	FBgn0040091	Ugt58Fa	-3.38
15	FBgn0040104	lectin-24A	-3.35
16	FBgn0031261	nAcRbeta-21C	-3.35
17	FBgn0031220	CG4822	-3.31
18	FBgn0020907	Scp2	-3.23
19	FBgn0023197	Jon74E	-3.22
20	FBgn0038878	CG3301	-3.20
21	FBgn0039472	CG17192	-3.16
22	FBgn0051041	CG31041	-3.07
23	FBgn0051774	fred	-3.07
24	FBgn0051266	CG31266	-3.02
25	FBgn0052379	CG32379	-2.99
26	FBgn0263250	CG43393	-2.98
27	FBgn0033541	CG12934	-2.98
28	FBgn0031653	Jon25Biii	-2.96
29	FBgn0010425	epsilonTry	-2.95
30	FBgn0263746		-2.92

Table 14: Control vs UPD & Dm0 overexpression: 30 candidates with strongest increase in transcript levels compared to control

Nr	Flybase gene id	external gene name	log2 fold change
1	FBgn0053508	ppk13	7.38
2	FBgn0035638	Tektin-C	6.98
3	FBgn0085386	CG34357	6.51
4	FBgn0039551	Or98a	6.21
5	FBgn0053509	CG33509	6.20
6	FBgn0031935	CG13793	6.13
7	FBgn0031936	CG13794	5.90
8	FBgn0035187	Trh	5.52
9	FBgn0250910	Octbeta3R	5.46
10	FBgn0039482	CG14258	5.42
11	FBgn0039479	CG14257	5.42
12	FBgn0038239	CG14850	5.36
13	FBgn0036654	CG9692	5.29
14	FBgn0034463	CG15125	5.23
15	FBgn0004956	UPD1	5.04
16	FBgn0263328		5.03
17	FBgn0261429		5.03
18	FBgn0053922	CG33922	4.98
19	FBgn0083945	CG34109	4.98
20	FBgn0034462	CG15905	4.97
21	FBgn0032713	CG17323	4.95
22	FBgn0034374	CG15086	4.87
23	FBgn0053543	CG33543	4.85
24	FBgn0053296	CG33296	4.82
25	FBgn0040602	CG14545	4.70
26	FBgn0052625	CG32625	4.70
27	FBgn0035777	CG8563	4.69
28	FBgn0053923	CG33923	4.69
29	FBgn0026255	clumsy	4.66
30	FBgn0035316	CG15878	4.63

Table 15: Control vs UPD & Dm0 overexpression: 30 candidates with strongest decrease in transcript levels compared to control

Nr	Flybase gene id	external gene name	log2 fold change
1	FBgn0033774	CG12374	-7.13
2	FBgn0004428	LysE	-5.23
3	FBgn0004430	LysS	-4.81
4	FBgn0038878	CG3301	-4.66
5	FBgn0040091	Ugt58Fa	-4.20
6	FBgn0036953	CG17145	-4.05
7	FBgn0023197	Jon74E	-3.97
8	FBgn0051774	fred	-3.97
9	FBgn0031220	CG4822	-3.89
10	FBgn0003358	Jon99Ci	-3.85
11	FBgn0040104	lectin-24A	-3.79
12	FBgn0039471	CG6295	-3.66
13	FBgn0003357	Jon99Ciii	-3.49
14	FBgn0004426	LysC	-3.45
15	FBgn0031219	CG13694	-3.45
16	FBgn0031630	CG15629	-3.39
17	FBgn0031261	nAcRbeta-21C	-3.29
18	FBgn0036833	CG3819	-3.27
19	FBgn0004427	LysD	-3.20
20	FBgn0011556	zetaTry	-3.17
21	FBgn0030756	CG9903	-3.06
22	FBgn0050090	CG30090	-3.05
23	FBgn0039470	CG6296	-3.00
24	FBgn0085415	CG34386	-2.98
25	FBgn0263020	CG43315	-2.93
26	FBgn0039778	Jon99Fi	-2.89
27	FBgn0033469	CG12133	-2.88
28	FBgn0039472	CG17192	-2.87
29	FBgn0043575	PGRP-SC2	-2.85
30	FBgn0263250	CG43393	-2.81

Table 16: Dm0 overexpression vs UPD overexpression: 30 candidates with strongest increase in transcript levels compared to control

Nr	Flybase gene id	external gene name	log2 fold change
1	FBgn0027578	CG14526	5.06
2	FBgn0004872	piwi	4.57
3	FBgn0042110	CG18765	4.29
4	FBgn0050104	NT5E-2	4.20
5	FBgn0052279	dro2	4.19
6	FBgn0004956	os	4.03
7	FBgn0032684	CG10178	4.02
8	FBgn0035926	CG5804	4.01
9	FBgn0053543	CG33543	3.92
10	FBgn0052302	CG32302	3.82
11	FBgn0036948	CG7298	3.79
12	FBgn0031935	CG13793	3.72
13	FBgn0031936	CG13794	3.65
14	FBgn0031693	Cyp4ac1	3.62
15	FBgn0050103	CG30103	3.51
16	FBgn0039053	CG6738	3.40
17	FBgn0034462	CG15905	3.36
18	FBgn0051057	tau	3.34
19	FBgn0014073	Tie	3.29
20	FBgn0038632	CG14301	3.26
21	FBgn0032683	kon	3.22
22	FBgn0040958	Peritrophin-15b	3.19
23	FBgn0031694	Cyp4ac2	3.12
24	FBgn0033574	Spn47C	3.06
25	FBgn0053337	CG33337	3.06
26	FBgn0015400	kek2	3.05
27	FBgn0034317	CG14499	3.04
28	FBgn0036225	CG5883	3.03
29	FBgn0032856	CG16798	3.02
30	FBgn0032336	Ast-C	3.02

Table 17: Dm0 overexpression vs UPD overexpression: 30 candidates with strongest decrease in transcript levels compared to control

Nr	Flybase gene id	external gene name	log2 fold change
1	FBgn0035638	Tektin-C	-6.66
2	FBgn0034415	CG15116	-6.51
3	FBgn0034692	CG13502	-6.26
4	FBgn0263250	CG43393	-6.14
5	FBgn0261804	CG42750	-5.93
6	FBgn0085386	CG34357	-5.57
7	FBgn0000337	cn	-5.12
8	FBgn0034506	CG13870	-4.99
9	FBgn0039551	Or98a	-4.92
10	FBgn0015038	Cyp9b1	-4.91
11	FBgn0263332		-4.80
12	FBgn0033469	CG12133	-4.78
13	FBgn0263219	Dscam4	-4.76
14	FBgn0259683	Ir40a	-4.64
15	FBgn0027109	npf	-4.53
16	FBgn0034505	CG16739	-4.50
17	FBgn0052207	CG32207	-4.39
18	FBgn0035476	CG12766	-4.33
19	FBgn0086408	stl	-4.30
20	FBgn0051774	fred	-4.17
21	FBgn0053494	CG33494	-4.03
22	FBgn0035776	CG8564	-4.03
23	FBgn0264721		-4.01
24	FBgn0034910	CG4763	-3.98
25	FBgn0051728	CG31728	-3.87
26	FBgn0037975	CG3397	-3.86
27	FBgn0040091	Ugt58Fa	-3.80
28	FBgn0033774	CG12374	-3.80
29	FBgn0263477	scaRNA:U1-6	-3.79
30	FBgn0051708	CG31708	-3.73

Table 18: DAVID 6.8 GO-annotation, Control vs Dm0, upregulated transcripts, biological process

Term	Count	-log10(FDR)
DNA recombination	7	3,37
telomere maintenance	7	2,78
regulation of protein stability	6	2,13
mRNA splicing, via spliceosome	21	2,06
hippo signaling	5	2,04
chromatin-mediated maintenance of transcription	4	1,37
nucleotide-excision repair	6	1,29
regulation of alternative mRNA splicing, via spliceosome	9	1,21
telomere capping	4	1,07
double-strand break repair	5	1,01

Table 19: DAVID 6.8 GO-annotation, Control vs Dm0, upregulated transcripts, cellular compartment

Term	Count	-log10(FDR)
nucleus	110	4,60
apical cortex	8	1,79
nucleolus	17	1,76
sarcomere	4	1,69
adherens junction	8	1,31

Table 20: DAVID 6.8 GO-annotation, Control vs Dm0, upregulated transcripts, molecular function

Term	Count	-log10(FDR)
zinc ion binding	47	2,59
helicase activity	8	2,01
ATP binding	42	1,56
DNA binding	38	1,28
nucleic acid binding	28	1,26
RNA helicase activity	5	1,12
ATP-dependent DNA helicase activity	5	1,12

Table 21: DAVID 6.8 GO-annotation, Control vs Dm0, downregulated transcripts, biological process

Term	Count	-log10(FDR)
proteolysis	77	12,85
glutathione metabolic process	15	6,04
neuropeptide signaling pathway	17	5,87
metabolic process	25	3,35
transmembrane transport	35	2,75
chitin metabolic process	17	2,32
synaptic vesicle exocytosis	8	2,21
heat shock-mediated polytene chromosome puffing	5	2,21
G-protein coupled receptor signaling pathway	20	2,01
oxidation-reduction process	40	1,76
response to hypoxia	8	1,58
neurotransmitter secretion	15	1,39
leg disc proximal/distal pattern formation	6	1,39
cellular acyl-CoA homeostasis	4	1,02

Table 22: DAVID 6.8 GO-annotation, Control vs Dm0, downregulated transcripts, cellular compartment

Term1	Count	-log10(FDR)
integral component of membrane	103	6,60
membrane	46	3,82
integral component of plasma membrane	30	3,62
intracellular membrane-bounded organelle	16	2,78
extracellular region	51	2,59
extracellular space	41	2,21
intracellular	13	2,01
synaptic vesicle	12	1,78
presynaptic active zone	6	1,75
voltage-gated calcium channel complex	4	1,70
plasma membrane	47	1,41
basolateral plasma membrane	7	1,09

Table 23: DAVID 6.8 GO-annotation, Control vs Dm0, downregulated transcripts, molecular function

Term	Count	-log10(FDR)
serine-type endopeptidase activity	52	8,88
transfer of acyl groups	13	6,34
glutathione transferase activity	14	4,64
neuropeptide receptor activity	13	3,49
voltage-gated calcium channel activity	5	2,41
neuropeptide hormone activity	10	2,15
metallopeptidase activity	10	1,97
oxidoreductase activity	8	1,84
chitin binding	18	1,70
serine-type peptidase activity	9	1,66
heme binding	19	1,53
diazepam binding	4	1,14
hormone activity	8	1,11
lysozyme activity	6	1,11

Table 24: DAVID 6.8 GO-annotation, Control vs UPD, upregulated transcripts, biological process

Term	Count	-log10(FDR)
cellular amino acid metabolic process	5	2,65
dopamine uptake involved in synaptic transmission	3	1,43
defense response	7	1,43
neurotransmitter transport	4	1,21
peptide catabolic process	4	1,03
immune response	5	1,01

Table 25: DAVID 6.8 GO-annotation, Control vs UPD, upregulated transcripts, cellular compartment

Term	Count	-log10(FDR)
extracellular region	24	4,36
integral component of plasma membrane	18	2,42
proteinaceous extracellular matrix	7	2,30
integral component of membrane	53	1,36

Table 26: DAVID 6.8 GO-annotation, Control vs UPD, upregulated transcripts, molecular function

Term	Count	-log10(FDR)
metallodipeptidase activity	4	2,88
aminoacylase activity	4	2,88
dopamine:sodium symporter activity	3	1,42
neurotransmitter:sodium symporter activity	4	1,32
choline dehydrogenase activity	3	1,28

Table 27: DAVID 6.8 GO-annotation, Control vs UPD, downregulated transcripts, biological process

Term	Count	-log10(FDR)
proteolysis	46	14,51
glutathione metabolic process	10	5,49
metabolic process	14	3,09
oxidation-reduction process	20	1,81
potassium ion transport	5	1,34
transmembrane transport	15	1,16
digestion	3	1,02

Table 28: DAVID 6.8 GO-annotation, Control vs UPD, downregulated transcripts, cellular compartment

Term	Count	-log10(FDR)
membrane	24	4,04
nucleolus	14	3,85
intracellular membrane-bounded organelle	8	1,62

Table 29: DAVID 6.8 GO-annotation, Control vs UPD, downregulated transcripts, molecular function

Term	Count	-log10(FDR)
serine-type endopeptidase activity	30	8,75
glutathione transferase activity	10	5,08
glucuronosyltransferase activity	7	3,32
metallocarboxypeptidase activity	6	2,53
glutathione peroxidase activity	4	1,81

Table 30: DAVID 6.8 GO-annotation, Control vs Dm0+UPD, upregulated transcripts, biological process

Term	Count	-log10(FDR)
telomere maintenance	7	2,72
DNA recombination	7	2,07
ecdysteroid metabolic process	5	2,00
dopamine uptake involved in synaptic transmission	4	1,75
double-strand break repair	6	1,75
meiotic cell cycle	5	1,69
crystal cell differentiation	4	1,52
serotonin receptor signaling pathway	4	1,34
nucleotide-excision repair	6	1,31
proteolysis	32	1,02

Table 31: DAVID 6.8 GO-annotation, Control vs Dm0+UPD, upregulated transcripts, cellular compartment

Term	Count	-log10(FDR)
integral component of plasma membrane	37	1,81
extracellular region	42	1,72
proteinaceous extracellular matrix	10	1,30
nuclear chromosome, telomeric region	4	1,20
synaptonemal complex	4	1,20
Mre11 complex	3	1,20

Table 32: DAVID 6.8 GO-annotation, Control vs Dm0+UPD, upregulated transcripts, molecular function

Term	Count	-log10(FDR)
damaged DNA binding	9	3,63
dopamine:sodium symporter activity	4	1,74
metalloendopeptidase activity	11	1,55
choline dehydrogenase activity	4	1,52
G-protein coupled serotonin receptor activity	4	1,33

Table 33: DAVID 6.8 GO-annotation, Control vs Dm0+UPD, downregulated transcripts, biological process

Term	Count	-log10(FDR)
proteolysis	61	9,53
neuropeptide signaling pathway	17	6,73
oxidation-reduction process	45	5,05
G-protein coupled receptor signaling pathway	22	3,94
transmembrane transport	33	3,71
metabolic process	22	3,58
flavonoid glucuronidation	10	3,41
flavonoid biosynthetic process	10	3,41
regulation of calcium ion-dependent exocytosis	5	2,58
glutathione metabolic process	10	2,32
ion transmembrane transport	5	2,29
neurotransmitter secretion	15	2,26
calcium ion transmembrane transport	6	1,94
insecticide catabolic process	7	1,71
response to DDT	7	1,53
cytoskeletal matrix organization at active zone	4	1,28
calcium ion-regulated exocytosis of neurotransmitter	4	1,28
synaptic vesicle exocytosis	6	1,11
cellular water homeostasis	4	1,10

Table 34: DAVID 6.8 GO-annotation, Control vs Dm0+UPD, downregulated transcripts, cellular compartment

Term	Count	-log10(FDR)
integral component of membrane	225	14,26
integral component of plasma membrane	60	8,15
intracellular membrane-bounded organelle	28	7,62
membrane	50	5,50
voltage-gated calcium channel complex	6	4,14
synaptic vesicle	14	3,43
plasma membrane	67	2,72
extracellular space	45	1,54
basolateral plasma membrane	7	1,14

Table 35: DAVID 6.8 GO-annotation, Control vs Dm0+UPD, downregulated transcripts, molecular function

Term	Count	-log10(FDR)
serine-type endopeptidase activity	42	6,79
oxidoreductase activity, acting on paired donors, with incorporation or reduction of molecular oxygen	19	4,60
neuropeptide hormone activity	11	3,88
electron carrier activity	22	3,66
neuropeptide receptor activity	12	3,58
monooxygenase activity	17	3,54
heme binding	21	3,33
iron ion binding	22	3,18
UDP-glycosyltransferase activity	10	2,82
glutathione peroxidase activity	9	2,64
voltage-gated calcium channel activity	5	2,40
calcium ion binding	26	2,33
glutathione transferase activity	10	2,19
oxidoreductase activity, acting on CH-OH group of donors	8	1,85
lysozyme activity	6	1,48
glycerol channel activity	4	1,17
water channel activity	4	1,17
oxidoreductase activity	19	1,08
metallocarboxypeptidase activity	6	1,00

Table 36: Control vs Dm0 overexpression: 5 hippo pathway candidates with increase in transcript levels compared to control

Nr	Flybase gene id	external gene name	log2 fold change
1	FBgn0030530	Ajuba(jub)	1,04
2	FBgn0000212	brahma(brm)	1,09
3	FBgn0053193	salvador(sav)	1,03
4	FBgn0086384	Merlin(Mer)	1,13
5	FBgn0001075	fat(ft)	1,81